Thermodynamics of the BCS-BEC Crossover

Ph.D. thesis by

Stefano Cerrito

Physik-Department

Technische Universität München

Technische Universität München
Physik-Department
Institut für Theoretische Physik T34
Univ.-Prof. Dr. W. Zwerger

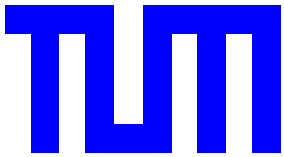

Thermodynamics of the BCS-BEC Crossover

Stefano Cerrito

Vollständiger Abdruck der von der Fakultät für Physik der Technischen Universität München zur Erlangung des akademischen Grades eines

Doktors der Naturwissenschaften (Dr. rer. nat.)

genehmigten Dissertation.

Vorsitzender: Univ.-Prof. Christian Pfleiderer, Ph. D.

Prüfer der Dissertation:

1. Univ.-Prof. Dr. Wilhelm Zwerger
2. Univ.-Prof. Dr. Wolfram Weise

Die Dissertation wurde am 28.03.2007 bei der Technischen Universität München eingereicht und durch die Fakultät für Physik am 06.06.2007 angenommen.

Abstract

In this thesis a self-consistent and conserving theory for the thermodynamics of an attractive, two-component Fermi gas near a Feshbach resonance is presented. The work is motivated by the numerous fascinating experiments which, in the last decade, have been carried out in the field of dilute ultra-cold atomic gases.

In order to cover both normal and super-fluid phase we extend the many-body formalism developed by Luttinger and Ward and by DeDominicis and Martin. Employing a ladder approximation to treat the formation of pairs at low densities, the resulting self-consistent integral equations for the normal and anomalous Green functions are solved numerically for arbitrary coupling.

The critical temperature, the equation of state and the entropy are determined as a function of the dimensionless parameter $1/k_F a$, which controls the crossover from the BCS-regime of extended pairs to the BEC-regime of tightly bound molecules. The associated dimers turn out to be described by a Popov-type approximation of a gapless, repulsive Bose-gas. The transition to the normal state in this approximation is weakly first order, in contrast to the expected continuous transition. In spite of this problem, our results compare well with recent numerical and field-theoretic approaches at the unitarity point.

Contents

List of Figures

Chapter 1

Introduction

The problem of quantum gases at low temperature has always aroused a lot of interest in the scientific community. In fact, below a certain critical temperature, both Bose gases [1] and Fermi gases with an attractive interaction assume a non-trivial behavior becoming superfluid. However the mechanisms which underly this phenomenon are quite different depending on the fermionic or bosonic nature of the particles.

A bosonic gas undergoes Bose-Einstein condensation for temperatures lower than a certain condensation temperature T_c. In this phase a macroscopic number of bosons condensates into the zero momentum state, thus the ground-state expectation value of the boson field operator $\langle\psi(\mathbf{r},t)\rangle$ remains finite in the thermodynamic limit. This reflects a macroscopic quantum coherence of the bosons in the condensate and may be viewed as the order parameter of the superfluid transition. While the theoretical background of Bose-Einstein condensation dates back to the original works of Bose [1] and Einstein [2], a Bose-Einstein condensate of atoms has been realized only at the end of the century in a gas of trapped alkali atoms [3, 4, 5]. Trapped alkali gases are relatively simple systems which behave like systems of point particles with a simple local interaction, therefore the study of weakly interacting Bose gases has become a very active field of research in the past ten years [6, 7, 8, 9].

On the other hand a fermionic system with an attractive interaction becomes superfluid at sufficiently low temperatures (electrons in a metal). The basic idea is that pairing between particles in the states $(\mathbf{k}\uparrow)$ and $(-\mathbf{k}\downarrow)$ occurs if the interparticle potential is attractive which makes the Fermi sea unstable. These pairs can condense into the zero momentum state and develop a macroscopic quantum coherence. In this case, the order parameter of the transition is given by the average of two fermion operators $\langle\psi_{\sigma_1}(\mathbf{r_1},t_1)\psi_{\sigma_2}(\mathbf{r_2},t_2)\rangle$. Cooper has shown [10] that in a weakly interacting Fermi gas an infinitesimal attractive interaction is already sufficient for the formation of bound momentum pairs, which are called Cooper pairs. Following this observation Bardeen, Cooper and Schrieffer developed a microscopic theory of superconductivity [11] (BCS-theory) which represents one of the most successful applications of many-body techniques and whose prediction are in very good agreement with

[1] In the case of repulsive interactions, superfluidity will only occur provided these are weak enough.

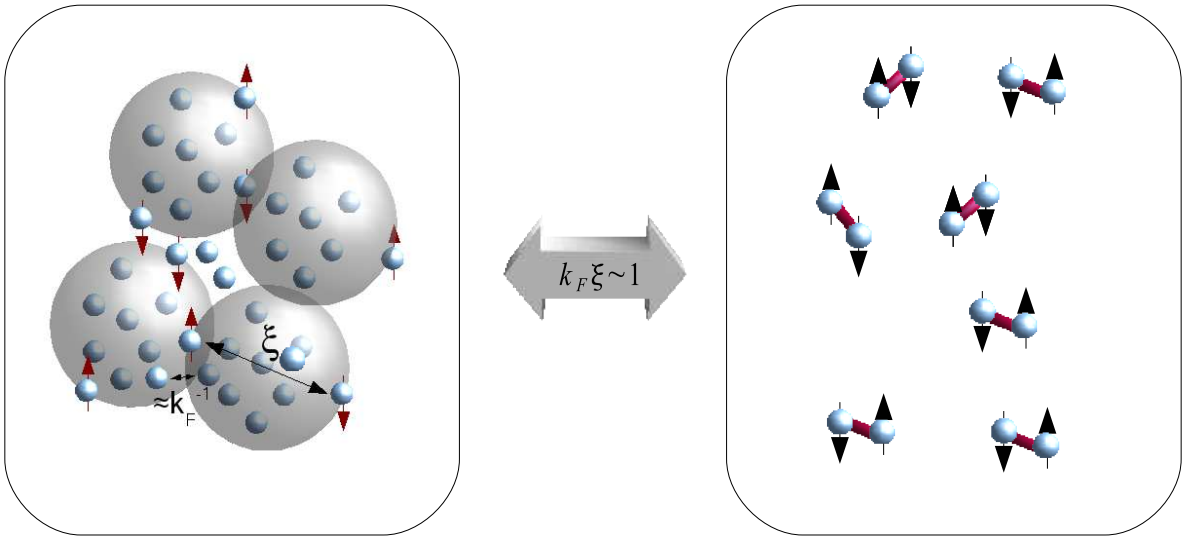

Figure 1.1: Pairing for weak and strong coupling. For weak coupling the fermions forms Cooper pairs which are very large and penetrate each other. In the limit of strong coupling the fermions are bound to form bosonic dimers which are far away from each other. The symbol ξ in the Figure is the size of a pair and k_F^{-1} represent the average distance between the fermions. The ratio $k_F\xi$ between the size of the pairs and the interparticle spacing defines different physical regimes. The weak coupling regime is defined by $k_F\xi \gg 1$, while $k_F\xi \ll 1$ indicates the strong coupling regime. The crossover region coincides with the intermediate regime defined by $k_F\xi \sim 1$.

experimental data.

1.1 From Cooper pairing to Bose Einstein condensation

The Cooper pairs, which are formed if the temperature is sufficiently low, are not well defined particles in real space. The pairs are normally very large and penetrate each other. On the other hand, if the attractive interaction becomes very strong the size of the pairs will eventually become smaller than the interparticle spacing defined by $1/k_F$ and the fermions will bind together to form bosonic dimers. The dimers form a dilute weakly interacting Bose gas which at low temperature becomes superfluid through Bose-Einstein condensation.

The BCS theory and the Bose-Einstein condensation of bosonic dimers can be viewed as two limiting cases of superfluidity in a Fermi system for weak and strong attractive interaction respectively.

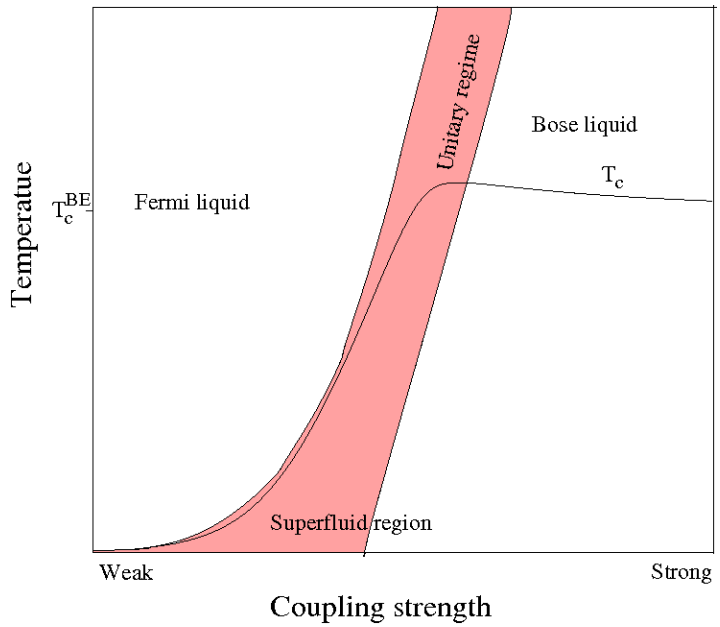

Figure 1.2: Phase diagram of a Fermi system with attractive interaction. The critical temperature of the superfluid transition is plotted as a function of the coupling strength. For weak coupling the system is a Fermi liquid while for strong coupling is a Bose liquid of molecules. The two limiting regimes are separated by an intermediate region where the Fermi liquid theory breaks down and one goes continuously from fermionic to bosonic statistics. In the region below the T_c-curve the system is in the superfluid state.

The strength of the interaction is characterized by the quantity $k_F\xi$, where ξ is the diameter of the pairs and k_F^{-1} represent the average distance between the fermions. Hence $k_F\xi$ is the ratio between the size of the pairs and the interparticle spacing. For weak coupling the diameter of the Cooper pairs is much larger than the average distance between the fermions, thus the BCS theory is valid in the regime defined by $k_F\xi \gg 1$. This situation is schematically shown in Figure 1.1 on the left hand side. On the other hand the regime of strong coupling is defined by the relation $k_F\xi \ll 1$. In this case the pairs are small and far away from each other as is depicted on the left hand side of Figure 1.1. The intermediate regime $k_F\xi \sim 1$ defines the region where the crossover from BCS superconductivity to Bose-Einstein condensation of dimers happens. Allowing the attractive interaction between the fermions to assume arbitrary strength one can describe how the fermionic system smoothly goes from being a superfluid system of BCS type (where the interaction is arbitrarily weak) to a Bose-Einstein condensate (BEC) of diatomic molecules or dimers (where the interaction is arbitrarily strong). The Cooper pairs, which need an attractive interaction to be formed, could be seen as ”bosonic-like” molecules which then are driven statistically to condense. BCS theory is a special case where the formation of the pairs and the condensation occurs at the same temperature.

The first attempt to extend the BCS theory to arbitrary coupling dates back to Eagles [12] and Leggett [13] which independently noted that the BCS ground state wave function is capable of describing a continuous evolution from BCS like behaviour to Bose-Einstein condensation as the strength of the attractive interaction between the fermions is increased. Using a variational ansatz with a BCS trial wave function it is possible to derive two equations to determine the energy gap Δ and the chemical potential μ as a function of the coupling strength for $T = 0$. Noziéres and Schmitt-Rink [14] first attempted to solve the problem at finite temperatures by using the many-particle quantum field theory with temperature dependent Green's functions and the so called ladder approximation. Within this theory they determined the critical temperature of the superfluid transition in the whole region from the weak coupling to the strong coupling limit. Another approach, based on a functional integral representation of the interacting fermion system is due to Drechsler and Zwerger [15]. This theory, originally designed for a two dimensional system was later extended to three dimensions [16]. A self-consistent quantum field theory approach to the crossover problem was given by Haussmann [17, 18]. The critical temperature of the superfluid transition as a function of the coupling strength obtained by the theories listed above qualitatively looks like the curve depicted in Figure 1.2. For weak coupling the system is a Fermi liquid where the gas is composed of fermionic particles, in the strong coupling regime the fermions are tightly bound into bosonic molecules. Outside the BCS regime, superfluidity emerge out of a non-Fermi liquid normal state where single fermions and bound pairs coexist. This intermediate regime, indicated in Figure 1.2 by the colored region, is also called "unitary regime".

Except for very weak coupling, pairs form and condens at different temperatures. For relatively strong coupling the temperature at which pairs are formed is related to the binding energy of the pairs $k_B T^* \propto \varepsilon_b$. Below a certain critical temperature the preformed bosonic molecules undergoes Bose-Einstein condensation at a critical temperature which is approximately given by the Bose-Einstein condensation temperature $T_{c,BE}$. Furthermore the binding energy ε_b depends on the strength of the interaction, thus for strong coupling T^* is much larger than T_c. If the coupling strength is reduced, the dissociation temperature T^* decreases sensibly while the critical temperature remains nearly constant. In the unitary region the dissociation temperature will reach the same order of magnitude of the critical temperature T_c. In the BCS limit the formation of Cooper pairs and superfluidity occur precipitously at the same temperature T_c. The critical temperature is thus given by the BCS critical temperature $T_{c,BCS}$ which decreases exponentially with the coupling strength.

1.2 Cold atomic gases

An experimental realization of the system described above can be achieved by using degenerate atomic gases. These gases can be manipulated with a high level of control, this fact together with the detailed understanding of the atomic interactions allows a precise comparison between experimental and theoretical results. The major step toward the realization of such a system was the development of cooling techniques which allowed to obtain first a degenerate gas of bosons at temperatures below the con-

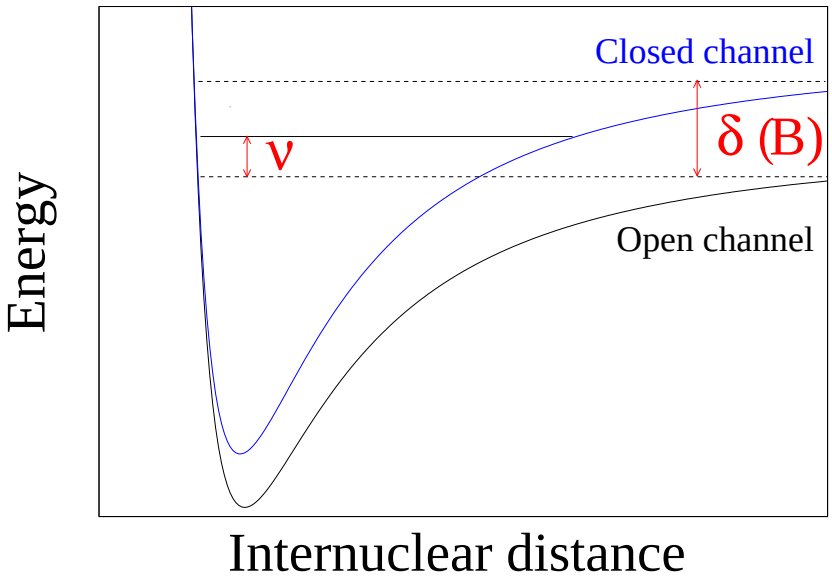

Figure 1.3: Schematic representation of the mechanism of a Feshbach resonance. A Feshbach resonance occurs when a bound state in the closed channel lies in proximity to the scattering threshold of an open channel potential. The symbol ν denotes the detuning of the bound state from the edge of the collision continuum. δ represents the energy shift between the two channels.

densation temperature [3, 4, 5] and then to achieve degeneracy in a Fermi gas of ^{40}K atoms [19]. The common technique to cool down bosonic gases is evaporative cooling. It consists in systematically removing only the more energetic atoms (i.e. the hottest atoms) in the trap. Effective evaporative cooling requires that the atoms in the gas undergo elastic thermalizing collisions. Although the way to obtain a degenerate Fermi gas is similar to the method employed in achieving BEC, it is necessary to take into account the Pauli statistics. In fact, due to their nature, fermions in the same state tend to avoid each other and a consequence is that s-wave interactions, which dominate the low energy scattering would vanish between a single species of fermions. The absence of s-wave scattering would prohibit the fermions to thermalize quickly, which is a necessary part of the cooling process. To overcome this problem the group at Jila [19] used a mixture of atoms within the two hyperfine levels: $|F = 9/2, m_F = 9/2\rangle$ and $|F = 9/2, m_F = 7/2\rangle$, where $F = 9/2$ is the total atomic spin and m_F is the magnetic quantum number. In this configuration fermions with the same spin will not interact, but two atoms in different spin states will. A more useful way to cool fermions is to sympathetically cool them with bosons: the bosons are evaporatively cooled as usual, while the fermions are cooled by interaction with the bosons. This technique was employed to create degenerate mixtures of ^6Li cooled to temperatures as low as 200 nK using either ^7Li ([20, 21, 22]) or ^{23}Na ([23]) as "refrigerant",

a degenerate mixture of ^{40}K and ^{87}Rb was obtained at the same time by the group in Firenze [24].

One of the most interesting features of cold atomic gases is the ability to finely tune the atomic interactions. This is achieved by using Feshbach resonances which can be precisely tuned by a magnetic field. Feshbach resonances in a dilute atomic gas were observed first in bosonic gases [25, 26, 27, 28] and later in Fermi systems [29, 30, 31, 32]. In Figure 1.3 is depicted a schematic representation of a Feshbach resonance. The open channel is associated with a triplet spin state, a Feshbach resonance arises when a bound state in the closed channel lies near the zero energy corresponding to the continuum of scattering states in the open channel. The electronic Zeeman coupling to the triplet state associated with the open channel makes it possible to shift the relative position of the two potentials by application of a magnetic field. This shift is indicated in the Figure by δ. In this way the resonance is magnetically tunable and the scattering length of the system will vary continuously with the magnetic field, becoming infinite at the value of the field which correspond to the Feshbach resonance. The deviation of the field from the resonance is indicated in Figure 1.3 by the detuning parameter ν. When ν is large and positive, the singlet state associated with the closed channel lies much above the open channel and does not play an important role. On the other hand if ν is large and negative the physics is defined by the closed channel.

The magnetic field, by detuning the two channels, influences the scattering properties of the system. At this stage it is useful to introduce the s-wave scattering length a, which in the low-energy limit is associated with the scattering amplitude of the two body scattering process. It turns out that the scattering length varies with the magnetic field according to

$$a = a_{bg}\left(1 - \frac{\Delta B}{B - B_0}\right), \tag{1.1}$$

where a_{bg} is the off-resonant background scattering length in the absence of the coupling to the closed channel. Furthermore ΔB is a measure of the width of the resonance, B_0 is the value of the magnetic field just on resonance and $B - B_0 \sim \nu$. Thus the scattering length a is negative when there is no bound state, it becomes $-\infty$ just before the bound state appears and $+\infty$ as the bound state stabilizes. As the interaction becomes increasingly strong, the scattering length approaches 0 from the positive side

The ability to tune the interparticle interactions in atomic gases via Feshbach resonances allows to control the process of molecular formation and dissociation. Fermionic molecules have lifetimes of the order of several seconds [33, 34, 35, 36]. This surprisingly long lifetime allows the realization of Bose-Einstein condensates of molecules [37, 38, 39] and the subsequent exploration of the crossover from a Bose-Einstein condensate to a BCS-like state of weakly bound fermion pairs [40, 41, 42, 43, 44].

1.3 Outlook and overview

The structure of this thesis will be as follows.

Chapter 2 will present the formalism of Luttinger and Ward for interacting fermions and the for-

malism of De Dominicis and Martin. A section will be dedicated to the Ward identity and the Thouless criterion. In Chapter 3 a set of self-consistent equations for the Green's function and the vertex function will be derived within the formalism of Luttinger and Ward previously described. The numerical results obtained by solving the self-consistent equation will be reported and commented. Chapter 4 is dedicated to the thermodynamics of the crossover. We will write explicitly the grand canonical thermodynamic potential within the formalism of Luttinger and Ward, and the entropy obtained from the theory developed by De Dominicis and Martin. Further we will show that, within our approximation the two formalism previously described are equivalent and produce the same set of self-consistent equations. The numerical results relative to the thermodynamic potentials are reported and commented in Chapter 5. Chapter 6 is dedicated to the description of the numerics we used to produce the present results.

Chapter 2

Many-body theory of interacting fermions

2.1 Luttinger-Ward formalism

2.1.1 Introduction

A system of interacting fermions can be successfully described in the many body formalism due Luttinger and Ward[45]. The formalism was originally developed to investigate the perturbation series for the ground state energy of a many-fermion system to arbitrary order in the interaction by using a Feynman diagrammatic technique. Starting from the grand canonical partition function for the system they obtain an expression for the grand canonical thermodynamic potential of an homogeneous interacting Fermi gas in a non-superfluid regime as unique functional of the Green's function.

This formalism, originally developed to explore the properties of non-superfluid Fermi systems, is also suited to describe superfluid systems. In more recent works the theory of Luttinger and Ward has been used to investigate the problem of the crossover of a Fermi liquid from BCS superfluidity to Bose-Einstein condensation [18, 17] which has been described in the previous Chapter. The crossover problem is more complicated than the original one, in fact the theory has to be capable to describe two different phenomena: the formation of pairs due to the attractive interaction and the transition to a superfluid regime below a certain critical temperature T_c. In the limit of weak interactions pairing between the fermions occurs simultaneously with the superfluid transition and the process is driven by individual excitations that can be described by a purely fermionic theory. On the other side, if the interaction is strong enough, the formation of pairs occurs at a temperature scale much higher than the critical temperature T_c. The superfluid transition in this regime is thus driven by collective excitations of a bosonic nature.

In section 2.1.2 we will describe the original formalism which, in Chapter 3, will be adapted to describe a fermionic system which can eventually become superfluid.

2.1.2 Formalism

Formally we start from the grand canonical partition function at finite temperature

$$Z = e^{-\beta\Omega} = \mathrm{Tr}\{\exp(-\beta[\hat{H} - \mu\hat{N}])\}. \tag{2.1}$$

The properties of the system are described by average of physical quantities which, in the grand canonical ensemble, are given by:

$$\langle \cdots \rangle = Z^{-1}\mathrm{Tr}\{\cdots \exp(-\beta[\hat{H} - \mu\hat{N}])\}. \tag{2.2}$$

From the definition (2.1) we can derive the grand canonical thermodynamic potential by taking the logarithm $\Omega = -k_B T \ln(Z)$. The partition function and the grand-potential are normally expressed by a perturbation series, to obtain it we decompose the Hamiltonian H into a free Hamiltonian $H_0 - \mu N$ which describes the noninteracting system and an interaction part H_1 (see for instance [46]). From the interacting part of the Hamiltonian H_1 we define the S-matrix

$$S = \mathrm{T}\exp\left\{-\hbar^{-1}\int_0^{\hbar\beta} d\tau H_1(\tau)\right\} \tag{2.3}$$

where τ is the imaginary time which varies in the interval $0 \leq \tau \leq \hbar\beta$ and $H_1(\tau)$ is defined by

$$H(\tau) = \exp\left[(H_0 - \mu N)\tau/\hbar\right] H_1\left[-(H_0 - \mu N)\tau/\hbar\right]. \tag{2.4}$$

The partition function can be rewritten in terms of the S-matrix as

$$Z = Z_0\langle \mathrm{T}\exp\left\{-\hbar^{-1}\int_0^{\hbar\beta} d\tau\, H_1(\tau)\right\}\rangle_0 \tag{2.5}$$

where $Z_0 = \mathrm{Tr}\{exp[-\beta H_0 - \mu N]\}$ is the partition function of the free fermions. The averages in the noninteracting system are defined by $\langle \ldots \rangle_0 = Z_0^{-1}\mathrm{Tr}\{\ldots \exp[-\beta H_0 - \mu N]\}$. The expression (2.5) is a very compact way to write the the perturbation series which is in practice generated by expanding the S-matrix in powers of the interaction and then evaluating the averages $\langle \ldots \rangle_0$ by using the Wick theorem. In this way we obtain a perturbation series where in the Feynman diagrams the propagator lines are identified by the free Green's function

$$G_{0,XX'} = \langle \mathrm{T}[\psi_X \psi^\dagger_{X'}]\rangle_0. \tag{2.6}$$

The Feynman diagrams can be partially resummed to obtain a perturbation series in terms of a smaller number of irreducible diagrams in which the propagator lines are now identified by the exact Green's function defined by

$$G_{XX'} = \langle \mathrm{T}[\psi_X \psi^\dagger_{X'}]\rangle. \tag{2.7}$$

The resummation can be performed by Legendre transformation [47]. This is achieved by introducing an external field which couples to a quadratic form of the fermionic field operators. In such a way a generalized partition function can be obtained which generates the Green's function by a functional derivative. A Legendre transformation is then performed to get an expression for the grand potential as a function of the Green's function. After having introduced the external field $A_{XX'}$ the generalized Partition function reads

$$Z[A] = Z\langle T e^{\psi^\dagger A \psi}\rangle. \tag{2.8}$$

The one-particle Green's function defined in (2.7) can be obtained from the generalized partition function (2.8) through a functional derivative:

$$\left.\frac{\delta Z[A]}{\delta A_{XX'}}\right|_{A=0} = -Z\langle \mathrm{T}[\psi_{X'}\psi_X^\dagger]\rangle = -ZG_{X'X}. \tag{2.9}$$

Alternatively we can obtain a generalized Green's function, which depend on the external field $A_{XX'}$, from the first variation of the free energy $F[A] = -\ln Z[A]$:

$$\frac{\delta F[A]}{\delta A_{XX'}} = G_{X'X}. \tag{2.10}$$

Instead of $F[A]$ we may consider the functional of the Green's function

$$\Omega[G] = F[A] - G_{X'X}A_{XX'}, \tag{2.11}$$

obtained by a Legendre transformation from the external field A to G. According to (2.11), the first variation of the functional $\Omega[G]$ with respect to the variable $G_{X'X}$ inverts the relation (2.9) expressing the external field $A_{XX'}$ as a function of the one-particle Green's function G:

$$\delta\Omega[G] = -A_{XX'}\delta G_{X'X}. \tag{2.12}$$

For an interacting system the functional $\Omega[G]$ reads

$$\Omega[G] = -\mathrm{Tr}\{-\ln G + [G_0^{-1}G - 1]\} - \Phi[G]. \tag{2.13}$$

The first term in (2.13) is obtained from the free energy for the noninteracting system. The trace Tr that appears in (2.13) is a very short hand notation for a fourfold trace defined with respect to the formal index $X = (\mathbf{r}, \tau, \sigma)$, which comprises the space-time coordinates and the spin index [1]. The functional $\Phi[G]$ contains all term due to the interaction and is definite by an infinite perturbation series of irreducible Feynman diagrams. The self-energy can be defined from $\Phi[G]$ trough a functional

[1] The formal index X can comprise another additional index α which distinguishes the fermion field operators between annihilation and creation operators.

derivative

$$\Sigma_{X'X} = -\frac{\delta\Phi[G]}{\delta G_{XX'}}. \tag{2.14}$$

We may now compare the first variation of the functional (2.13) with (2.12). The field $A_{XX'}$ is an auxiliary parameter introduced to perform the Legendre transformation, therefore it should vanish in a real physical system. Using this fact and the relation (2.14) we get a stationarity condition which determines the full matrix Green's function:

$$\frac{\delta\Omega[G]}{\delta G} = G^{-1} - G_0^{-1} + \Sigma = 0. \tag{2.15}$$

The condition (2.15) is also known as Dyson equation and is usually written in the form

$$G^{-1}_{XX'} = G^{-1}_{0,XX'} - \Sigma_{XX'}. \tag{2.16}$$

Equation (2.16) together with the functional derivative (2.14) forms a set of self-consistent equations for the Green's function. The numerical value of the functional (2.13) at the stationary point defined by (2.15) is the grand canonical potential $\Omega(T,\mu)$ of the system:

$$\Omega(T,\mu) = -k_B T \ln Z = k_B T F[0] = k_B T \mathrm{extr}\{\Omega[G]\}, \tag{2.17}$$

where extr$\{\Omega[G]\}$ is an extremum in the sense of a saddle point. The grand thermodynamic potential is then defined by the equation (2.13) and the stationarity condition (2.15).

2.1.3 Resummation of the perturbation series

To get an explicit form for the functionals $\Omega[G]$ and $\Phi[G]$ we start from the perturbation series for the partition function $Z[A]$ which is generated by expanding the S-matrix as anticipated in section 2.1.2

$$Z[A] = Z_0[A]\{1 + \text{sum over all vacuum diagrams}\}. \tag{2.18}$$

The expansion contains all the diagrams, including the disconnected ones. A first resummation is obtained by taking the logarithm $F[A] = -\ln Z[A]$. Indeed the perturbation series which is obtained for the functional $F[A]$ contains only the subclass of connected diagrams

$$F[A] = F_0[A] - \{1 + \text{sum over all } \textbf{connected} \text{ vacuum diagrams}\}. \tag{2.19}$$

From $F[A]$ we can obtain the Green's function by the functional derivative (2.10). In terms of Feynman diagrams $G_{XX'}$ is represented by an open propagator line ad closed loops connected by interaction lines. Such a diagram fall into pieces if a propagator line is cut at a certain point, anyway the diagrams can be regrouped and the Green's function can be written in terms of a series which contains only

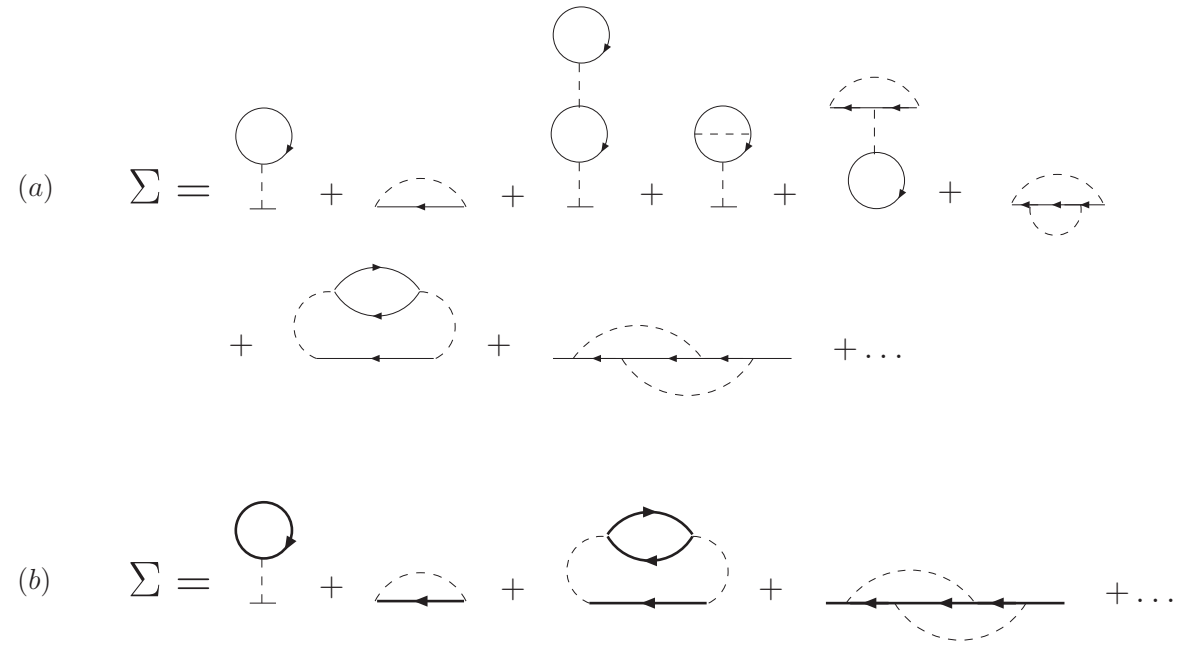

Figure 2.1: Perturbation series for the self-energy in terms of the bare Green's function $G_{0,XX'}$ (a) and in terms of skeleton diagrams with thick propagator lines (b). The thick propagator lines are identified with the exact Green's function $G_{XX'}$.

one-particle irreducible diagrams (i.e. diagrams that don't fall into pieces if a propagator line is cut):

$$G = G_0 + G_0\Sigma G_0 + G_0\Sigma G_0\Sigma G_0 + \dots, \tag{2.20}$$

where Σ is the self energy and contains only *one-particle irreducible* diagrams with amputated external lines. The series of Feynman diagrams that gives the self energy is depicted in Figure 2.1a. The self-energy can be resummed further by taking only the *skeleton diagrams* (i.e. those diagrams that don't contain self-energy sub-diagrams) and substituting the propagator line with a thick line. In practice this correspond to substituting the free fermion Green's function with the exact Green's function. As an example we can look at Figure 2.1, the diagrams 3 and 4, and 5 and 6 in Figure 2.1a, contain self-energy sub-diagrams while the rest are skeleton diagrams, thus in the resummation procedure are resummed in the first and second diagram in Figure 2.1b respectively. The functional $\Phi[G]$ is related to the self-energy by the functional derivative (2.14). In term of Feynman diagrams a functional derivative correspond to cut a propagator line in a closed loop, thus by comparing (2.14) with the diagrams for the self-energy, which to the second order can be represented by the skeleton diagrams in Figure 2.1b, we can derive the infinite perturbation series for the functional $\Phi[G]$ where the amputated external propagator lines are closed to form a loop. Hence, by means of (2.13), for the grand thermodynamic potential we get the series of diagrams

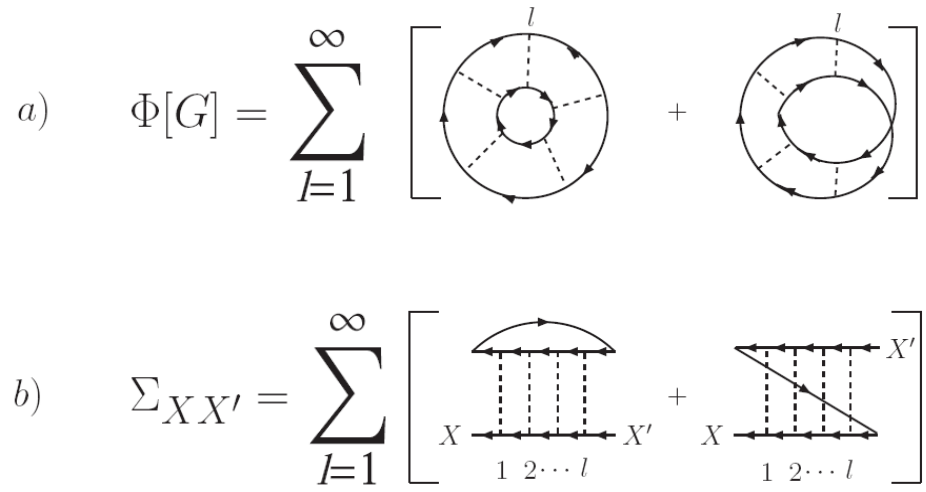

Figure 2.2: Self-consistent ladder approximation for the functional $\Phi[G]$ and for the self-energy Σ

$$\Phi[G] = \left\{ \begin{array}{l} \text{Sum of all vacuum irreducible diagrams} \\ \text{with thick propagator lines identified by } G \end{array} \right\} . \tag{2.21}$$

An approximation for $\Phi[G]$ is obtained by truncating the series, so that an infinite subclass of diagrams is resummed exactly . This kind of approximations are called conserving approximations [48, 49]. The name derives from the fact that, whenever the self-energy Σ can be written as derivative of a functional $\Phi[G]$, the approximation satisfies certain conservation laws if $\Phi[G]$ possess the relative symmetries. Thus if, for instance, the functional $\Phi[G]$ is invariant under the local Gauge transformation $G_{XX'} \rightarrow \exp(i\lambda_X) G_{XX'} \exp(-i\lambda_{X'})$ then the particle number is locally conserved. Furthermore if $\Phi[G]$ is invariant under spatial and time translation, the total momentum and the total energy are conserved respectively. In particular, for Fermi systems conserving approximations satisfy the Luttinger theorem [50] which states that the volume enclosed in the Fermi sphere only depends on the particle density. A suitable approximation that treats two-particle collision and the formation of pairs correctly is a ladder approximation. In this approximation the functional $\Phi[G]$ and his functional derivative $\Sigma_{XX'}$ are expressed by the infinite series of Feynman diagrams depicted in Figure 2.2. The approximation is self-consistent because the propagator lines are identified with the full matrix Green's function.

The one-particle Green's function, which is determined self-consistently in ladder approximation, describes the properties of the single fermions. In the present work we are also interested in the collective modes of the interacting Fermi system which are described by the two-particle Green's function. A generalized two-particle Green's function can be generated by the second functional

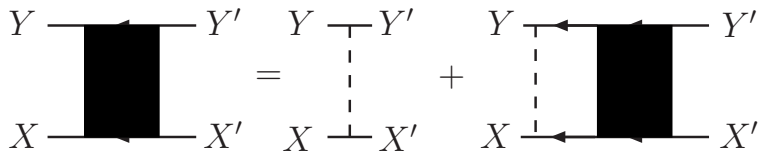

Figure 2.3: Bethe-Salpeter equation for the vertex function in self-consistent ladder approximation

derivative of the partition function

$$\frac{\delta^2 Z[A]}{\delta A_{XX'}\delta A_{YY'}} = Z[A]\langle T[\psi_{X'}\psi_{Y'}\psi_Y^\dagger\psi_X^\dagger]\rangle, \tag{2.22}$$

where the two-particle Green's function is defined by

$$G^{(2)}_{XX',YY'} = \langle T[\psi_X\psi_Y\psi_{Y'}^\dagger\psi_{X'}^\dagger]\rangle. \tag{2.23}$$

Inserting the usual perturbation series for the partition function (2.18) it is possible to obtain a perturbation series of $G^{(2)}_{XX',YY'}$ [51]. The diagrams of the two-particle Green's function can be partially resummed to get

$$G^{(2)}_{XX',Y'Y} = G_{XX'}G_{Y'Y} + \chi_{XX',Y'Y} - \chi_{XX',U'U}\Gamma_{UU',W'W}\chi_{WW',Y'Y}, \tag{2.24}$$

where $\chi_{XX',Y'Y}$ is the pair propagator and is defined by

$$\chi_{XX',YY'} = -G_{XY'}G_{YX'} \tag{2.25}$$

and $\Gamma_{XX',YY'}$ is the vertex function. It is possible to expand $\Gamma_{XX',YY'}$ in terms of an irreducible vertex function, thus we get a series that can be resummed to obtain the integral equation

$$\Gamma_{XX',Y'Y} = \Gamma_{1,XX',Y'Y} - \Gamma_{1,XX',U'U}\chi_{UU',W'W}\Gamma_{WW',Y'Y}. \tag{2.26}$$

Equation (2.26) is also known as Bethe-Salpeter equation. For a normal fluid system the Bethe-Salpeter equation (2.26) is represented in ladder approximation by the Feynman diagrams in figure 2.3.

2.2 Ward identity and Thouless criterion

The symmetries of a system implies relation between Green's functions and vertex function which are known as Ward identities. These identities can be also derived for systems which presents a spontaneously broken symmetry related to a second-order phase transition. In this section we will

derive a Ward identity which involve the variation of the self-energy. We consider the Jacobi matrix of the Legendre transformation from $A_{XX'}$ to $G_{XX'}$. The functional derivative that defines the matrix is related to the second functional derivative of the free energy functional $F[A]$:

$$\frac{\delta G_{XX'}}{\delta A_{YY'}} = \frac{\delta^2 F[A]}{\delta A_{XX'}\delta A_{YY'}}. \tag{2.27}$$

Using the definitions (2.7) and (2.9) for the one-particle Green's function and (2.22) for the two-particles Green's function, the Jacobi matrix can be rewritten in terms of the pair propagator and the vertex function:

$$\frac{\delta G_{XX'}}{\delta A_{YY'}} = -\left[G^{(2)}_{XX',Y'Y} - G_{XX'}G_{Y'Y}\right] = -\left[\chi_{XX',Y'Y} - \chi_{XX',W'W}\Gamma_{WW',U'U}\chi_{UU',Y'Y}\right], \tag{2.28}$$

where in the last equality the relation (2.24) has been used. The inverse Jacobi matrix can be written using the result (2.27) and the identity $\chi - \chi\Gamma\chi = [\chi^{-1} + \Gamma_1]^{-1}$:

$$\frac{\delta A_{XX'}}{\delta G_{YY'}} = \frac{\delta^2 \Omega[G]}{\delta G_{XX'}\delta G_{YY'}} = -\left[\chi_{XX',Y'Y} - \chi_{XX',W'W}\Gamma_{WW',U'U}\chi_{UU',Y'Y}\right]^{-1} = -\left[\chi^{-1}_{XX',Y'Y} + \Gamma_{1,XX',Y'Y}\right]. \tag{2.29}$$

We can now calculate the variation of the self-energy with respect to $G_{XX'}$. In order to do that we need first to calculate the variation of the functional $\Phi[G]$. Using the equation (2.13) we can write

$$\frac{\delta\Phi[G]}{\delta G_{XX'}} = \left(G^{-1}_{XX'} - G^{-1}_{0,XX'}\right) - \frac{\delta\Omega[G]}{\delta G_{XX'}}. \tag{2.30}$$

Recalling the definition (2.14) of the self energy and using the result (2.29) we obtain the first variation of the self-energy $\Sigma_{XX'}$

$$\frac{\delta\Sigma_{XX'}}{\delta G_{YY'}} = -\chi^{-1}_{XX'Y'Y} + \left(\chi^{-1}_{XX'Y'Y} + \Gamma_{1,XX',Y'Y}\right) = \Gamma_{1,XX',Y'Y}. \tag{2.31}$$

Next we consider a transformation which depend on a continuous parameter λ. We assume that the variation of the Green's function $\delta_\lambda G_{XX'}$ and of the external parameter $\delta_\lambda A_{XX'}$ can be determined explicitly. From the relation (2.29) we can get the variation of the inverse external parameter with respect to λ:

$$\delta_\lambda A^{-1}_{XX'} = -\left[\chi^{-1}_{XX',Y'Y} + \Gamma_{1,XX',Y'Y}\right]\delta_\lambda G_{YY'}. \tag{2.32}$$

The previous relation can be used to get a Ward identity correlated to the existence of massless Goldstone modes due to a spontaneously broken symmetry. Using the identity $\chi^{-1} + \Gamma_1 = \chi^{-1}\Gamma^{-1}\Gamma_1$ we can rewrite (2.32) to get

$$-\Gamma^{-1}_{XX',Y'Y}\Gamma_{1,YY',U'U}\delta_\lambda G_{UU'} = \chi_{XX',Y'Y}\delta_\lambda A_{YY'}. \tag{2.33}$$

Inserting result (2.31) into (2.33) we obtain a Ward identity for the self-energy $\delta_\lambda \Sigma_{XX'}$:

$$-\Gamma^{-1}_{XX',Y'Y}\delta_\lambda \Sigma_{YY'} = \chi_{XX',Y'Y}\delta_\lambda A_{YY'}. \tag{2.34}$$

Let's now consider a continuous transformation which is related to a global change of phase of the fermionic fields

$$\psi_\sigma(\mathbf{r}) \to e^{i\lambda}\psi_\sigma(\mathbf{r}), \quad \psi^\dagger_\sigma(\mathbf{r}) \to e^{-i\lambda}\psi^\dagger_\sigma(\mathbf{r}), \tag{2.35}$$

the system is invariant under this transformation hence the variation $\delta_\lambda \Omega[G]$ vanishes for all G, thus we can argue, by means of the definition (2.12), that $\delta_\lambda A_{XX'} = -\delta[\delta_\lambda \Omega[G]]/\delta G_{X'X} = 0$. Finally we obtain the Ward identity

$$\Gamma^{-1}_{XX',Y'Y}\delta_\lambda \Sigma_{YY'} = 0. \tag{2.36}$$

This symmetry is broken in the superfluid phase of the system where the average $\langle \mathrm{T}[\psi_X \psi_{X'}]\rangle$ assumes a finite value. In this phase the order parameter $\Delta \sim \langle \mathrm{T}[\psi_X \psi_{X'}]\rangle$ is transformed by (2.35) as $\Delta \to e^{2i\lambda}\Delta$. Clearly the thermodynamic potentials must remain invariant under a global change of phase both in the normal and in the superfluid state, thus the Ward identity (2.36) must be always verified. The previous identity is trivially satisfied if the system is in his disordered phase in fact, above T_c the order parameter of the system vanishes and hence the variation $\delta_\lambda \Sigma_{XX'}(\Delta)$ is always zero. Below the critical temperature $\delta_\lambda \Sigma_{XX'}(\Delta) \neq 0$, thus, in order to satisfy the identity (2.36), the inverse of the vertex function must have a zero eigenvalue, this corresponds to a pole in the vertex function which is related to physical phenomena as sound, pair formation, superconductivity and is an evidence of the existence of massless Goldstone modes of a second order phase transition. The consequence of the identity (2.36) that the vertex function has a pole below the critical temperature T_c is known as Thouless criterion for superconductivity [52].

2.3 De Dominicis and Martin formalism

2.3.1 Introduction

De Dominicis and Martin [47] went beyond the theory developed by Luttinger and Ward: they showed that the dynamical and thermodynamical properties of an interacting quantum system may be expressed in terms of renormalized propagators and vertices. Their formulation is sufficiently general to describe Bose or Fermi systems with several component either in the normal and in the superfluid state. The formalism developed by De Dominicis and Martin is particularly well suited to describe the crossover problem because it deals with the one-particle Green's function, which describes the properties of the single fermions , and, trough the two-particle Green's function, with the vertex function, which describes the bosonic properties of the bound fermions. They introduce up to four external fields that couple with products of the field operators and then perform up to four Legendre transformation. For normal and superfluid fermionic systems, which is the case we are interested in, only

two external fields are needed which couple to even products of the fields operators. The conjugate variables are the one-particle Green's function and the two-particles Green's function.

2.3.2 Formalism

We follow what has been done in section 2.1.2. First we make a Legendre transformation from the external field to the Green's function to obtain a functional which generates the one-particle Green's function. Next we proceed with a second Legendre Transformation by introducing an external field which couples to second order product of the field operators ψ_X and $\psi_X^\dagger$. The resulting functional is a function of both the one-particle Green's function and two-particles Green's function, the latter being related to the vertex function by the relation [47]:

$$\begin{aligned} G_{2,X_1X_2X_3X_4} =& G_{X_1X_3}G_{X_2X_4} - G_{X_1X_4}G_{X_2X_3} - G_{X_1X_2}G_{X_3X_4} \\ & - G_{X_1Y_1}G_{X_2Y_2}\Gamma_{Y_1Y_2Y_3Y_4}G_{Y_3X_3}G_{Y_4X_4}. \end{aligned} \tag{2.37}$$

The two-particles Green's function can be thus expressed in terms of products of the one-particle Green's function and the connected part of the two-particles Green's function. Both $G_2 = G_{2,X_1X_2X_3X_4}$ and the vertex function $\Gamma = \Gamma_{X_1X_2X_3X_4}$ have four arguments which are indicated by the four formal indices X_i. The last term of equation (2.37) represent the connected part of the two-particles Green's function and describes the correlation effects. The vertex function $\Gamma_{X_1X_2X_3X_4}$ can be obtained from this term by complete amputation of the four external propagator lines and is a more convenient variable to deal with.

The natural functional for the bare coupling constants is the logarithm of the partition function, while the functional for the renormalized variables turns out to be:

$$\begin{aligned} F^{(2)}[G,\Gamma] =& \tfrac{1}{2}\mathrm{Tr}\{-\ln G + [(-i\hbar\omega_n)G - 1]\} \\ & + \tfrac{1}{2}\mathrm{Tr}\{\ln[1 - \tfrac{1}{2}\bar{\Gamma}] + \tfrac{1}{2}\bar{\Gamma} + \tfrac{1}{2}[\tfrac{1}{2}\bar{\Gamma}]^2 - (1/4!)[\bar{\Gamma}]^2\} \\ & + \mathcal{K}^{(2)}[G,\Gamma]. \end{aligned} \tag{2.38}$$

The connected part of the two-particle Green's function appears explicitly in the functional (2.38) and is expressed with the help of the modified vertex function $\bar{\Gamma}$ defined by

$$\bar{\Gamma}_{X_1X_2X_3X_4} = G^{1/2}_{X_1Y_1}G^{1/2}_{X_2Y_2}\Gamma_{Y_1Y_2Y_3Y_4}G^{1/2}_{Y_3X_3}G^{1/2}_{Y_4X_4}, \tag{2.39}$$

where the four external propagator lines are amputated only half way. For a proper definition of the second trace and the related matrix products the four indices of the modified vertex function must be grouped into pairs according to $\bar{\Gamma} = \bar{\Gamma}_{(X_1X_2)(X_3X_4)}$. The last term in (2.38), the functional $\mathcal{K}^{(2)}[G,\Gamma]$, is defined with the infinite perturbation series of 2-line irreducible Feynman diagrams depicted in Figure 2.4, where the propagator lines and the vertices are dressed and identified by the one-particle Green's function G and by the vertex function Γ, respectively.

$\mathcal{K}^{(2)}[G,\Gamma] =$ 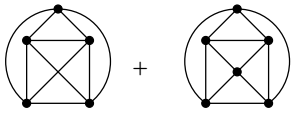 $+ \cdots$

Figure 2.4: The functional $\mathcal{K}^{(2)}[G,\Gamma]$ is the sum of all 2-line irreducible diagrams. The propagator lines and the vertices (full circles) are dressed and identified with G and Γ, respectively.

A stationary principle for the functional $F^{(2)}[G,\Gamma]$, subject to the constraint that all conserved quantities are kept constant, provides a fully renormalized description of the system. The numerical value of the functional at its stationary point is the dimensionless entropy of the system $S/k_B = F^{(2)}$. In the original work of De Dominicis and Martin the maximum of the entropy is found, under the constraint of given values of the internal energy and particles number, starting from the functional:

$$W[G,\Gamma] = F^{(2)}[G,\Gamma] - \lambda_U U[G,\Gamma] - \lambda_N N[G], \tag{2.40}$$

where λ_U and λ_N are the two Lagrange parameters for the constraints, while in the present work the grand thermodynamic potential will be equivalently used:

$$\Omega[G,\Gamma] = U[G,\Gamma] - T\,S[G,\Gamma] - \mu\,N[G], \tag{2.41}$$

here the Lagrange parameters are the temperature T and the chemical potential μ. Both the functionals (2.40) and (2.41) must be stationary under small variation of the one-particle Green's function and the vertex function. The one-particle Green's function G and the vertex function Γ are thus uniquely determined by the stationarity criteria

$$\delta\Omega[G,\Gamma]/\delta G = 0 \;\text{ and }\; \delta\Omega[G,\Gamma]/\delta\Gamma = 0. \tag{2.42}$$

At the beginning of the paragraph it was pointed out that De Dominicis and Martin go beyond the theory of Luttinger and Ward, now it is important to stress in which sense the theory described in this section is an extension of the one described in section 2.1.

Within the formalism of Luttinger and Ward a Legendre transformation is performed which defines a functional of the one-particle Green's function. The saddle point value of this functional can be then identified with the grand canonical potential. The Green's function is obtained by the stationary condition (2.15), while the vertex function has to be derived by using a further equation, i.e. the Bethe-Salpeter equation, which is not obtained by a stationarity condition of the functional. In the theory of De Dominicis and Martin a second Legendre transformation from the bare two particle interaction to the two-particle Green's function leads to a functional associated with the physical entropy which is a functional of the one-particle Green's function and, through the two-particle Green's function, of the vertex function. From the entropy (2.38) we can then obtain the grand canonical potential as a function

of the Green's function and the vertex function (see equation (2.41)). The vertex function is in this case obtained from the second of the stationarity conditions (2.42). The two formalism are related to each other by a Legendre transformation which can be interpreted as a resummation procedure that renormalizes the vertex.

We can now compare the two functionals (2.13) and (2.38). The first trace in the two functionals (2.13) and (2.38) describes the single particle contribution to the grand canonical potential and to the entropy respectively. A comparison between the two terms shows that the two traces are identical. The second trace in (2.38) represent, together with the functional $\mathcal{K}^{(2)}[G,\Gamma]$, the inverted perturbation series of the ladder diagrams. It includes both the particle-particle and particle-hole interaction which describe the formation of pairs and the screening of the interaction. Keeping only the particle-particle contribution in the second trace of (2.38) and putting the functional $\mathcal{K}^{(2)}[G,\Gamma]$ to zero, it is possible to recover the functional $\Phi[G]$ obtained within the formalism of Luttinger and Ward.

The equivalence of the two formalisms in this approximation can be verified by getting the vertex function Γ from the second stationarity condition in (2.42) and inserting the resulting function in the grand-thermodynamic potential obtained from the entropy functional through the relation (2.41). The resulting functional coincides with the grand-potential of the Luttinger and Ward formalism.

Chapter 3

Solution of the self-consistent equations

The results described on a general level in Chapter 2, can be successfully applied to a fermionic system with an attractive interaction.

In the following we will focus on a Fermi system where the attractive interaction can be tuned to explore the interplay between pairing phenomena and superfluidity when the system goes from weak to strong coupling.

By solving the self-consistent equations for the Green's and the vertex function we can directly calculate parameter of the system like the critical temperature T_c, the order parameter of the superfluid transition Δ and the chemical potential μ over the whole crossover. The numerical results will be compared in the two limits with the BCS-theory and the theory of weakly interacting Bose gases.

3.1 Derivation of the Green's and the vertex functions within the formalism of Luttinger and Ward

The interacting Fermi system, in second quantization representation is described by the Hamiltonian:

$$\begin{aligned}\hat{H} = &\int d^d r \sum_{\sigma} \frac{\hbar^2}{2m} [\nabla \psi^{\dagger}_{\sigma}(\mathbf{r})][\nabla \psi_{\sigma}(\mathbf{r})] \\ &+ \frac{1}{2} \int d^d r \int d^d r' \sum_{\sigma\sigma'} V_{\sigma\sigma'}(\mathbf{r}-\mathbf{r}') \psi^{\dagger}_{\sigma}(\mathbf{r}) \psi^{\dagger}_{\sigma'}(\mathbf{r}') \psi_{\sigma'}(\mathbf{r}') \psi_{\sigma}(\mathbf{r}),\end{aligned} \tag{3.1}$$

where $\psi^{\dagger}_{\sigma}(\mathbf{r})$ and $\psi_{\sigma}(\mathbf{r})$ are the fermionic creation and destruction operators, σ labels the internal degree of freedom such as , for example, two different hyperfine states. We assume that the range of the resonant interaction is much smaller that the background scattering length a_{bg} and the Fermi wavelength λ_F. In this approximation we take the range of the effective interaction to zero so that the interaction potential can be replaced by a delta potential $V(\mathbf{r}) \sim \delta(\mathbf{r})$ between fermions of opposite

spin

$$V(\mathbf{r}-\mathbf{r}') = g_0\delta(\mathbf{r}-\mathbf{r}'), \tag{3.2}$$

here g_0 is a parameter corresponding to the bare coupling strength. For dimensions $d \geq 2$ the delta potential interaction causes an ultraviolet divergence in the Feynman diagrams, thus a renormalization of the coupling strength will be required.

The quantum field-theoretic description of an interacting fermionic system that undergoes a superfluid transition can be described, at finite temperature T by the Matsubara formalism which introduces an imaginary time variable τ defined on the interval $0 \leq \tau \leq \hbar\beta$ where $\beta = 1/k_B T$. In this formalism we can define the following averages of the fermionic fields

$$\langle \mathrm{T}[\psi_\sigma(\mathbf{r},\tau)\psi^\dagger_{\sigma'}(\mathbf{r}',\tau')]\rangle = \delta_{\sigma\sigma'}\mathcal{G}(\mathbf{r}-\mathbf{r}',\tau-\tau') \tag{3.3}$$

and

$$\langle \mathrm{T}[\psi_\sigma(\mathbf{r},\tau)\psi_{\sigma'}(\mathbf{r}',\tau')]\rangle = \varepsilon_{\sigma\sigma'}\mathcal{F}(\mathbf{r}-\mathbf{r}',\tau-\tau'), \tag{3.4}$$

where $\varepsilon_{\sigma\sigma'}$ is the spin function of a fermion pair with zero spin and $\delta_{\sigma\sigma'}$ is the Kronecker delta. The equation (3.3) represent the normal Matsubara Green's function while (3.4) is also known as the anomalous Matsubara Green's function. The latter is proportional to the order parameter of the superfluid transition and vanish when the system is in its disordered phase. The normal and anomalous Green's function (3.3) and (3.4) can be written in a more compact way using Nambu's notation [53]. In this notation a new index α is introduced which will distinguish the fermion field operators between annihilation and creation operators:

$$(\Phi^\alpha_\sigma) = \begin{pmatrix} \psi_\sigma \\ \psi^\dagger_\sigma \end{pmatrix}, \qquad \left(\bar{\Phi}^\alpha_\sigma\right) = (\psi^+_\sigma, \psi_\sigma). \tag{3.5}$$

The average of the fields (3.5) defines a Green's function which includes both the normal and the anomalous Green's functions

$$\langle \mathrm{T}[\Phi^\alpha_\sigma(\mathbf{r},\tau)\bar{\Phi}^{\alpha'}_{\sigma'}(\mathbf{r}',\tau')]\rangle = G^{\alpha\alpha'}_{\sigma\sigma'}(\mathbf{r}-\mathbf{r}',\tau-\tau'). \tag{3.6}$$

Thus the Green's function will become a matrix whose off-diagonal elements are the anomalous Green's functions

$$G^{\alpha\alpha'}_{\sigma\sigma'}(\mathbf{r}-\mathbf{r}',\tau-\tau') = \begin{pmatrix} \delta_{\sigma\sigma'}\mathcal{G}(\mathbf{r}-\mathbf{r}',\tau-\tau') & \varepsilon_{\sigma\sigma'}\mathcal{F}(\mathbf{r}-\mathbf{r}',\tau-\tau') \\ -\varepsilon_{\sigma\sigma'}\mathcal{F}^*(\mathbf{r}'-\mathbf{r},\tau-\tau') & -\delta_{\sigma\sigma'}\mathcal{G}(\mathbf{r}'-\mathbf{r},\tau'-\tau) \end{pmatrix}. \tag{3.7}$$

In the Nambu representation the propagator lines in the Feynman diagrams are undirected because the matrix Green's function includes both direction. Moreover, this representation allows the introduction of a symmetric interaction vertex which is invariant under permutation of the four external lines and

can be identified with the bare interaction vertex Γ_0. Since the interaction (3.2) is spin independent, the spin indices don't need to be treated explicitly. Hence the matrix structure due to the spin indices can be simplified and the 4×4 matrix (3.7) can be reduced to a 2×2 matrix

$$G(\mathbf{r}-\mathbf{r}', \tau-\tau') = \begin{pmatrix} \mathcal{G}(\mathbf{r}-\mathbf{r}', \tau-\tau') & \mathcal{F}(\mathbf{r}-\mathbf{r}', \tau-\tau') \\ -\mathcal{F}^*(\mathbf{r}'-\mathbf{r}, \tau-\tau') & -\mathcal{G}(\mathbf{r}'-\mathbf{r}, \tau'-\tau) \end{pmatrix}. \tag{3.8}$$

The spin degrees of freedom will be taken into account multiplying by a factor 2 each closed fermion loop in the Feynman diagrams.

For a homogeneous system we can define the Fourier transformation for the matrix Green's function and the matrix self-energy

$$G_{\alpha,\alpha'}(\mathbf{r}, \tau) = \frac{1}{\beta} \int \frac{d^3k}{(2\pi)^3} \sum_{\omega_n} e^{i(\mathbf{k}\cdot\mathbf{r}-\omega_n\tau)} G_{\alpha,\alpha'}(\mathbf{k}, \omega_n), \tag{3.9}$$

where $\omega_n = \pi(2n+1)/\hbar\beta$ are the fermionic Matsubara frequencies. Defining the inverse free fermions matrix Green's function

$$G_0^{-1}(\mathbf{k}, \omega_n) = \begin{pmatrix} -i\hbar\omega_n + (\varepsilon_{\mathbf{k}} - \mu) & 0 \\ 0 & -i\hbar\omega_n - (\varepsilon_{\mathbf{k}} - \mu) \end{pmatrix} \tag{3.10}$$

we can write the Dyson equation obtained from the stationarity condition (2.15) as a function of the momentum and the Matsubara frequencies:

$$G^{-1}_{\alpha\alpha'}(\mathbf{k}, \omega_n) = G^{-1}_{0,\alpha\alpha'}(\mathbf{k}, \omega_n) - \Sigma_{\alpha\alpha'}(\mathbf{k}, \omega_n), \tag{3.11}$$

where, according to (2.14), the self-energy $\Sigma_{\alpha\alpha'}(\mathbf{k}, \omega_n)$ is defined by the functional derivative

$$\Sigma_{\alpha\alpha'}(\mathbf{k}, \omega_n) = -\frac{1}{\beta V} \frac{\delta\Phi[G]}{\delta G_{\alpha'\alpha}}, \tag{3.12}$$

here the factor $\frac{1}{\beta V}$ is the correct normalization factor in Fourier space.

The interaction term in the Hamiltonian (3.1) implies that the equation of motion involves the two-particles Green's function. A more suitable variable to deal with is the the vertex function which can be expressed by the Bethe-Salpeter equation (2.26) in terms of the irreducible vertex function Γ_1. The irreducible vertex function is also represented by an infinite series of irreducible diagrams thus an approximation is needed. To the lowest order it is possible to replace Γ_1 by the bare interaction vertex Γ_0 which can be identified with the interaction strength g_0. Within this approximation and exploiting the local nature of the interaction, the integral equation (2.26) becomes, after a partial diagonalization in Fourier space [18], a simple matrix equation. For dimensions $d \geq 2$ the Bethe-Salpeter equation

can be written as:

$$\Gamma^{-1}_{\alpha_1\alpha'_1,\alpha'_2\alpha_2}(\mathbf{K},\Omega_n) = \Gamma^{-1}_{0,\alpha_1\alpha'_1,\alpha'_2\alpha_2} + \chi_{\alpha_1\alpha'_1,\alpha'_2\alpha_2}(\mathbf{K},\Omega_n) \tag{3.13}$$

where $\chi_{\alpha_1\alpha'_1,\alpha'_2\alpha_2}$ is the pair propagator defined in (2.25) and can be expressed in terms of the matrix Green's function $G_{\alpha\alpha'}(\mathbf{k},\omega_n)$

$$\chi_{\alpha_1\alpha'_1,\alpha'_2\alpha_2}(\mathbf{K},\Omega_n) = \int \frac{d^3k}{(2\pi)^3}\frac{1}{\beta}\sum_{\omega_n} G_{\alpha_1\alpha_2}(\mathbf{K}-\mathbf{k},\Omega_n-\omega_n)G_{\alpha'_1\alpha'_2}(\mathbf{k},\omega_n). \tag{3.14}$$

The local interaction with the delta potential implies an ultraviolet divergence in the pair propagator thus we need to regularize it by redefining the interaction strength. Consequently, the tensors $\Gamma^{-1}_{\alpha_1\alpha'_1,\alpha'_2\alpha_2}(\mathbf{K},\Omega_n)$ and $\chi_{\alpha_1\alpha'_1,\alpha'_2\alpha_2}(\mathbf{K},\Omega_n)$ reduce into 2×2 matrices. The simplification arises from the fact that only part of the pair propagator is ultraviolet divergent. In particular the contribution of the particle holes excitations to the pair propagator $\chi_{ph} = \chi_{11,11}$ together with the component of $\chi_{\alpha_1\alpha'_1,\alpha'_2\alpha_2}(\mathbf{K},\Omega_n)$ which involve the anomalous Green's functions are finite while the particle-particle contribution, which is given by the component $\chi_{12,12}$ is ultraviolet divergent. To renormalize the divergence we define the interaction parameter g as follows

$$\frac{1}{g} = \frac{1}{g_0} + \int \frac{d^dk}{(2\pi)^d}\frac{m}{\hbar^2\mathbf{k}^2}. \tag{3.15}$$

The interaction (3.2) is the zero limit of a potential which implies only low-energy s-wave scattering, this implies that the scattering amplitude do not depend on the angle so g is a constant parameter. In $d = 3$ the scattering amplitude g is connected to the scattering length by the simple relation

$$g = \frac{4\pi\hbar^2}{m}\cdot a. \tag{3.16}$$

We now look at the renormalized interaction parameter g, by introducing an ultraviolet cutoff Λ, the integral in (3.15) becomes

$$\int_{|\mathbf{k}|<\Lambda} \frac{d^dk}{(2\pi)^d}\frac{m}{\hbar^2\mathbf{k}^2} = \frac{\Omega_d}{(2\pi)^d}\frac{m}{\hbar^2}\frac{\Lambda^{d-2}}{d-2}, \tag{3.17}$$

which is, in the three-dimensional case, ultraviolet divergent in the limit $\Lambda\to\infty$. Since the scattering amplitude g is kept constant, the bare interaction vertex g_0 must be taken to zero in the limit where the cut-off Λ diverges, this implies that the diagrams which involve the finite contribution to the pair-propagator will vanish because of $g_0\to -0$. The only contribution that remains is the particle-particle contribution which is renormalized by (3.15) and generates the ladder diagrams depicted in Figure 2.3. This argument is also used by Strinati and Pieri [54] but it is not clear weather these vanishing terms do not contribute after the re-summation of infinitely many terms of the perturbation series. In the following we will anyway concentrate only on the particle-particle contribution. If we now look at the particle-particle contribution to the pair propagator, we note that the four tensor indices

are pairwise identical which means that two of them are redundant. The tensor $\chi_{\alpha_1\alpha_1',\alpha_2'\alpha_2}$ can be thus described through a matrix defined by only two indices. The renormalization of the remaining term of the interaction vertex can be performed as follows: in the pair propagator we separate the ultraviolet divergence by introducing the renormalized propagator $M_{\alpha\alpha'}(\mathbf{K},\Omega_n)$

$$\chi_{\alpha\alpha'}(\mathbf{K},\Omega_n) = M_{\alpha\alpha'}(\mathbf{K},\Omega_n) + \int \frac{d^dk}{(2\pi)^d}\frac{m}{\hbar^2\mathbf{k}^2}.$$

Inserting the expression (3.14) in the Bethe-Salpeter equation (3.13) and taking the ultraviolet divergence to the renormalized coupling strength (3.15), we obtain the renormalized Bethe-Salpeter equation

$$\Gamma^{-1}_{\alpha\alpha'}(\mathbf{K},\Omega_n) = g^{-1}\delta_{\alpha\alpha'} + M_{\alpha\alpha'}(\mathbf{K},\Omega_n), \tag{3.18}$$

where

$$M_{\alpha\alpha'}(\mathbf{K},\Omega_n) = \int \frac{d^3k}{(2\pi)^3}\left[\frac{1}{\beta}\sum_{\omega_n} G_{\alpha\alpha'}(\mathbf{K}-\mathbf{k},\Omega_n-\omega_n)G_{\alpha\alpha'}(\mathbf{k},\omega_n) - \frac{m}{\hbar\mathbf{k}^2}\delta_{\alpha\alpha'}\right] \tag{3.19}$$

is the renormalized pair propagator. Performing a Fourier back transformation we obtain the regularized pair propagator in real space and imaginary time

$$M_{\alpha\alpha'}(\mathbf{r},\tau) = [G_{\alpha\alpha'}(\mathbf{r},\tau)]^2 - C\,\delta_{\alpha\alpha'}\delta(\mathbf{r})\delta_B(\tau/\hbar), \tag{3.20}$$

where the divergence of the first term is canceled by the constant C defined by the integral (3.17) which is infinite in the limit $\Lambda \to \infty$. The function $\delta_B(\tau/\hbar)$ is the Bosonic delta function defined by

$$\delta_B(\tau/\hbar) = \frac{1}{\beta}\sum_{\Omega_n} e^{-i\Omega_n\tau} = \sum_n \delta(\tau/\hbar + n\beta), \tag{3.21}$$

which is periodic in the variable τ. Once the renormalized pair-propagator is known, it is possible to calculate the functional $\Phi[G]$ defined by the ladder approximation in Figure 2.2 [18]

$$\Phi[G] = -\beta L^d\; g|F(\mathbf{r}=0,\tau=0)|^2 - \frac{1}{2}\beta L^d \int \frac{d^dK}{(2\pi)^d}\frac{1}{\beta}\sum_{\Omega_n}\mathrm{Tr}\left\{\ln\left[1+g_0\chi\right]\right\}. \tag{3.22}$$

An analytical expression for the self-energy can be obtained by the functional derivative of (3.22) which gives

$$\Sigma_{\alpha\alpha'}(\mathbf{r},\tau) = \Sigma_{1,\alpha\alpha'}\delta(\mathbf{r})\delta_F(\tau/\hbar) + G_{\alpha\alpha'}(-\mathbf{r},-\tau)\Gamma_{\alpha\alpha'}(\mathbf{r},\tau). \tag{3.23}$$

The second term of equation (3.23) includes the particle-particle contribution to the self-energy while $\Sigma_{1,\alpha\alpha'}$ is the non-diagonal part of the Fock term, which involves the anomalous propagator and is given

by

$$\Sigma_1 = \begin{pmatrix} 0 & g_0 F(\mathbf{r}=0,\tau=0) \\ g_0 F^*(\mathbf{r}=0,\tau=0) & 0 \end{pmatrix}. \tag{3.24}$$

In the first term of equation (3.23), $\delta_F(\tau/\hbar)$ is the fermionic delta function defined by

$$\delta_F(\tau/\hbar) = \frac{1}{\beta}\sum_{\omega_n} e^{-i\omega_n\tau} = \sum_n (-1)^n \delta(\tau/\hbar + n\beta), \tag{3.25}$$

which is anti-periodic in the variable τ.

The non-diagonal terms in the matrix (3.24) define the order parameter

$$\Delta = g\mathcal{F}(\mathbf{r}=0,\tau=0) = g\int \frac{d^dk}{(2\pi)^d}\frac{1}{\beta}\sum_{\omega_n}\mathcal{F}(\mathbf{k},\omega_n), \tag{3.26}$$

which is expected to be nonzero for a superfluid fermion system. For a zero range interaction the integral in equation (3.26) results to be also ultraviolet divergent, thus the order parameter needs to be renormalized too. Using (3.15) we can replace the interaction parameter g_0 by the scattering amplitude obtaining

$$\Delta = g\int \frac{d^dk}{(2\pi)^d}\left[\mathcal{F}(\mathbf{k},\tau=0) + \Delta\frac{m}{\hbar^2\mathbf{k}^2}\right]. \tag{3.27}$$

The equations (3.11), (3.23) and (3.18) together with (3.20) form the set of self-consistent equations

$$\boxed{\begin{aligned} G^{-1}_{\alpha\alpha'}(\mathbf{k},\omega_n) &= G^{-1}_{0,\alpha\alpha'}(\mathbf{k},\omega_n) - \Sigma_{\alpha\alpha'}(\mathbf{k},\omega_n), \\ \Sigma_{\alpha\alpha'}(\mathbf{r},\tau) &= \Sigma_{1,\alpha\alpha'}\delta(\mathbf{r})\,\delta_F(\tau/\hbar) + G_{\alpha\alpha'}(-\mathbf{r},-\tau)\,\Gamma_{\alpha\alpha'}(\mathbf{r},\tau), \\ \Gamma^{-1}_{\alpha\alpha'}(\mathbf{K},\Omega_n) &= g^{-1}\delta_{\alpha\alpha'} + M_{\alpha\alpha'}(\mathbf{K},\Omega_n), \\ M_{\alpha\alpha'}(\mathbf{r},\tau) &= [G_{\alpha\alpha'}(\mathbf{r},\tau)]^2 - C\,\delta_{\alpha\alpha'}\delta(\mathbf{r})\delta_B(\tau/\hbar). \end{aligned}} \tag{3.28}$$

which can be numerically solved to get the full matrix Green's function $G_{\alpha\alpha'}(\mathbf{k},\omega_n)$ and the vertex function $\Gamma_{\alpha\alpha'}(\mathbf{K},\Omega_n)$.

3.2 Validity of the Ward identity in the self-consistent approximation

In Chapter 2 the Ward identity (2.36) was derived for exact theory and we said that it is true up to all the orders in perturbation theory. However, in the present theory it is only an approximation due to the fact that the exact functional which enters either in the Luttinger and Ward theory or in the theory of De Dominicis and Martin is truncated. A consequence of this truncation is that the functional derived within this approximation will not obey the Ward identity. The function $\Gamma_{\alpha\alpha'}(\mathbf{K},\Omega_n)$ obtained from the self-consistent equations is equivalent to the vertex function Γ defined by the Bethe-Salpeter equation depicted in Figure 3.1, where the irreducible vertex function Γ_1 defined by the

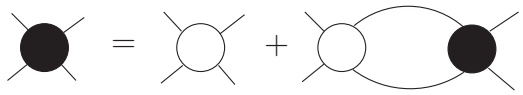

Figure 3.1: Bethe-Salpeter equation in the lowest order approximation. The irreducible vertex function Γ_1 is replaced by the bare vertex function Γ_0

functional derivative (2.31) is replaced, in the lowest order approximation, by the bare vertex Γ_0 [18]. In this approximation the vertex Γ_0 is given by the second functional derivative of the Hartree-Fock functional $\Phi_{HF}[G]$, which is equivalent to the functional derivative of the Hartree-Fock self-energy. Thus, the Ward identity (2.36) in this self-consistent approximation will involve the variation $\delta_\lambda \Sigma_{HF}$, where Σ_{HF} does not depend either on the Fermi wave vector or on the fermionic Matsubara frequencies. The off-diagonal terms of Σ_{HF} are given by $\Sigma_{1,\alpha\alpha'}$ defined in (3.24) which is the order parameter $(\Delta_\alpha) = (\Delta, \Delta^*)$. However, to derive the self-consistent equations (6.5)- (6.8) we used a self-consistent ladder approximation for the functional $\Phi[G]$ hence in equation (2.34) the variation $\delta_\lambda A_{HF}$ does not vanish. If we now compare the variation of the functional $\delta\Omega[G]/\delta G$ in self-consistent ladder approximation and in Hartree-Fock approximation using the definitions (2.12) and (2.15), we can estimate how large is the parameter A_{HF}

$$A_{HF} = \Sigma - \Sigma_{HF}. \tag{3.29}$$

The variation δ_λ is related to a global change of phase, thus the variation $\delta_\lambda A_{HF}$ possesses only the off-diagonal elements. From the definition (3.23) for the self-energy we note that the first term $\Sigma_{1,\alpha\alpha'}$, whose off-diagonal components are proportional to Δ, is canceled by the off-diagonal part of the Hartree-Fock self-energy Σ_{HF}. The leading off-diagonal term of the external parameter A_{HF} is thus given, according to (3.29), by the product $G(-\mathbf{r}, -\tau)\Gamma(\mathbf{r}, \tau)$. Now, if we look at the Dyson equation (3.11), we see that the leading off-diagonal term of the Green's function is included in the self-energy, hence it is of the order $O(|\Delta|)$. This implies that the renormalized pair propagator (3.20) and the vertex function defined by the Bethe-Salpeter equation (3.18) have off-diagonal terms which are proportional to $|\Delta|^2$. Finally, we can say that the off-diagonal terms of $G \cdot \Gamma$ are of the order $O(|\Delta|^3)$. Thus close to T_c, where the order parameter is exponentially small the variation $\delta_\lambda A_{HF} = O(|\Delta|^3)$. Finally the Ward identity in our self-consistent approximation can be written in the following way:

$$\Gamma^{-1}_{\alpha\alpha'}(\mathbf{K} = \mathbf{0}, \Omega_n = 0)\Delta_{\alpha'} = O\left(|\Delta|^3\right). \tag{3.30}$$

As a consequence of the violation of the Ward identity (3.30), the present theory does not have a collective mode whose energy vanishes in the long wavelength limit, i.e. it violates the Thouless criterion. For $T = T_c$ the vertex function is diagonal and both the eigenvalues are zero. In this case the Thouless criterion is valid. The fact that the theory does not satisfy the Goldstone theorem for

continuous symmetries is a general problem of conserving approximations based on the Luttinger and Ward formalism. This fact has already been pointed out by Hohenberg and Martin [55] for superfluid Bose systems where it is known as violation of the Hugenholtz-Pines theorem.

3.3 Weak coupling limit

In the regime of weak couplings the s-wave scattering length a is small, consiquently the bare vertex function Γ_0, which is represented in Figure 3.1 by a open circle is small. Thus a correct description of the system is given by the lowest order approximation where we replace the vertex function by the bare one which, in the limit $a \to 0$, is given by

$$\Gamma(\mathbf{K}, \Omega_n) = \frac{4\pi\hbar^2}{m} \cdot a. \tag{3.31}$$

Expression (3.31) corresponds to the scattering amplitude of low-energy s-wave scattering. If we retain the Hartree-Fock terms only, the self-energy Σ is then given by

$$\Sigma_{HF} = \begin{pmatrix} \Gamma_{HF} G(\mathbf{r} = \mathbf{0}, \tau = -0) & \Delta \\ \Delta^* & -\Gamma_{HF} G(\mathbf{r} = \mathbf{0}, \tau = -0) \end{pmatrix} = \begin{pmatrix} -\frac{2\pi\hbar^2}{m} a \cdot n_F & \Delta \\ \Delta^* & \frac{2\pi\hbar^2}{m} a \cdot n_F \end{pmatrix} \tag{3.32}$$

to obtain the last identity we made use of the density equation

$$n_F = -2\mathcal{G}(\mathbf{r} = \mathbf{0}, \tau = -0). \tag{3.33}$$

From the self-energy Σ_{HF}, using the Dyson equation, the Hartree-Fock equation for the matrix Green's function can be obtained, which turns out to be the Gorkov equation for the normal and anomalous Green's functions:

$$G_{HF}^{-1}(\mathbf{k}, \omega_n) = G_0^{-1}(\mathbf{k}, \omega_n) - \Sigma_{HF} = \begin{pmatrix} -i\hbar\omega_n + (\bar{\varepsilon}_k - \mu) & -\Delta \\ -\Delta^* & -i\hbar\omega_n - (\bar{\varepsilon}_k - \mu) \end{pmatrix}, \tag{3.34}$$

where $\bar{\varepsilon}_k$ is the Hartree-Fock energy

$$\bar{\varepsilon}_k = \varepsilon_k + \frac{4}{3\pi} \varepsilon_F \cdot k_F a. \tag{3.35}$$

Inverting the 2×2 matrix (3.34) we obtain the normal Green's function

$$\mathcal{G}_{HF}(\mathbf{k}, \omega_n) = u_k^2 \frac{1}{-i\hbar\omega_n + E_k} - v_k^2 \frac{1}{i\hbar\omega_n + E_k} \tag{3.36}$$

and the anomalous Green's function

$$\mathcal{F}_{HF}(\mathbf{k},\omega_n) = \frac{\Delta}{2E_k}\left(\frac{1}{-i\hbar\omega_n + E_k} + \frac{1}{i\hbar\omega_n + E_k}\right), \tag{3.37}$$

where E_k is the usual spectrum of the fermionic quasi-particles

$$E_k = \sqrt{(\bar{\varepsilon}_k - \mu)^2 + |\Delta|^2} \tag{3.38}$$

and the coefficient u_k and v_k are given by

$$u_k^2 = \frac{1}{2}\left[1 + \frac{\bar{\varepsilon}_k - \mu}{\sqrt{(\bar{\varepsilon}_k - \mu)^2 + |\Delta|^2}}\right] \tag{3.39}$$

$$v_k^2 = \frac{1}{2}\left[1 - \frac{\bar{\varepsilon}_k - \mu}{\sqrt{(\bar{\varepsilon}_k - \mu)^2 + |\Delta|^2}}\right]. \tag{3.40}$$

The standard equation of the BCS-theory for the gap can be obtained by inserting the anomalous Green's function $\mathcal{F}_{HF}(\mathbf{k},\omega_n)$ into the equation (3.27) for the order parameter:

$$1 = -\frac{4\pi\hbar^2}{m}a\int \frac{d^3k}{(2\pi)^3}\left[\frac{1}{2E_{\mathbf{k}}}\tanh\left(\frac{E_{\mathbf{k}}}{2k_BT}\right) - \frac{m}{\hbar^2\mathbf{k}^2}\right]. \tag{3.41}$$

The integral (3.41) is regularized by the last term in the square bracket. By solving the gap-equation (3.41) for $T = 0$ the energy gap is obtained

$$\Delta^{(BCS)}(T=0) = \frac{8\varepsilon_F}{e^2}\exp(-\pi/2k_F|a|), \tag{3.42}$$

while setting $\Delta = 0$ in (3.41) it is possible to obtain the critical temperature for the superfluid transition

$$k_BT_c^{BCS} = \frac{8e^{\gamma_E}}{\pi e^2}\varepsilon_F\exp\left(-\pi/2k_F|a|\right) \approx 0.61\varepsilon_F\exp\left(-\pi/2k_F|a|\right), \tag{3.43}$$

here $\gamma_E = 0.5772...$ is the Euler's constant and $2k_F|a|/\pi = N(0)g$ is the dimensionless coupling constant, with $N(0) = mk_F/2\pi^2\hbar^2$ the standard density of state per spin at the Fermi energy. Corrections to the leading order of the BCS-result have been given by Gorkov and Melik-Barkhudarov [56], who went beyond the first order approximation by considering density fluctuations, the corrections to the first order are due to induced interactions, where one fermion sees the polarization in the Fermi gas due to a second fermion. In the gap equation the interaction $g = 4\pi\hbar^2/m\cdot a$ is replaced by an effective interaction $g \to g + \delta V$. In the new effective interaction are retained all the irreducible diagrams up to the second order, which are depicted in Figure 3.2. The density induced interaction leads to a positive

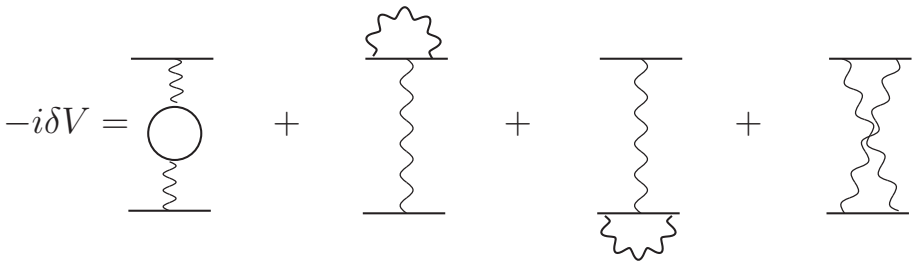

Figure 3.2: Second order correction to the interaction g

correction of the dimensionless coupling constant according to

$$g \to g + g^2 N(0) \frac{1 + 2\ln 2}{3}. \tag{3.44}$$

Since the correction to the attractive two-body scattering amplitude g is positive, the induced interaction weaken the interaction between the fermions and leads to a reduction of the transition temperature by a factor $(4e)^{-1/3} \approx 0.45$. The critical temperature obtained by Gorkov and Melik-Barkhudarov is thus given by

$$k_B T_c^{GM-B} = \frac{e^{\gamma_E}}{\pi} \left(\frac{2}{e}\right)^{7/3} \varepsilon_F \exp\left(-\pi/2k_F|a|\right) \approx 0.28 \varepsilon_F \exp\left(-\pi/2k_F|a|\right). \tag{3.45}$$

3.4 Strong coupling limit

In the weakly interacting limit $-\infty < \nu = 1/k_F a \lesssim -1$ our fermionic system converge to the BCS-theory. Increasing the strength of the interaction reflects in our model an increase of the dimensionless parameter ν. As long as $\nu < 0$, there are only unbound scattering states but when the inverse scattering length crosses zero, the fermions will start to bind into pairs with a diameter of the order of a while the average distance between the fermions is given by k_F^{-1}. If we require the system to be in the strong coupling regime, where

$$\nu = \frac{1}{k_F a} \gg 1, \tag{3.46}$$

then the distance between the pairs is much larger than their size and at low frequency and momenta the system behaves like a bosonic system. In fact for a two particle system the binding energy of a pair is

$$\varepsilon_b = \frac{\hbar^2}{m a^2}. \tag{3.47}$$

The ratio $\varepsilon_b/\varepsilon_F \propto \nu^2$ implies that in the regime defined by (3.46), $\varepsilon_F \ll \varepsilon_b$, hence at low energies quantum fluctuation are too small to break up the pairs and the physics of the system is dominated by bosonic degrees of freedom. The present crossover theory described by the set of equation (3.28),

converges in the strong coupling regime to the Hartree-Fock-Bogoliubov theory [17, 18]. Under the condition that we are in the low energy limit, where k_BT, $\hbar\Omega_n$ and $\hbar^2\mathbf{K}_F^2/4m$ are much smaller than the binding energy ε_b, the vertex function can be written in the following way

$$\Gamma^{-1}_{\alpha\alpha'}(\mathbf{K},\Omega_n) = -[8\pi\varepsilon_b^2 a^3]^{-1}\cdot\begin{pmatrix} -i\hbar\Omega_n + \frac{\hbar^2\mathbf{K}^2}{4m} + \frac{|\Delta|^2}{2\varepsilon_b} & -\frac{\Delta^2}{2\varepsilon_b} \\ -\frac{(\Delta^*)^2}{2\varepsilon_b} & i\hbar\Omega_n + \frac{\hbar^2\mathbf{K}^2}{4m} + \frac{|\Delta|^2}{2\varepsilon_b}\end{pmatrix} \tag{3.48}$$

up to the leading order in ε_b. On the other hand the Green's function of a weakly interacting Bose gas is given by the matrix [57]

$$G^{-1}_{B,\alpha\alpha'}(\mathbf{K},\Omega_n) = \begin{pmatrix} -i\hbar\Omega_n + \frac{\hbar^2\mathbf{K}^2}{4m} + T_B|\Psi_B|^2 & T_B\Psi_B^2 \\ T_B(\Psi_B^*)^2 & i\hbar\Omega_n + \frac{\hbar^2\mathbf{K}^2}{4m} + T_B|\Psi_B|^2\end{pmatrix}, \tag{3.49}$$

where $T = 4\pi\hbar^2 a_{dd}/2m$ is the bosonic T-matrix and Ψ_B is the average Bose field operator. If we identify the order parameter Δ with the bosonic order parameter Ψ_B through the relation

$$\Delta = \pm i[8\pi\varepsilon_b^2 a^3]^{1/2}\Psi_B, \tag{3.50}$$

the vertex function (3.48) resembles, up to the factor $-[8\pi\varepsilon_b^2 a^3]^{-1}$, the inverse Green's function of a superfluid interacting bosonic system

$$G_B(\mathbf{K},\Omega) = [8\pi\varepsilon_b^2 a^3]^{-1}\cdot\Gamma(\mathbf{K},\Omega_n), \tag{3.51}$$

where the bosonic scattering length is given by $a_{bb}^{(B)} = 2a$ and the T-matrix for the bosonic system reads $T_B = 4\pi\hbar^2 a/m$. It is important to note that the validity of the relation between the vertex (3.48) and the bosonic Green's function is only assured in the limit of strong coupling and low frequency and momenta. Indeed only in this limit the particles behave like bosons. In fact, in the limit $|k| \to \infty$, the diagonal part of the vertex function asymptotically behaves like (see also section 6.2)

$$\Gamma(\mathbf{K},\Omega_n) \approx 8\pi\frac{1}{\frac{1}{k_F a} - \sqrt{-i\frac{\Omega_n}{2} + \frac{K^2}{4} - \mu}}. \tag{3.52}$$

The different behaviour $G_B(\mathbf{K},\Omega_n) \sim \Omega_n^{-1}$ of the Green's function compared to that of the vertex function $\Gamma(\mathbf{K},\Omega_n) \sim \Omega_n^{-1/2}$, due to the two particle continuum associated with broken pairs, is evidence of the composite nature of the bosonic dimers. However, if the coupling constant becomes very large $\nu \gg 1$, the two particle continuum moves up to very large frequencies of the order of the binding energy $\varepsilon_b \sim \nu^2$.

According to this approximation, the scattering length of the weakly interacting bosons is found to be twice the fermionic scattering length. However Petrov *et al.* [58] have recently calculated the exact dimer-dimer scattering length by studying the four fermion problem and found the value $a_{dd} = 0.62\,a$.

Since in this regime the gas behaves like a weakly interacting gas of Bosons with a positive scattering length we expect that the system becomes superfluid below a critical temperature T_c which, to the zeroth order approximation, is the temperature $T_c^{(BEC)}$ where an ideal Bose gas with density $n_B = n/2$ and mass $m_B = 2m$ undergoes Bose-Einstein condensation:

$$k_B T_c^{(BEC)} = 3.31 \frac{\hbar^2 n_B^{2/3}}{m_B} = 0.218 \varepsilon_F. \tag{3.53}$$

The leading correction to this results arise from the residual interaction between the tightly bound bosonic dimers and the exact dependence of the critical temperature of the dilute repulsive bosonic gas on the interaction strength. The correction results to be positive and linear in the scattering length [59][60][61]

$$T_c / T_c^{(BEC)} = 1 + c n_B^{1/3} a_{dd}, \tag{3.54}$$

where the numerical constant assumes the value $c \approx 1.31$. The result (3.54) tells us that for the homogeneous case the evolution of the critical temperature from the BCS-regime to the BEC-regime as a function of the dimensionless coupling constant $\nu = 1/k_F a$ necessarily exhibits a maximum, since the asymptotic result for the ideal Bose gas is approached from above. The maximum in the curve of the critical temperature has been already predicted in early studies of the critical temperature along the BCS-BEC crossover by Nozières and Schmitt-Rink [14] and by Randeria [62] but still the high and the location of the maximum has not been determined in a reliable manner.

3.5 Global phase diagram

To study the physics of the system in the intermediate regime $-1 \lesssim \nu = 1/k_F a \lesssim 1$, we need to numerically solve the set of equations (3.28). In order to do this we use as input parameter the temperature and the order parameter. The coupling constant ν and the chemical potential of the system are then determined self-consistently. Thus, the solution of the self-consistent equations (3.28) determines the state of the system by giving, as direct result the temperature of the system, the order parameter of the superfluid transition, the coupling constant and the chemical potential. In Figures 3.3 and 3.4 is depicted the order parameter of the system as a function of the dimensionless coupling constant and the dimensionless temperature. The order parameter vanishes in the limit of weak coupling according to the exponential law predicted by the BCS theory. In the opposite limit of strong coupling, the behaviour can be derived from $\mu n \to -\Delta^2/2g$. This behaviour reflects the fact that the fermion chemical potential in the strong coupling limit is governed by the potential energy which is, in the limit $\nu \to \infty$, the binding energy. From Figure 3.3 one can clearly see that there is a region where the gap is multivalued. This region of multivaluedness near T_c, which is evidence of a first order transition, is an artefact of our approximation and will be present in all the thermodynamic potentials calculated within our theory.

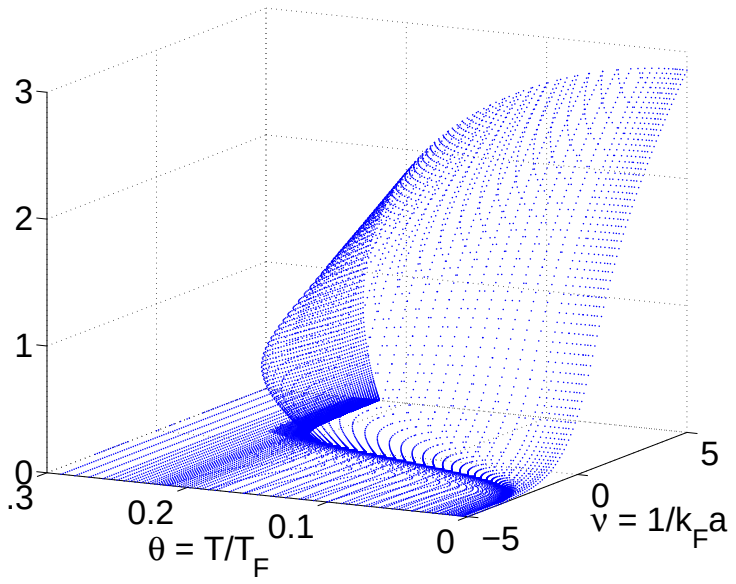

Figure 3.3: Three dimensional view of the order parameter. From this picture one can clearly see the region around the critical temperature where the order parameter becomes multivalued. This multivalued behaviour is charaterisitc of a first-order transition.

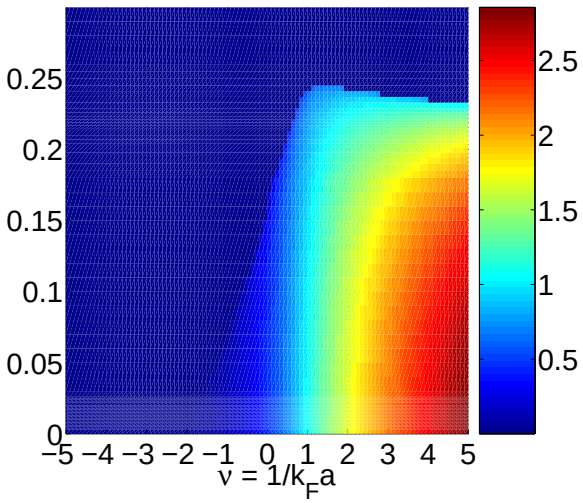

Figure 3.4: Projection of the order parameter on the $\theta - \nu$ plane.

The crucial quantity which determines the overall structure of the phase diagram is then the critical temperature T_c where the transition from the normal system to the superfluid system occurs. As we have pointed out in sections 3.3 and 3.4, the behaviour of the critical temperature is well known in the two extreme limits. For weak coupling the fermionic gas can be described by a BCS-like theory, while for strong attractive interaction the fermions are bound into dimers and the theory converge to an effective theory of repulsively interacting bosons. These approximation works fine because the relevant quasi-particles, the fermions in the weak coupling limit and the bosons in the strong coupling limit, are well defined and have long life times. This is not the case for intermediate couplings $-1 \lesssim \nu = 1/k_F a \lesssim 1$ where the quasi-particles are short-lived. The range of temperatures around T_c where the order parameter and the thermodynamic potentials are multivalued can be clearly identified in Figure 3.5 as the region bounded by the upper and lower T_c curves respectively. In the above-mentioned figure the critical temperature is depicted as dimensionless ratio $\theta_c = T_c/T_F$ together with the limits in the BSC and BEC regime.

The lower T_c curve (depicted in Figure 3.5 by the red dashed line) has been determined by implementing the Thouless criterion and is defined as the lowest temperature for which the normal-fluid state is stable. Such a definition for T_c was already used in previous works [63] and [18], and produces for the critical temperature a curve which increases monotonically as a function of the coupling constant ν. Consequently, the value $T_c^{(BEC)}$ for the ideal Bose gas is approached from below, which is in contrast with the result (3.54) and with the previous works of Nozières and Schmitt-Rink [14], Randeria [62], Drechsler and Zwerger [15], and Sá De Melo *et al.* [64].

In order to determine a sensible value for the critical temperature within our approach we have determined T_c from the criterion that it is the maximum temperature at which the order parameter $\Delta(T)$ is nonzero. The T_c curve (full black line in Figure 3.5) obtained from the last criterion exhibits a maximum on the BEC-side of the crossover around $\nu \approx 1$, which is the behaviour expected on general grounds. As a consequence of the maximum in the T_c curve our theory approaches the critical temperature of the ideal Bose gas from above which is consistent with the enhancement of the critical temperature predicted by the functional form (3.54) in the BEC limit ($\nu \gg 1$).

As a comparison we plotted in Figure 3.5 two additional curves in the strong coupling regime which are obtained from the relation (3.54). The data depicted by the red squares are obtained by substituting the exact result for the dimer-dimer scattering length $a_{dd} = 0.62a$ and the numerical constant $c \approx 1.31$ obtained from Monte Carlo calculations [65, 66, 67] while the dash-dotted blue line is obtained by using the Born approximation for the dimer-dimer scattering length $a_{dd}^{(B)} = 2a$ and the numerical constant $c \approx 0.58$ which are consistent with our Popov-approximate theory. Even though our theory predicts a scattering length which differs from the exact value the agreement of our results with the exact results is very good.

On the BCS-side our estimate of the critical temperature is compared with the BCS result (3.43) for the critical temperature (yellow dashed line) and the Gorkov Melik-Barkhudarov correction to this result (green squares). Even in this regime, the agreement of the present theory with the approximation

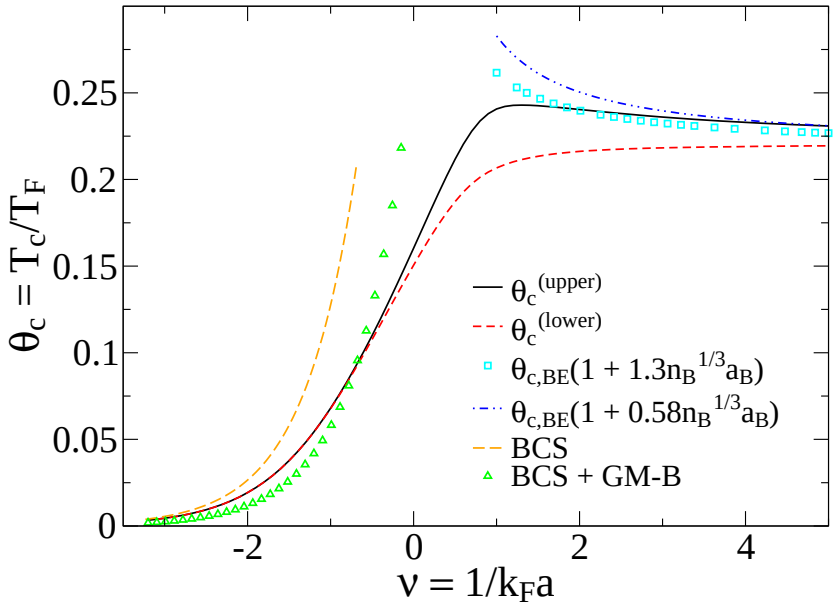

Figure 3.5: (Color online) $\theta_c^{(lower)}$ (red dashed line) and $\theta_c^{(upper)}$ (solid black line, identified as T_c) compared with the Shohno result (blue dotted-dashed line) with $a_{dd}^{(B)} = 2\,a$ and the exact result (light-blue squares) with $\Delta T_c/T_{BEC} = c\,n_B^{1/3} a_{dd}^{(0)}$ and $c = 1.31$ (QMC) and $a_{dd} = 0.62\,a$. Yellow dashed line and green triangles show the BCS result without and with Gorkov and Melik-Barkhudarov corrections.

for extremely weak coupling is evident.

The other physical parameter which can be directly calculated in the self-consistent approximation is the chemical potential. Since our calculation extends to all temperature and coupling strength, we are able to calculate the chemical potential in a wider range of temperatures for arbitrary values of the coupling constant. Figure 3.6 and 3.7 depict surface plot of the chemical potential as a function of the dimensionless temperature and coupling constant and its projection onto the $\theta - \nu$ plane. In the weak coupling limit the numerical results approach the result expected for an ideal Fermi gas $\mu \to \varepsilon_F$ as can be seen in the surface plot depicted in Figure 3.6. On this side of the crossover there are essentially no bound pairs, the system is a Fermi liquid and only below the critical temperature T_c there will be a few cooper pairs. On the Bose side the difference between the chemical potential and the binding energy $\varepsilon_b = \hbar^2/ma^2 = \varepsilon_F \cdot 2\nu^2$ is plotted. In the strong coupling limit $1/k_F a \gg 1$ the fermions are bound together into dimers and we expect $\mu \to -\varepsilon_b/2 = -\varepsilon_F \nu^2$. The difference $\mu + \varepsilon_b/2$ approaches zero from the positive side which is an evidence of the repulsive interaction between the pairs.

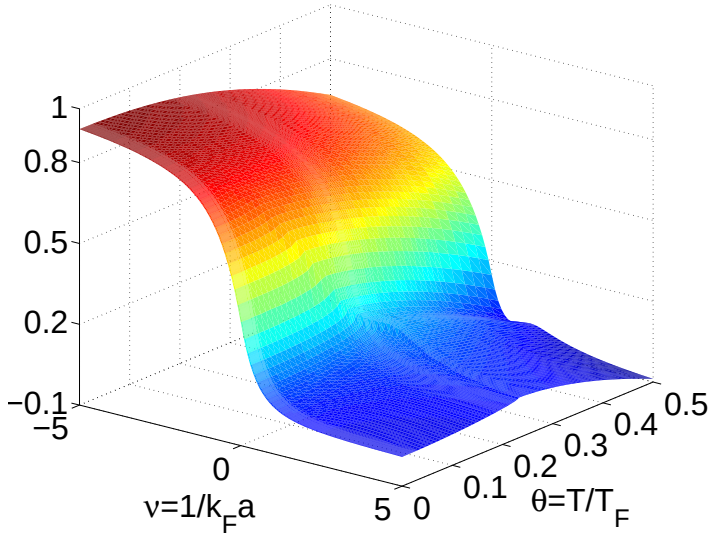

Figure 3.6: Surface plot of the chemical potential μ a function of the coupling constant $\nu = 1/k_F a$ and the dimensionless temperature $\theta = T/T_F$. On the Bose side the difference $\mu + \varepsilon_b/2$ in units of the Fermi energy ε_F is plotted, where $\varepsilon_b/2 = \varepsilon_F \nu^2$.

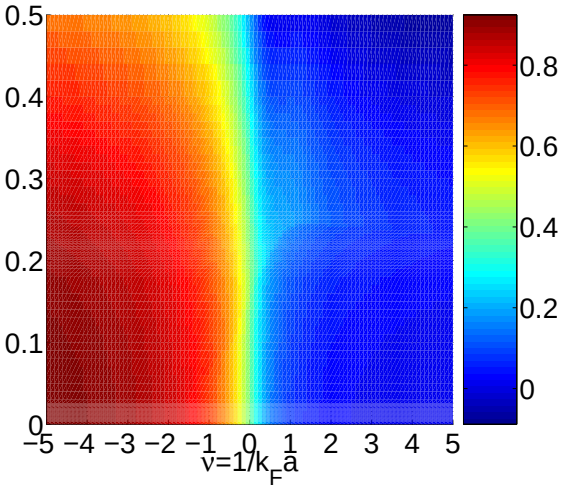

Figure 3.7: Projection of the chemical potential onto the $\theta - \nu$ plane. The numerical value of the chemical potential is indicated by the different color according to the color bar on the right of the plot.

Chapter 4

Thermodynamics of the crossover

4.1 Thermodynamic potentials

The functional $\Omega[G]$ obtained within the formalism of Luttinger and Ward can be explicitly derived starting from the functional (2.13) with the stationarity condition (2.15) and inserting the ladder approximation for the functional $\Phi[G]$, which has already been explicitly calculated in a previous work [18]

$$\begin{aligned}\Omega[G] = -L^d \int \frac{d^d k}{(2\pi)^d} \frac{1}{\beta} \sum_{\omega_n} \mathrm{Tr}\{-\ln[G(\mathbf{k},\omega_n)] + [G_0(\mathbf{k},\omega_n)^{-1} G(\mathbf{k},\omega_n) - 1]\} \\ + L^d\, g_0 |\mathcal{F}(\mathbf{0},0)|^2 \;+\; \frac{1}{2} L^d \int \frac{d^d K}{(2\pi)^d} \frac{1}{\beta} \sum_{\Omega_n} \mathrm{Tr}\{\ln[1 + g_0 \chi(\mathbf{K},\Omega_n)]\}.\end{aligned} \tag{4.1}$$

The functional (2.13) is written in a very compact way, in fact the trace that appears in it is fourfold. In (4.1) the four traces have been written explicitly: the first one is taken with respect to the position $\mathbf{r}$, which is represented by the integral over the wave vector $\mathbf{k}$. The second trace is taken with respect to the imaginary time τ and is represented by the sum over the Matsubara frequencies. The trace over the spin indices has been suppressed and replaced by an extra factor 2. Finally in the formula (4.1) survives only one trace which is the one over the Nambu indices. The matrix Green's functions $G_0(\mathbf{k},\omega_n)$ and $G(\mathbf{k},\omega_n)$ are defined by (3.10) and (3.7) while the pair propagator $\chi(\mathbf{K},\Omega_n)$ is defined by (3.14). The kinetic energy and the chemical potential are included via the free matrix Green's function $G_0(\mathbf{k},\omega_n)$, the temperature T is included directly by means of the factor β and indirectly through the fermionic and bosonic Matsubara frequencies $\omega_n = 2\pi(n+1)/\beta$ and $\Omega_n = 2\pi n/\beta$. The interaction is included in (4.1) by the bare interaction parameter, which needs to be renormalized following the procedure which is explained in section 3.1. Fermionic and bosonic functions are distinguished by their arguments. Fermionic wave vectors and the fermionic Matsubara frequencies are denoted by small letters while the bosonic wave vectors and Matsubara frequencies are denoted by capital letters.

The fermionic Green's function and the pair propagator as a function of the wave vector and the

Matsubara frequencies are obtained through a Fourier transformation with respect to the position $\mathbf{r}$ and the imaginary time τ. The second term in the (4.1) is defined by the anomalous Green's function (3.4). The volume L^d is supposed to be a cube with edge length L and the limit $L \to \infty$ is taken in the renormalization procedure.

In the formalism of De Dominicis and Martin the renormalization of the coupling strength is obtained replacing the bare coupling constant with the vertex function via a Legendre transformation. The resulting functional is the dimensionless entropy given by (2.38). From the functional $F^{(2)}[G,\Gamma]$ we can derive an explicit expression for the entropy. If we restrict the second trace of (2.38) to the particle-particle ladders and set $\mathcal{K}^{(2)}[G,\Gamma]$ to zero as described in section 2.3, the entropy functional reads

$$\begin{aligned} S[G,\Gamma]/k_B = \beta L^d \int \frac{d^dk}{(2\pi)^d}\,\frac{1}{\beta}\sum_{\omega_n} \mathrm{Tr}\{-\ln[G(\mathbf{k},\omega_n)] + [-i\hbar\omega_n G(\mathbf{k},\omega_n) - 1]\} \\ + \frac{1}{2}\beta L^d \int \frac{d^dK}{(2\pi)^d}\,\frac{1}{\beta}\sum_{\Omega_n} \mathrm{Tr}\{\ln[1-\chi(\mathbf{K},\Omega_n)\,\Gamma(\mathbf{K},\Omega_n)] + \chi(\mathbf{K},\Omega_n)\,\Gamma(\mathbf{K},\Omega_n)\}. \end{aligned} \tag{4.2}$$

The first term of the functional (4.2) is the same as in (2.38) where the trace is written explicitly and it doesn't need any further explanation, on the other hand, the second term needs a more careful analysis. In our approximation the restriction to particle-particle ladders implies that the Nambu indices are pairwise identical, that means they reduce from four to two. In this way the vertex function Γ can be represented by a 2×2 matrix like for the matrix Green's function. With this simplification the pre-factor of Γ in equation (2.38) changes. The factor $1/2$ disappears and the quadratic terms in the second trace cancels. With the further simplification $\mathcal{K}^{(2)}[G,\Gamma] = 0$ the trace reduces to

$$\frac{1}{2}\mathrm{Tr}\left\{\ln[1-\bar{\Gamma}] + \bar{\Gamma}\right\}. \tag{4.3}$$

Using the definition of $\bar{\Gamma}$ given by (2.39), together with the definition (3.14) of the pair propagator $\chi(\mathbf{K},\Omega_n)$, the modified vertex function can be rewritten in the following way

$$\bar{\Gamma}(\mathbf{K},\Omega_n) = \chi^{1/2}(\mathbf{K},\Omega_n)\Gamma(\mathbf{K},\Omega_n)\chi^{1/2}(\mathbf{K},\Omega_n) = \chi(\mathbf{K},\Omega_n)\Gamma(\mathbf{K},\Omega_n). \tag{4.4}$$

Furthermore, we note that the two-particle Green's function and hence the vertex function Γ, depend on four wave vectors, where only three of them are independent because of the momentum conservation. Since we restrict ourself only to particle-particle ladder in the present approximation, Γ is the scattering amplitude of two fermions in the many particle system. The three independent wave vectors can be then chosen as the center of mass wave vector $\mathbf{K}$, the relative incoming wave vector and the relative outcoming wave vector. Since the interaction is assumed to be elastic and of s-wave type, the scattering amplitude does not depend on the incoming and outcoming wave vectors, hence the vertex function Γ depends only on the center of mass wave vector $\mathbf{K}$. The same argument can be repeated for the

Matsubara frequencies so that, in the end we can assume that the vertex function is a function of the center of mass wave vector $\mathbf{K}$ and the center of mass Matsubara frequencies Ω_n only. The spin dependence can be factored just as it has been done for the Green's function and can be incorporated in the pre-factors including a factor 2 for each closed fermionic loop.

From the entropy functional we can obtain an explicit expression for the grand-thermodynamic potential in the formalism of De Dominicis and Martin. According to (2.41), in order to do that we need to find an explicit expression for the internal energy and for the particle number. Within the present formalism the internal energy can be explicitly evaluated in terms of the Green's function G and the vertex function Γ. From the thermal average

$$U = \langle \hat{H} \rangle = Z^{-1} \operatorname{Tr}\{\hat{H} \exp(-\beta[\hat{H} - \mu\hat{N}])\}, \tag{4.5}$$

using the delta potential interaction and inserting the Hamiltonian (3.1) in the (4.5) we obtain:

$$\begin{aligned} U = &\int d^d r \sum_\sigma \frac{\hbar^2}{2m} \langle [\nabla \psi^\dagger_\sigma(\mathbf{r})][\nabla \psi_\sigma(\mathbf{r})] \rangle \\ &+ \frac{1}{2} \int d^d r \sum_{\sigma\sigma'} g_0 \langle \psi^\dagger_\sigma(\mathbf{r}) \psi^\dagger_{\sigma'}(\mathbf{r}) \psi_{\sigma'}(\mathbf{r}) \psi_\sigma(\mathbf{r}) \rangle. \end{aligned} \tag{4.6}$$

The first term in the (4.6) represent the kinetic energy and can be expressed in terms of the Green's function, it contains, in fact, an average of two fermionic fields, that can be expressed through equation (3.3) in terms of the normal Green's function. The first integral of the (4.6) can be rewritten as follows:

$$\begin{aligned} &\int d^d r \sum_\sigma \frac{\hbar^2}{2m} \langle [\nabla \psi^+_\sigma(\mathbf{r})][\nabla \psi_\sigma(\mathbf{r})] \rangle \\ &\qquad = -2 \int d^d r \int \frac{d^d k}{(2\pi)^d} \int \frac{d^d k'}{(2\pi)^d} \cdot \frac{\hbar^2}{2m} \mathbf{k} \cdot \mathbf{k}' e^{-i\mathbf{r}\cdot(\mathbf{k}-\mathbf{k}')} \langle a(\mathbf{k}, \tau)^\dagger a(\mathbf{k}', \tau) \rangle \\ &\qquad = -2 \int \frac{d^d k}{(2\pi)^d} \frac{\hbar^2 k^2}{2m} \mathcal{G}(\mathbf{k}, \tau = -0). \end{aligned} \tag{4.7}$$

The second integral in the (4.6) can be expressed by four terms. It contains an average of four fermionic fields which, using the Wick theorem and following De Dominicis and Martin, can be separated into three products of single particle Green's functions plus a term which take into account the correlations:

$$\begin{aligned} \langle \mathrm{T}[\psi(X_1)\psi(X_2)\psi^\dagger(X_3)\psi^\dagger(X_4)] \rangle = &\langle \mathrm{T}[\psi(X_1)\psi^\dagger(X_3)] \rangle \langle \mathrm{T}[\psi(X_2)\psi^\dagger(X_4)] \rangle \\ &- \langle \mathrm{T}[\psi(X_1)\psi^\dagger(X_4)] \rangle \langle \mathrm{T}[\psi(X_2)\psi^\dagger(X_3)] \rangle \\ &- \langle \mathrm{T}[\psi(X_1)\psi(X_2)] \rangle \langle \mathrm{T}[\psi^\dagger(X_3)\psi^\dagger(X_4)] \rangle \\ &- \bar{\Gamma}_{X_1 X_2 X_3 X_4}. \end{aligned} \tag{4.8}$$

The three product of one-particle Green's function represent the Hartree energy, the Fock energy and the Bogoliubov energy. The connected part of the two-particle Green's function provides the correlation energy. The third product can be finally expressed in terms of the anomalous Green's function. Instead of calculating directly the averages in (4.8) we can get an explicit expression of the potential energy in a simpler way. We have applied the self-consistent ladder approximation to get a closed formula for the grand thermodynamic potential, thus we will apply the same approximation to evaluate the potential energy. In order to evaluate the average

$$\langle H_{pot}\rangle = \frac{1}{2}\int d^d r \sum_{\sigma\sigma'} g_0 \,\langle \psi^\dagger_\sigma(\mathbf{r})\psi^\dagger_{\sigma'}(\mathbf{r})\psi_{\sigma'}(\mathbf{r})\psi_\sigma(\mathbf{r})\rangle \tag{4.9}$$

we note that

$$\langle H_{pot}\rangle = Z^{-1}\mathrm{Tr}\,\left\{\hat{H}_{pot}\; e^{-\beta(\hat{H}_{kin}-\mu\hat{N}+\hat{H}_{pot})}\right\} = -\frac{1}{\beta}g_0\frac{\partial \ln Z}{\partial g_0} = g_0\frac{\partial\Omega}{\partial g_0}, \tag{4.10}$$

where Ω is the grand thermodynamic potential, g_0 the bare interaction strength and the partial derivative are taken at constant T and μ and volume. As can be seen from (4.1), the functional Ω depends explicitly on the interaction strength. However there is also an implicit dependence due to the presence of the full Green's function $G(\mathbf{k},\omega_n)$. Anyway at equilibrium the grand thermodynamic potential is defined by its value at the saddle point

$$\frac{\delta\Omega[G]}{\delta G} = 0,$$

hence we don't have to worry about the implicit derivative $\delta\Omega/\delta G\cdot\partial G/\partial g_0$ and the calculation reduces to a straightforward partial derivative of the last two term of the functional (4.1):

$$\langle H_{pot}\rangle = g_0\left[L^d|\mathcal{F}(\mathbf{0},0)|^2 + \frac{1}{2}L^d\int\frac{d^dK}{(2\pi)^d}\,\frac{1}{\beta}\sum_{\Omega_n}\mathrm{Tr}\{[1+g_0\chi(\mathbf{K},\Omega_n)]^{-1}\cdot\chi(\mathbf{K},\Omega_n)\}\right] \tag{4.11}$$

the quantity in the trace can be further rewritten with the help of the Bethe-Salpeter equation $[1 + g_0\chi(\mathbf{K},\Omega_n)]^{-1} = \Gamma(\mathbf{K},\Omega_n)/g_0 = 1-\chi(\mathbf{K},\Omega_n)\Gamma(\mathbf{K},\Omega_n)$ and the internal energy take then the following explicit form:

$$\begin{aligned} U[G,\Gamma] = &-2L^d\int\frac{d^dk}{(2\pi)^d}\,\varepsilon_{\mathbf{k}}\,\mathcal{G}(\mathbf{k},\tau=-0) \;+\; L^d\,g_0|\mathcal{F}(\mathbf{0},0)|^2 \\ &+\frac{1}{2}L^d\int\frac{d^dK}{(2\pi)^d}\,\frac{1}{\beta}\sum_{\Omega_n} g_0\,\mathrm{Tr}\{\chi(\mathbf{K},\Omega_n)-\chi(\mathbf{K},\Omega_n)\,\Gamma(\mathbf{K},\Omega_n)\,\chi(\mathbf{K},\Omega_n)\}. \end{aligned} \tag{4.12}$$

An explicit expression for the particles number in terms of the one-particle Green's function can be derived starting from the definition

$$N = \langle\hat{N}\rangle = \int d^d r\sum_\sigma\langle\psi^\dagger_\sigma(\mathbf{r})\psi_\sigma(\mathbf{r})\rangle. \tag{4.13}$$

Proceeding as for the internal energy, the equation for the particle number can be rewritten in the standard form:

$$N[G] = -2\,L^d \int \frac{d^d k}{(2\pi)^d}\, \mathcal{G}(\mathbf{k}, \tau = -0). \tag{4.14}$$

Combining the expression for the entropy and the results obtained for the internal energy and the particle number, we can now write the grand-thermodynamic potential in a explicit way by exploiting the thermodynamic relation (2.41). As a result we get, within the formalism of De Dominicis and Martin a functional for the grand thermodynamic potential which is essentially different from the one calculated within the formalism of Luttinger and Ward:

$$\begin{aligned}\Omega[G,\Gamma] = &-2\,L^d \int \frac{d^d k}{(2\pi)^d}\,(\varepsilon_{\mathbf{k}} - \mu)\,\mathcal{G}(\mathbf{k}, \tau = -0) \;+\; L^d\, g_0 |\mathcal{F}(\mathbf{0}, 0)|^2 \\ &- L^d \int \frac{d^d k}{(2\pi)^d}\,\frac{1}{\beta}\sum_{\omega_n} \mathrm{Tr}\{-\ln[G(\mathbf{k},\omega_n)] + [-i\hbar\omega_n G(\mathbf{k},\omega_n) - 1]\} \\ &+ \frac{1}{2}\,L^d \int \frac{d^d K}{(2\pi)^d}\,\frac{1}{\beta}\sum_{\Omega_n} g_0\,\mathrm{Tr}\{\chi(\mathbf{K},\Omega_n) - \chi(\mathbf{K},\Omega_n)\,\Gamma(\mathbf{K},\Omega_n)\,\chi(\mathbf{K},\Omega_n)\} \\ &- \frac{1}{2}\,L^d \int \frac{d^d K}{(2\pi)^d}\,\frac{1}{\beta}\sum_{\Omega_n} \mathrm{Tr}\{\ln[1 - \chi(\mathbf{K},\Omega_n)\,\Gamma(\mathbf{K},\Omega_n)] + \chi(\mathbf{K},\Omega_n)\,\Gamma(\mathbf{K},\Omega_n)\}.\end{aligned} \tag{4.15}$$

Although at this stage the functionals (4.1) and (4.15) are formally different, it can be shown that the value of the functional (4.15) at stationarity coincides exactly with the grand-thermodynamic potential $\Omega[G]$ expressed by (4.1) (see Appendix A).

Alternatively, a functional for the entropy can be derived from the Luttinger and Ward grand-potential according to the thermodynamic relation $S = -\partial\Omega/\partial T$. Again we will obtain a formal expression for the entropy which is different from (4.2). However, if G and Γ satisfy the self-consistent equation the two functionals will become identical. The equivalence of the different functionals in thermal equilibrium is necessary for the consistency of the theory and the compatibility of the self-consistent ladder approximation for all thermodynamic quantities.

4.2 Derivation of the self-consistent equations within the formalism of De Dominicis and Martin

In this section the Dyson equation (3.11) and the Bethe-Salpeter equation (3.18), already written in Chapter 3 within the formalism of Luttinger and Ward, will be derived from the first variation of the functional (2.42) by means of the stationarity criteria (2.42).

First we will derive the Bethe-Salperter equation (3.13) from the variation $\delta_\Gamma \Omega[G,\Gamma]$, where Γ is

varied and G is kept constant:

$$\delta_\Gamma \Omega[G,\Gamma] = \frac{1}{2} L^d \int \frac{d^d\mathbf{K}}{(2\pi)^d} \frac{1}{\beta} \sum_{\Omega_n} \mathrm{Tr}\Big\{ \Big[-g_0 \chi(\mathbf{K},\Omega_n) - 1 + [1 - \chi(\mathbf{K},\Omega_n)\Gamma(\mathbf{K},\Omega_n)]^{-1} \Big] \times \chi(\mathbf{K},\Omega_n)\delta\Gamma(\mathbf{K},\Omega_n) \Big\}. \tag{4.16}$$

The quantity $\delta\Gamma(\mathbf{K},\Omega_n)$ is arbitrary thus the condition $\delta\Omega[G,\Gamma]/\delta\Gamma = 0$ implies that the the argument of the integral (4.16) must vanish:

$$-g_0\chi(\mathbf{K},\Omega_n) + [1 - \chi(\mathbf{K},\Omega_n)\Gamma(\mathbf{K},\Omega_n)]^{-1} - 1 = 0 \tag{4.17}$$

Equation (4.17) is nothing but the Bethe-Salpeter equation. In fact, if we multiply it from the right side by $[1 - \chi(\mathbf{K},\Omega_n)\Gamma(\mathbf{K},\Omega_n)]$ and from the left side by $\chi(\mathbf{K},\Omega_n)$, we get

$$\Gamma(\mathbf{K},\Omega_n) = g_0 - g_0\chi(\mathbf{K},\Omega_n)\Gamma(\mathbf{K},\Omega_n) \tag{4.18}$$

which is exactly the Bethe-Salpeter equation and can be written in the same form as in (3.13) by multiplying it by $\Gamma(\mathbf{K},\Omega_n)^{-1}$ from the right.

Considering the variation of $\Omega[G,\Gamma]$ with respect to G, where Γ is kept constant we get the Dyson equation (3.11). In order to perform the variation explicitly, we need to express the dependence on the Green's function $G(\mathbf{k},\omega_n)$ of the first two terms in the grand-canonical potential (4.15). To this purpose we rewrite the kinetic energy in the following form:

$$\begin{aligned} 2L^d \int \frac{d^dk}{(2\pi)^d} \frac{1}{\beta} \sum_{\omega_n} (\varepsilon_k - \mu)\mathcal{G}(\mathbf{k},\omega_n) &= \\ = L^d \int \frac{d^dk}{(2\pi)^d} \frac{1}{\beta} \sum_{\omega_n} \mathrm{Tr} \left\{ \begin{pmatrix} (\varepsilon_\mathbf{k} - \mu) & 0 \\ 0 & -(\varepsilon_\mathbf{k} - \mu) \end{pmatrix} \begin{pmatrix} \mathcal{G}(\mathbf{k},\omega_n) & \mathcal{F}(\mathbf{k},\omega_n) \\ \mathcal{F}^*(\mathbf{k},\omega_n) & -\mathcal{G}^*(\mathbf{k},\omega_n) \end{pmatrix} \right\} \\ = L^d \int \frac{d^dk}{(2\pi)^d} \frac{1}{\beta} \sum_{\omega_n} \mathrm{Tr} \left\{ \Big(G_0^{-1}(\mathbf{k},\omega_n) + i\hbar\omega_n \Big) G(\mathbf{k},\omega_n) \right\}, \end{aligned} \tag{4.19}$$

The term $L^d\, g_0 |\mathcal{F}(\mathbf{0},0)|^2$ has to be treated in the same way. Noting that $\Delta = g_0\mathcal{F}(\mathbf{0},0)$ we can write

$$\begin{aligned} 2L^d\, g_0 |\mathcal{F}(\mathbf{0},0)|^2 &= L^d \mathrm{Tr} \begin{pmatrix} \Delta F^*(\mathbf{r}=0,\tau=0) & 0 \\ 0 & \Delta^* F(\mathbf{r}=0,\tau=0) \end{pmatrix} \\ &= L^d \int \frac{d^dk}{(2\pi)^d} \frac{1}{\beta} \sum_{\omega_n} \mathrm{Tr} \left\{ \begin{pmatrix} 0 & \Delta \\ \Delta^* & 0 \end{pmatrix} \begin{pmatrix} \mathcal{G}(\mathbf{k},\omega_n) & \mathcal{F}(\mathbf{k},\omega_n) \\ \mathcal{F}^*(\mathbf{k},\omega_n) & -\mathcal{G}^*(\mathbf{k},\omega_n) \end{pmatrix} \right\} \\ &= L^d \int \frac{d^dk}{(2\pi)^d} \frac{1}{\beta} \sum_{\omega_n} \mathrm{Tr} \left\{ \Sigma_1 G(\mathbf{k},\omega_n) \right\} \end{aligned} \tag{4.20}$$

where Σ_1 is the Fock contribution to the self-energy defined by the matrix (3.24). The two terms (4.19) and (4.20) can be now grouped together with the third integral in the functional (4.15), thus the first three contribution to the grand-thermodynamic potential read:

$$L^d \int \frac{d^d k}{(2\pi)^d} \frac{1}{\beta} \sum_{\omega_n} \mathrm{Tr}\left\{\ln[G(\mathbf{k},\omega_n)] + \left[-G_0^{-1}(\mathbf{k},\omega_n) + \Sigma_1\right] G(\mathbf{k},\omega_n)\right\} - L^d \frac{|\Delta|^2}{g_0}. \tag{4.21}$$

Noting that the pair propagator $\chi(\mathbf{K},\Omega_n)$ is a product of Green's functions, the variation with respect to $G(\mathbf{k},\omega_n)$ of the grand-potential functional finally reads:

$$\begin{aligned}\delta_G\Omega[G,\Gamma] = L^d \int \frac{d^d k}{(2\pi)^d} \frac{1}{\beta} \sum_{\omega_n} \mathrm{Tr}\left\{[G(\mathbf{k},\omega_n)^{-1} - G_0(\mathbf{k},\omega_n)^{-1} + \Sigma_1]\delta G(\mathbf{k},\omega_n)\right\} \\ + \frac{L^d}{2} \int \frac{d^d K}{(2\pi)^d} \frac{1}{\beta} \sum_{\Omega_n} \mathrm{Tr}\Big\{g_0\,[1 - \chi(\mathbf{K},\Omega_n)\Gamma(\mathbf{K},\Omega_n)]\delta\chi(\mathbf{K},\Omega_n) \\ - g_0\,\delta\chi(\mathbf{K},\Omega_n)\,\Gamma(\mathbf{K},\Omega_n)\,\chi(\mathbf{K},\Omega_n) \\ + [1 - \chi(\mathbf{K},\Omega_n)\,\Gamma(\mathbf{K},\Omega_n)]^{-1}\delta\chi(\mathbf{K},\Omega_n)\,\Gamma(\mathbf{K},\Omega_n) \\ - \delta\chi(\mathbf{K},\Omega_n)\,\Gamma(\mathbf{K},\Omega_n)\Big\}.\end{aligned} \tag{4.22}$$

The second integral can be simplified by using the Bethe-Salpeter equation. Equation (4.17) implies that the last three terms of this integral cancel. Applying (4.18) to the remaining term, for the second integral we obtain

$$\frac{1}{2}\, L^d \int \frac{d^d K}{(2\pi)^d}\, \frac{1}{\beta} \sum_{\Omega_n} \mathrm{Tr}\{\Gamma(\mathbf{K},\Omega_n)\,\delta\chi(\mathbf{K},\Omega_n)\}\,. \tag{4.23}$$

From (3.14) we obtain the variation of the pair propagator

$$\delta\chi_{\alpha\alpha'}(\mathbf{K},\Omega_n) = 2 \int \frac{d^d k}{(2\pi)^d}\, \frac{1}{\beta} \sum_{\omega_n} G_{\alpha\alpha'}(\mathbf{K}-\mathbf{k},\Omega_n-\omega_n)\,\delta G_{\alpha\alpha'}(\mathbf{k},\omega_n)\,. \tag{4.24}$$

We insert this result into (4.23), interchange the order of boson and fermion integration/summation, and write the trace and the matrix product explicitly in terms of the Nambu indices. Thus, equation (4.23) is transformed into

$$L^d \int \frac{d^d k}{(2\pi)^d}\, \frac{1}{\beta} \sum_{\omega_n} \sum_{\alpha\alpha'} \Big[\int \frac{d^d K}{(2\pi)^d}\, \frac{1}{\beta} \sum_{\Omega_n} \Gamma_{\alpha\alpha'}(\mathbf{K},\Omega_n)\, G_{\alpha'\alpha}(\mathbf{K}-\mathbf{k},\Omega_n-\omega_n)\Big]\delta G_{\alpha'\alpha}(\mathbf{k},\omega_n)\,. \tag{4.25}$$

According to (3.23), we recognize the term in the square brackets in equation (4.25) as the particle-particle contribution to the self energy $\tilde{\Sigma}_{\alpha\alpha'}(\mathbf{k},\omega_n)$. Putting everything together leads to

$$\delta_G\Omega[G,\Gamma] = L^d \int \frac{d^d k}{(2\pi)^d}\, \frac{1}{\beta} \sum_{\omega_n} \mathrm{Tr}\{[G(\mathbf{k},\omega_n)^{-1} - G_0(\mathbf{k},\omega_n)^{-1} + \Sigma_1 + \tilde{\Sigma}(\mathbf{k},\omega_n)]\delta G(\mathbf{k},\omega_n)\}\,. \tag{4.26}$$

Since the variation δG is arbitrary, the the stationarity condition $\delta\Omega[G,\Gamma]/\delta\Gamma = 0$ yields

$$G(\mathbf{k},\omega_n)^{-1} = G_0(\mathbf{k},\omega_n)^{-1} - \Sigma_1 - \tilde{\Sigma}(\mathbf{k},\omega_n), \tag{4.27}$$

which is the Dyson equation (3.11) with $\Sigma(\mathbf{k},\omega_n) = \Sigma_1 + \tilde{\Sigma}(\mathbf{k},\omega_n)$ the self energy.

4.3 Thermodynamics in the weak coupling limit

We can now obtain the mean-field approximation for the thermodynamic potentials. In order to do that we first need to write explicitly the mean-field Green's function (3.34) in the functionals (4.1) and (4.12). To this purpose we replace the free fermions Green's function $G_0(\mathbf{k},\omega_n)$ with $G_1(\mathbf{k},\omega_n)$ by rewriting the Dyson in the following way

$$G^{-1}(\mathbf{k},\omega_n) = G_1^{-1}(\mathbf{k},\omega_n) - \tilde{\Sigma}_{\alpha\alpha'}(\mathbf{k},\omega_n), \tag{4.28}$$

where $\tilde{\Sigma}_{\alpha\alpha'}(\mathbf{k},\omega_n)$ is the particle-particle contribution to the self-energy (see equation (3.23)).

First we consider the grand-thermodynamic potential (4.1). Using result (4.20) we can rewrite the first two terms of $\Omega[G]$ as follows

$$-L^d \int \frac{d^dk}{(2\pi)^d}\,\frac{1}{\beta}\sum_{\omega_n} \mathrm{Tr}\{-\ln[G(\mathbf{k},\omega_n)] + [G_1(\mathbf{k},\omega_n)^{-1}G(\mathbf{k},\omega_n) - 1]\} - L^d\frac{|\Delta|^2}{g_0}, \tag{4.29}$$

thus, rewriting the last term of (4.1) by means of the Bethe-Salpeter equation, the grand-thermodynamic potential reads

$$\begin{aligned}\Omega[G] = &- L^d \int \frac{d^dk}{(2\pi)^d}\,\frac{1}{\beta}\sum_{\omega_n} \mathrm{Tr}\{-\ln[G(\mathbf{k},\omega_n)] + [G_1(\mathbf{k},\omega_n)^{-1}G(\mathbf{k},\omega_n) - 1]\} \\ &- L^d\frac{|\Delta|^2}{g_0} + \frac{1}{2}L^d \int \frac{d^dK}{(2\pi)^d}\,\frac{1}{\beta}\sum_{\Omega_n} \mathrm{Tr}\{-\ln[\Gamma(\mathbf{k},\omega_n)/g_0]\}.\end{aligned} \tag{4.30}$$

The internal energy and the particle number can be combined thus, using (4.19), (4.20), the mean-field Dyson equation (3.34) and the Bethe-Salpeter equation (4.18), we obtain

$$\begin{aligned}U[G,\Gamma] - \mu N[G] = &- L^d \int \frac{d^dk}{(2\pi)^d}\,\frac{1}{\beta}\sum_{\omega_n} \mathrm{Tr}\{(G_1(\mathbf{k},\omega_n)^{-1} + i\hbar\omega_n)G(\mathbf{k},\omega_n)\} \\ &- L^d\frac{|\Delta|^2}{g_0} - \frac{1}{2}L^d \int \frac{d^dK}{(2\pi)^d}\,\frac{1}{\beta}\sum_{\Omega_n} \mathrm{Tr}\{\Gamma(\mathbf{k},\omega_n)/g_0 - 1\}.\end{aligned} \tag{4.31}$$

The entropy functional (4.2) contains neither $G_0(\mathbf{k},\omega_n)$ nor $G_1(\mathbf{k},\omega_n)$, anyway we can simplify the

formula by using the Bethe-Salpeter equation [1]

$$\begin{aligned} S[G,\Gamma]/k_B = \beta L^d \int \frac{d^dk}{(2\pi)^d}\,\frac{1}{\beta}\sum_{\omega_n} \mathrm{Tr}\{-\ln[G(\mathbf{k},\omega_n)] + [-i\hbar\omega_n G(\mathbf{k},\omega_n) - 1]\} \\ + \frac{1}{2}\beta L^d \int \frac{d^dK}{(2\pi)^d}\,\frac{1}{\beta}\sum_{\Omega_n} \mathrm{Tr}\{\ln[\Gamma(\mathbf{k},\omega_n)/g_0] + [\Gamma(\mathbf{k},\omega_n)/g_0 - 1]\}. \end{aligned} \tag{4.32}$$

The mean-field approximation for the potentials can be obtained by substituting the matrix Green's function $G(\mathbf{k},\omega_n)$ by $G_1(\mathbf{k},\omega_n)$ and by neglecting all terms containing the vertex function. Thus, for the grand-thermodynamic potential, we obtain:

$$\Omega_{MF}[G] = -L^d \int \frac{d^dk}{(2\pi)^d}\,\frac{1}{\beta}\sum_{\omega_n} \mathrm{Tr}\{-\ln[G_1(\mathbf{k},\omega_n)] - L^d\frac{|\Delta|^2}{g_0}, \tag{4.33}$$

for the combination of the internal energy and the particle number we get the approximation

$$U_{MF}[G,\Gamma] = -L^d \int \frac{d^dk}{(2\pi)^d}\,\frac{1}{\beta}\sum_{\omega_n} \mathrm{Tr}\{(G_1(\mathbf{k},\omega_n)^{-1} + i\hbar\omega_n)G_1(\mathbf{k},\omega_n)\} - L^d\frac{|\Delta|^2}{g_0}, \tag{4.34}$$

finally for the mean-field entropy we obtain

$$S_{MF}[G,\Gamma]/k_B = \beta L^d \int \frac{d^dk}{(2\pi)^d}\,\frac{1}{\beta}\sum_{\omega_n} \mathrm{Tr}\{-\ln[G_1(\mathbf{k},\omega_n)] + [-i\hbar\omega_n G_1(\mathbf{k},\omega_n) - 1]\}. \tag{4.35}$$

4.4 Evaluation of the sums over the fermionic Matsubara frequencies

In all the thermodynamic functionals which have been derived in the previous sections appear sums over Matsubara frequencies of matrices of the type

$$A(\mathbf{k},\omega_n) = \begin{pmatrix} \mathcal{A}(\mathbf{k},\omega_n) & \mathcal{B}(\mathbf{k},\omega_n) \\ -\mathcal{B}(\mathbf{k},\omega_n)^* & \mathcal{A}(\mathbf{k},\omega_n)^* \end{pmatrix}. \tag{4.36}$$

Most of these sums are not well defined, in fact the functions which need to be summed do not decay to zero fast enough to make the series converge. However this problem can be avoided by performing a Fourier back transformation of the function from the frequencies ω_n to the imaginary time τ. The Fourier transformations results,in fact, to be finite for every τ, thus we can obtain a finite result from the Fourier back transformation by taking the limit $\tau \to 0^-$.

[1] If we simplify in the entropy functional the term involving the vertex function by using the Bethe-Salpeter equation we can easily see that the thermodynamic relation $\Omega = U - Ts - \mu N$ yields the same result for the grand-thermodynamic potential obtained within the formalism of Luttinger and Ward.

We define the sums in the functionals (4.29), (4.30) and (4.31) in the following way

$$\frac{1}{\beta}\sum_{\omega_n}\mathrm{Tr}\{A(\mathbf{k},\omega_n)\} = 2\mathcal{A}(\mathbf{k},\tau=-0), \tag{4.37}$$

where $\mathcal{A}(\mathbf{k},\tau)$ is assumed to be real and is defined as the Fourier transformation of function of the type $A(\mathbf{k},\omega_n) = -\ln[G(\mathbf{k},\omega_n)]$ or $A(\mathbf{k},\omega_n) = [G_0(\mathbf{k},\omega_n)^{-1}G(\mathbf{k},\omega_n) - 1]$. It is thus possible to compute the mean-field functionals (4.33), (4.34) and (4.35). In the grand canonical potential we have the sum

$$\sum_{\omega_n}\mathrm{Tr}\{-\ln[G_1(\mathbf{k},\omega_n)]\} = \sum_{\omega_n}\ln\left(-E_k^2-\hbar^2\omega_n^2\right),$$

which can be computed by taking the limit

$$\lim_{\tau\to 0^-}\sum_{\omega_n}e^{-i\omega_n\tau}\ln\left(-E_k^2-\hbar^2\omega_n^2\right) = \lim_{\tau\to 0^-}\left[-\frac{2}{|\tau|}+\ln\left(1+e^{\beta E_k}\right)\ln\left(1+e^{-\beta E_k}\right)\right]. \tag{4.38}$$

The result is obviously divergent in the limit $\tau\to 0^-$ but the series can be regularized by subtracting the free fermion result $\sum_{\omega_n}\ln[-(\varepsilon_k-\mu)^2-\hbar^2\omega_n^2]$, thus for the regularized sum we get the result

$$\sum_{\omega_n}\ln\left(\frac{-E_k^2-\hbar^2\omega_n^2}{-(\varepsilon_k^2-\mu)^2-\hbar^2\omega_n^2}\right) = \left[2\ln\left(1+e^{-\beta E_k}\right)+\beta E_k-\beta(\varepsilon_k-\mu)-2\ln\left(1+e^{-\beta\xi_k}\right)\right]. \tag{4.39}$$

The last term is the result in the limit $\Delta\to 0$, which is exactly the free fermions term which we subtracted to renormalize the sum, thus if we neglect the last logarithm in the (4.39), the grand thermodynamic potential reads:

$$\Omega_{MF} = -L^d\int\frac{d^dk}{(2\pi)^d}\left[E_k-(\varepsilon_k-\mu)\right]-\frac{1}{\beta}\int\frac{d^dk}{(2\pi)^d}\left[2\ln\left(1+e^{-\beta E_k}\right)\right]-L^d\frac{|\Delta|^2}{g_0}. \tag{4.40}$$

Using the same recipe we can calculate the mean-field approximation for the internal energy which reads:

$$U_{MF}-\mu N_{HF} = 2L^d\int\frac{d^dk}{(2\pi)^d}\left\{\frac{E_k}{1+e^{\beta E_k}}+\frac{1}{2}\left[E_k-(\varepsilon_k-\mu)\right]\right\}-L^d\frac{|\Delta|^2}{g_0}, \tag{4.41}$$

where

$$E_0 = -2L^d\int\frac{d^dk}{(2\pi)^d}\left\{\frac{1}{2}\left[E_k-(\varepsilon_k-\mu)\right]\right\}-L^d\frac{|\Delta|^2}{g_0} \tag{4.42}$$

reduces to the BCS condensation energy after the renormalization of the coupling constant $g_0\to g$ defined in (3.15). To get the energy functional in the form (4.41), we considered the first two terms of the functional (4.12) and the particle number, and used the relation

$$L^d\,g_0|\mathcal{F}(\mathbf{0},0)|^2 = 2L^d\,\Delta\int\frac{d^dk}{(2\pi)^d}\mathcal{F}(\mathbf{k},\tau=0)-L^d\frac{|\Delta|}{g_0}.$$

Looking at the entropy functional (4.35) we note that, multiplying the second term in the trace by $G_1^{-1}(\mathbf{k},\omega_n)\cdot G_1(\mathbf{k},\omega_n)$, we obtain exactly the argument of the trace in the internal energy functional (4.34). On the other hand, the first term of the mean-field entropy coincides with the first term in the mean-field grand thermodynamic potential. Combining the results (4.40) and (4.41) we obtain the mean-field expression for the entropy:

$$\begin{aligned} S_{MF}/k_B &= 2L^d \int \frac{d^dk}{(2\pi)^d}\left\{\ln\left(1+e^{-\beta E_k}\right)+\beta\frac{E_k}{1+e^{\beta E_k}}\right\} \\ &= -2L^d \int \frac{d^dk}{(2\pi)^d}\left\{(1-n_k)\ln(1-n_k)+n_k\ln n_k\right\}, \end{aligned} \tag{4.43}$$

where $n_k = 1/[1+\exp(\beta E_k)]$ is the Fermi distribution of the quasi-particles.

If we look more carefully at the equations (4.40) and (4.41) we note that the convergence of the integrals over the wave vector is assured by the term $L^d|\Delta|/g_0$, which compensates the divergence of the term $[E_k-(\varepsilon_k-\mu)]$. The regularization has been chosen in such a way that, in the non-interacting case, the results for the ideal Fermi gas are obtained, i.e. the term E_0 vanishes. On the other hand, the Entropy functional (4.43) does not need to be regularized.

4.5 Corrections to the mean-field approximation

In section 4.3 we derived the general form of the thermodynamics potentials of the system in ladder approximation and we got, starting from these functional, an explicit expression for the grand-thermodynamic potential, for the internal energy combined with the particle number and for the entropy of the system in mean-field approximation by computing the sums over the fermionic Matsubara frequencies. In the present section we will go beyond the mean-field approximation, in fact, while it describes correctly a fermionic system at zero temperature for arbitrary coupling strength [68], the mean-field approximation is not suited to describe properly the transition from the Fermi superfluidity to Bose-Einstein condensation at finite temperature. In fact, in this approximation the condensation and formation of pairs occurs at the same temperature and the superfluidity is destroyed by fermionic excitations. This picture describes correctly the system in the case of weak coupling, where the transition to superfluidity is driven by a gain in the potential energy associated to the formation of pairs, but doesn't apply when the interaction is sufficiently strong. In the latter case the transition from the normal to the superfluid system is driven by a gain in the kinetic energy, associated with the condensation of the pairs, which are formed at higher temperatures. A proper description of the BCS-BEC crossover at finite temperatures requires then to include excitations, which drive the superfluid parameter to zero without destroying pairs. The correction to the mean-field grand-thermodynamic potential, energy and entropy can be obtained by subtracting the mean-field functionals (4.40), (4.41) and (4.43) from the general formulas (4.33)- (4.35). This decomposition in a mean-field part plus a correction results to be very convenient for the numerical calculations. In fact, the Matsubara sums in the mean-field

approximation can be computed analytically, as has been shown in section 4.4 and we are left only with the integrals over the wave vectors which need to be computed numerically.

The most challenging part, at this stage, is the computation of the corrections $\Delta\Omega = \Omega - \Omega_{MF}$, $\Delta S = S - S_{MF}$ and $\Delta(U - \mu N) = U - U_{MF} - \mu(N - N_{MF})$. If we write the difference explicitly, we obtain for the grand thermodynamic potential the following correction

$$\begin{aligned}\Delta\Omega = &- L^d \int \frac{d^d k}{(2\pi)^d} \frac{1}{\beta} \sum_{\omega_n} \mathrm{Tr}\{-\ln[G_1(\mathbf{k},\omega_n)^{-1} G(\mathbf{k},\omega_n)] + [G_1(\mathbf{k},\omega_n)^{-1} G(\mathbf{k},\omega_n) - 1]\} \\ &+ \frac{1}{2} L^d \int \frac{d^d K}{(2\pi)^d} \frac{1}{\beta} \sum_{\Omega_n} \mathrm{Tr}\{-\ln[\Gamma(\mathbf{K},\Omega_n)/g_0]\} \,,\end{aligned} \tag{4.44}$$

the correction for the combination of the internal energy and the particle number read

$$\begin{aligned}\Delta U - \mu\Delta N = &- L^d \int \frac{d^d k}{(2\pi)^d} \frac{1}{\beta} \sum_{\omega_n} \mathrm{Tr}\{[G_1(\mathbf{k},\omega_n)^{-1} + i\hbar\omega_n][G(\mathbf{k},\omega_n) - G_1(\mathbf{k},\omega_n)]\} \\ &- \frac{1}{2} L^d \int \frac{d^d K}{(2\pi)^d} \frac{1}{\beta} \sum_{\Omega_n} \mathrm{Tr}\{[\Gamma(\mathbf{K},\Omega_n)/g_0 - 1]\} \,,\end{aligned} \tag{4.45}$$

and the correction for the entropy is given by

$$\begin{aligned}\Delta S/k_B = &\beta L^d \int \frac{d^d k}{(2\pi)^d} \frac{1}{\beta} \sum_{\omega_n} \mathrm{Tr}\{-\ln[G_1(\mathbf{k},\omega_n)^{-1} G(\mathbf{k},\omega_n)] + (-i\hbar\omega_n)[G(\mathbf{k},\omega_n) - G_1(\mathbf{k},\omega_n)]\} \\ &- \frac{1}{2}\beta L^d \int \frac{d^d K}{(2\pi)^d} \frac{1}{\beta} \sum_{\Omega_n} \mathrm{Tr}\{-\ln[\Gamma(\mathbf{K},\Omega_n)/g_0] + [\Gamma(\mathbf{K},\Omega_n)/g_0 - 1]\} \,.\end{aligned} \tag{4.46}$$

In formulas (4.44)-(4.46) the sums over the fermionic Matsubara frequencies ω_n converge so that the regularization described in section 4.4 is not needed. However, the sums over the bosonic Matsubara frequencies Ω_n are not well defined and must be regularized. Thus, for a numerical evaluation the formulas (4.44)-(4.46) must be transformed further, which will be done in section 4.6.

4.6 Renormalization of the thermodynamic potentials

The formulas derived in the sections 4.4 and 4.5 are still divergent and need a further renormalization, in fact the term $1/g_0$ diverges thus the interaction strength has to be replaced by the scattering amplitude g following (3.15).

First we look at the mean-field formulas (4.40)- (4.43). As has been already pointed out, the formulas are finite except for the term defined by (4.42). The condensation energy E_0 is composed by two diverging terms, an infinite integral and a term proportional to $1/g_0$, which compensate each other.

After the renormalization of the coupling constant $1/g = 1/g_0 + \int d^dk/(2\pi)^d m/(\hbar^2\mathbf{k}^2)$ we obtain

$$E_0 = -2L^d \int \frac{d^dk}{(2\pi)^d} \left\{ \frac{1}{2}\left[E_k - (\varepsilon_k - \mu)\right] - \frac{|\Delta|^2}{2\varepsilon_k} \right\} - L^d \frac{|\Delta|^2}{g}. \tag{4.47}$$

In this expression for the condensation energy both the integral over the wave vector and the last term converge separately[2].

The next step is to regularize the correction to the mean-field functionals (4.44)- (4.46). We start with the last term of the correction to the grand thermodynamic potential (4.44). The logarithm containing the interaction strength g_0 can be rewritten as

$$\ln\left[\Gamma(\mathbf{K}, \Omega_n)/g_0\right] = \ln\left[\Gamma(\mathbf{K}, \Omega_n)/g\right] + \ln[1\, g/g_0].$$

The second logarithm does not depend on the bosonic Matsubara frequencies thus the back Fourier transformation of this term is proportional to

$$\frac{1}{\beta}\sum_{\Omega_n} e^{-i\Omega_n\tau} = \sum_n \delta(\tau/\hbar + n\beta) = \delta_B(\tau/\hbar) \tag{4.48}$$

hence, following what had been already done in section 4.4, the sum defined as

$$\frac{1}{\beta}\sum_{\Omega_n} \mathrm{Tr}\{A(\mathbf{K}, \Omega_n)\} = 2\mathcal{A}(\mathbf{K}, \tau = -0) \tag{4.49}$$

vanishes. In the renormalized correction formula $\Delta\Omega[G]$ the last term can be thus replaced by

$$\frac{1}{2} L^d \int \frac{d^dK}{(2\pi)^d} \frac{1}{\beta}\sum_{\Omega_n} \mathrm{Tr}\{-\ln[\Gamma(\mathbf{K}, \Omega_n)/g]\}. \tag{4.50}$$

Finally the complete renormalized correction to the mean-field functional for the grand thermodynamic potential reads

$$\begin{aligned} \Delta\Omega = &- L^d \int \frac{d^dk}{(2\pi)^d} \frac{1}{\beta}\sum_{\omega_n} \mathrm{Tr}\{-\ln[G_1(\mathbf{k}, \omega_n)^{-1} G(\mathbf{k}, \omega_n)] + [G_1(\mathbf{k}, \omega_n)^{-1} G(\mathbf{k}, \omega_n) - 1]\} \\ &+ \frac{1}{2} L^d \int \frac{d^dK}{(2\pi)^d} \frac{1}{\beta}\sum_{\Omega_n} \mathrm{Tr}\{-\ln[\Gamma(\mathbf{K}, \Omega_n)/g]\}\,. \end{aligned} \tag{4.51}$$

The integral over the wave vector is finite and can be computed without problem. However for the computation of the sum over the bosonic Matsubara frequencies, the definition (4.49) has to be used.

Next we have to renormalize the second term of the correction (4.45). Using the Bethe-Salpeter equation $\Gamma(\mathbf{K}, \Omega_n) = g_0 - g_0\chi(\mathbf{K}, \Omega_n)\Gamma(\mathbf{K}, \Omega_n)$, we can rewrite the trace as the product of the matrix

[2]The integrals over the wave vector in all the formulas that we will use are convergent in any dimension $2 < d < 4$

vertex function Γ and the pair propagator χ. Furthermore, we can rewrite the pair propagator as product of one-particle Green's function by using definition (3.14). By interchanging the order of integration we can then combine the vertex function and the Green's function into the particle-particle contribution of the self-energy by using $\Sigma(\mathbf{r},\tau) = G(-\mathbf{r},-\tau)\Gamma(\mathbf{r},\tau)$. Finally, by means of the Dyson equation $G(\mathbf{k},\omega_n)^{-1} = G(\mathbf{k},\omega_n)_0^{-1} - \Sigma_1 - \tilde{\Sigma}(\mathbf{k},\omega_n) = G(\mathbf{k},\omega_n)_1^{-1} - \tilde{\Sigma}(\mathbf{k},\omega_n)$, we can replace the self-energy in favor of the Green's function G and the mean-field Green's function G_1. Thus, we get

$$
\begin{aligned}
&- L^d \int \frac{d^dK}{(2\pi)^d}\, \frac{1}{\beta} \sum_{\Omega_n} \mathrm{Tr}\,\{\Gamma(\mathbf{K},\Omega_n)/g_0 - 1\} \\
&= L^d \int \frac{d^dK}{(2\pi)^d}\, \frac{1}{\beta} \sum_{\Omega_n} \mathrm{Tr}\,\{\Gamma(\mathbf{K},\Omega_n)\chi(\mathbf{K},\Omega_n)\} \\
&= L^d \int \frac{d^dK}{(2\pi)^d}\, \frac{1}{\beta} \sum_{\Omega_n} \sum_{\alpha\alpha'} \left\{ \Gamma_{\alpha\alpha'}(\mathbf{K},\Omega_n) \cdot \int \frac{d^dk}{(2\pi)^d}\, \frac{1}{\beta} \sum_{\omega_n} G_{\alpha\alpha'}(\mathbf{K}-\mathbf{k},\Omega_n-\omega_n) G_{\alpha\alpha'}(\mathbf{k},\omega_n) \right\} \\
&= L^d \int \frac{d^dk}{(2\pi)^d}\, \frac{1}{\beta} \sum_{\omega_n} \sum_{\alpha\alpha'} \left\{ \int \frac{d^dK}{(2\pi)^d}\, \frac{1}{\beta} \sum_{\Omega_n} G_{\alpha\alpha'}(\mathbf{K}-\mathbf{k},\Omega_n-\omega_n) \Gamma_{\alpha\alpha'}(\mathbf{K},\Omega_n) \cdot G_{\alpha\alpha'}(\mathbf{k},\omega_n) \right\} \\
&= L^d \int \frac{d^dk}{(2\pi)^d}\, \frac{1}{\beta} \sum_{\omega_n} \mathrm{Tr}\left\{ \tilde{\Sigma}(\mathbf{k},\omega_n) G(\mathbf{k},\omega_n) \right\} \\
&= L^d \int \frac{d^dk}{(2\pi)^d}\, \frac{1}{\beta} \sum_{\omega_n} \mathrm{Tr}\left\{ G_1^{-1}(\mathbf{k},\omega_n) \left[G(\mathbf{k},\omega_n) - G_1(\mathbf{k},\omega_n) \right] \right\}.
\end{aligned}
\tag{4.52}
$$

In the equalities (4.52) we replaced, by inverting the order of integration the bosonic integral and the bosonic Matsubara sum, by fermionic ones thus it is now possible to combine the first term and the second term of the functional (4.45). Hence, noting that $G_1^{-1}(\mathbf{k},\omega_n) + 2i\hbar\omega_n = G_1^{-1}(\mathbf{k},-\omega_n)$, we can considerably simplify the correction $\Delta U - \mu\Delta N$ to get:

$$
\Delta U - \mu\Delta N = -\frac{1}{2} L^d \int \frac{d^dk}{(2\pi)^d}\, \frac{1}{\beta} \sum_{\omega_n} \mathrm{Tr}\{G_1^{-1}(\mathbf{k},-\omega_n)[G(\mathbf{k},\omega_n) - G_1(\mathbf{k},\omega_n)]\}. \tag{4.53}
$$

Again the integral is finite while to perform the sum over the fermionic frequencies we need to use definition (4.37).

Concerning the correction to the entropy, we can rewrite the second term in the first integral of the functional (4.46) as

$$
-\left[i\hbar\omega_n + G_1^{-1}(\mathbf{k},\omega_n) \right] [G(\mathbf{k},\omega_n) - G_1(\mathbf{k},\omega_n)] + G_1^{-1}(\mathbf{k},\omega_n)[G(\mathbf{k},\omega_n) - G_1(\mathbf{k},\omega_n)].
$$

The first term results to be the same as the first term in the energy functional, hence we can combine the integral of this term with the last term of (4.46) and renormalize it by using the result (4.52). Furthermore, we can use (4.50) to renormalize the other diverging logarithm in the formula (4.46).

Putting the two results together we get the renormalized form of the correction to the mean-field entropy [3]:

$$\begin{aligned}\Delta S/k_B =& \beta L^d \int \frac{d^d k}{(2\pi)^d} \frac{1}{\beta} \sum_{\omega_n} \mathrm{Tr}\{-\ln[G_1(\mathbf{k},\omega_n)^{-1} G(\mathbf{k},\omega_n)] + [G_1(\mathbf{k},\omega_n)^{-1} G(\mathbf{k},\omega_n) - \mathbb{I}] \\ &- \frac{1}{2}\beta L^d \int \frac{d^d k}{(2\pi)^d} \frac{1}{\beta} \sum_{\omega_n} \mathrm{Tr}\{G_1^{-1}(\mathbf{k},\omega_n)[G(\mathbf{k},\omega_n) - G_1(\mathbf{k},\omega_n)]\} \\ &- \frac{1}{2}\beta L^d \int \frac{d^d K}{(2\pi)^d} \frac{1}{\beta} \sum_{\Omega_n} \mathrm{Tr}\{-\ln[\Gamma(\mathbf{K},\Omega_n)/g]\} \,.\end{aligned} \tag{4.54}$$

The final results for the thermodynamic potential can be written by putting together the mean-field result (4.40)-(4.43) and the correction formulas (4.51)-(4.54). Each term of the general formulas $\Omega = \Omega_{MF} + \Delta\Omega$, $S = S_{MF} + \Delta S$ and $\Delta(U - \mu N) = U - U_{MF} - \mu(N - N_{MF})$ is now finite and can be numerically computed.

[3] The same result can be obtained by using the thermodynamic relation $\Omega = U - TS - \mu N$.

Chapter 5

Numerical results of the thermodynamic potentials

In the following we will use the results obtained in the previous Chapters and we will give an overview of the thermodynamics of the interacting fermionic system at arbitrary coupling in both the superfluid and the normal regime. We calculate the thermodynamic potential in the region of the phase diagram where the dimensionless temperature $\theta = k_B T/\varepsilon_F$ varies in the interval $0 < \theta \leq 0.5$ and the dimensionless coupling strength $\nu = 1/k_F a$ varies in the interval $-5 \leq \nu \leq 5$. We will also have a section focusing at the physics at the nontrivial point, usually called *unitary point*, where the scattering length of the system becomes infinite. Our numerical data will be then compared with other numerical and experimental results.

5.1 Entropy and pressure

From the knowledge of the Green's function and the vertex function, by combining the the mean-field formulas (4.40) and (4.43) and the correction to the mean-field approximation (4.44) and (4.54) derived in section 4.1, we are able to calculate the entropy and the pressure of the system.

In Figure 5.1 we show the entropy as a function of the dimensionless temperature $\theta = T/T_F$ at five different coupling constant starting from $\nu = -2$ in the weak coupling limit to $\nu = 2$ in the strong coupling limit. This picture highlights the multi-valued character of the entropy which has already been discussed before, moreover it is also to see a rather sharp drop in the entropy for values of the coupling constant $\nu \gtrsim 1$. Figures 5.2 and 5.3 depict a surface plot of the entropy as a function of the dimensionless temperature $\theta = T/T_F$ and the dimensionless coupling constant ν and a projection of this surface onto the ν-θ plane respectively. Looking at the three dimensional surface plot in Figure 5.2 one can clearly see that the drop in the entropy occurs in the region $-1 \lesssim \nu \lesssim 1$ where the Fermi gas becomes a bosonic gas of dimers. This feature is seen in the projection onto the ν-θ plane by a drastic change in the color indicating the value of $S/k_B T$. From the analysis of the entropy we can

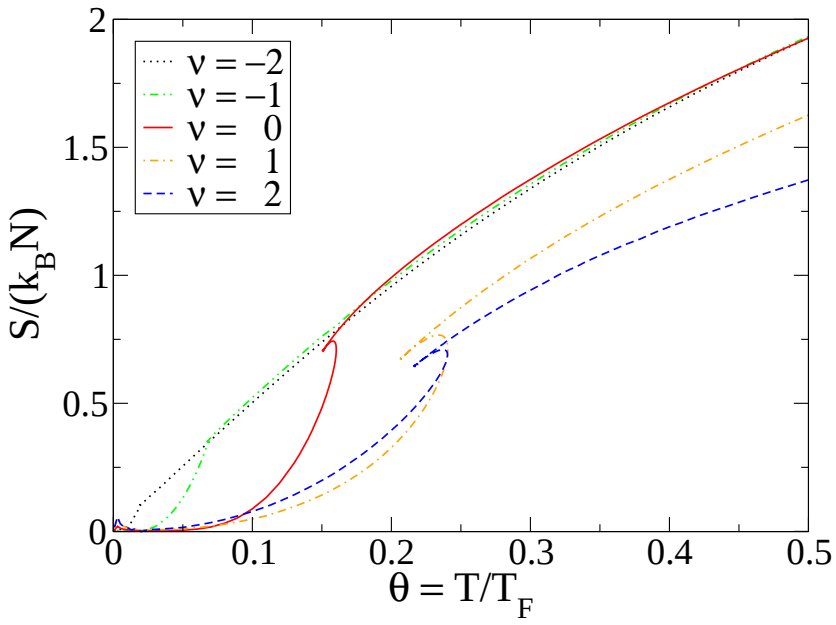

Figure 5.1: Entropy as a function of the dimensionless temperature $\theta = T/T_F$ at various coupling strength.

derive a criterion to determine the critical temperature of the super-fluid transition which is essentially equivalent to the one used in section 3.5. We use the fact that the entropy is continuous at T_c, hence the best approximation for the critical temperature is where the jump in the entropy between the two branches characterizing the super-fluid and the normal regime has a minimum. This criterion would lead to a curve for the critical temperature which is identical to the one depicted on Figure 3.5 by the full black line.

In Figures 5.4 and 5.5 we show the pressure of the system obtained from the formulas (4.40) and (4.51) for the grand thermodynamic potential by using the relation $p = -\Omega/V$. As can be noticed from the three dimensional view in Figure 5.4 also the pressure present a marked drop beyond $\nu \sim 1$ where the bosonic dimers dominate. At zero temperature and in the region of weak coupling $\nu \ll -1$ the numerics approaches the result of the ideal gas $p(T = 0)/n\varepsilon_F \to 2/5$. At higher temperatures, when the thermal energy is comparable with the binding energy $k_B T \sim O(\varepsilon_b = 2\varepsilon_F \nu^2)$ the pairs break up and on both sides we will have free fermions. In this regime the results approaches the Boltzmann limit over the whole crossover.

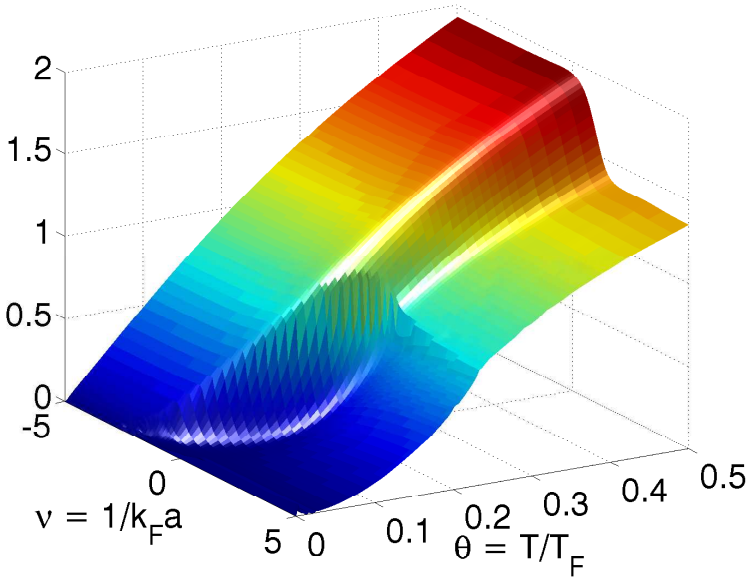

Figure 5.2: Entropy as a function of θ and ν obtained using the formulas (4.43) and (4.54).

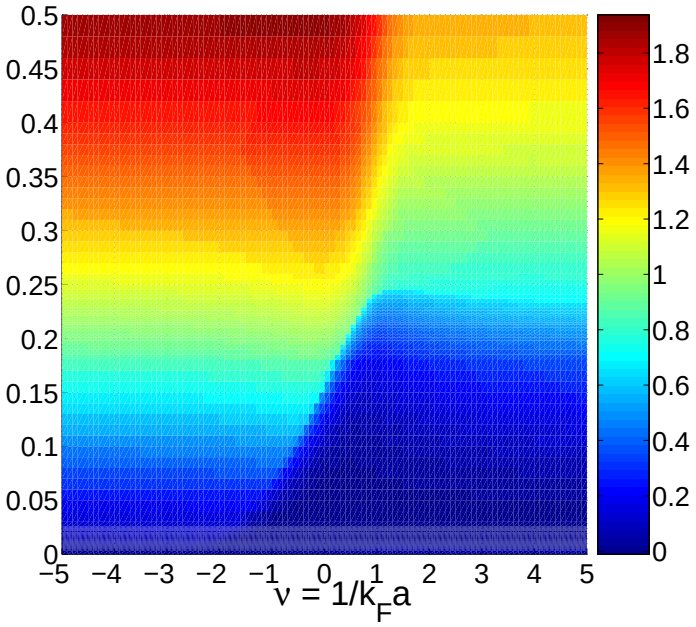

Figure 5.3: Entropy projected onto the θ-ν plane

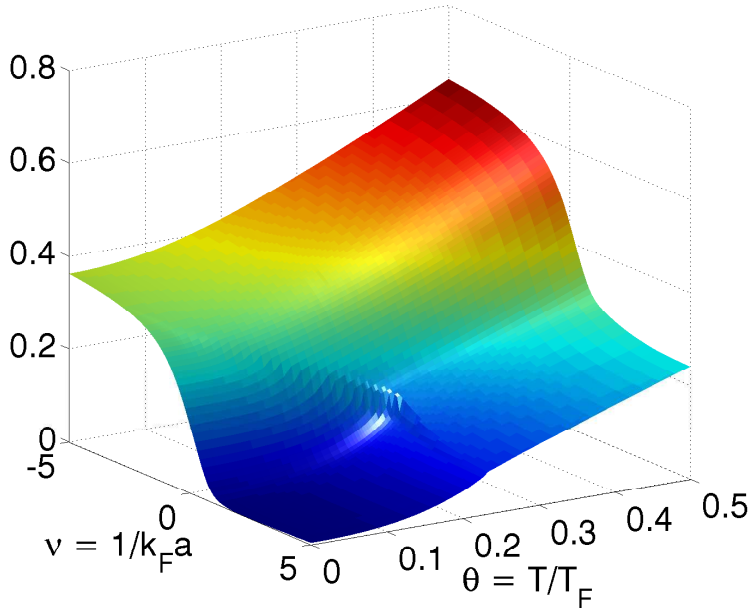

Figure 5.4: Pressure as a function of the dimensionless temperature $\theta = T/T_F$ at various coupling strength.

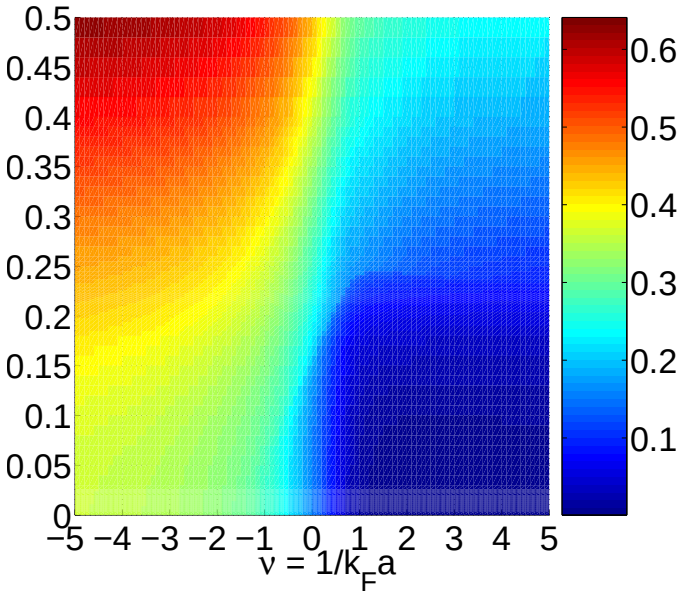

Figure 5.5: Projection of pressure onto the $\theta - \nu$ plane.

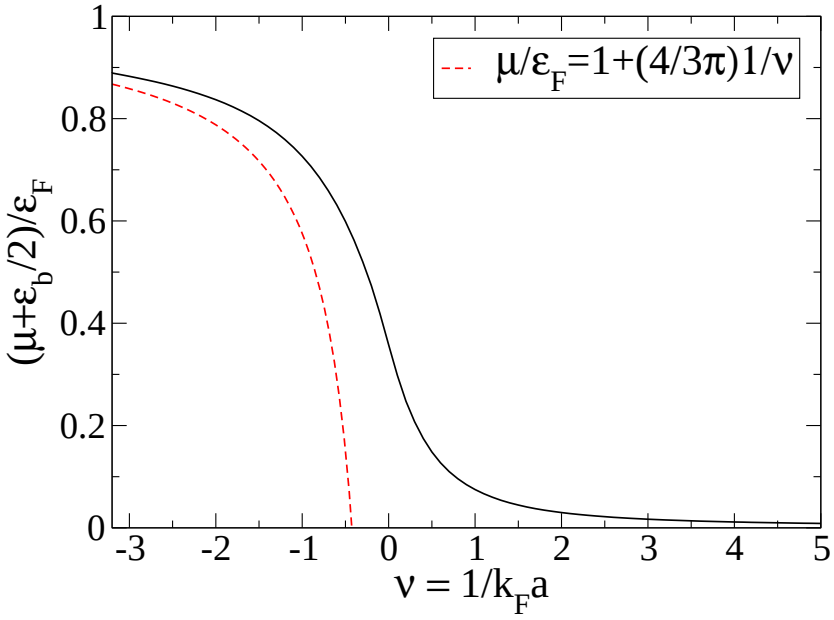

Figure 5.6: Chemical potential μ at the super-fluid transition as a function of the coupling constant $\nu = 1/k_F a$. On the Fermi side the numerical result is compared with the asymptotic result for the weakly interacting Fermi gas $\mu = \varepsilon_F[1 + (3/4\pi) \cdot 1/\nu]$. On the Bose side the difference $\mu + \varepsilon_b/2$ in units of the Fermi energy ε_F is plotted, where $\varepsilon_b/2 = \varepsilon_F \nu^2$.

5.2 Zero temperature results

In this section we will report about the parameters of the system as a function of the dimensionless coupling constant ν at zero temperature. These data are then compared with numerical and experimental results in section 5.4. The two parameter which, together with the critical temperature T_c, define the state of the system are the order parameter of the super-fluid transition Δ and the chemical potential μ. The first is an input parameter of the problem while the latter is calculated self-consistently by solving the set of equations (3.28).

The behavior of the chemical potential μ reflects directly the effects of BEC-BCS crossover. This can be clearly seen in Figure 5.6 and 5.7 where the chemical potential is plotted over the whole crossover. In Figure 5.6 is depicted the chemical potential μ as a function of the dimensionless coupling constant in units of the Fermi energy ε_F at zero temperature where we subtracted, on the Bose side, the binding energy of the pairs divided by two $\varepsilon_b/2 = \varepsilon_F \nu^2$. In the weak coupling limit the numerical results approach the result expected for an ideal Fermi gas $\mu \to \varepsilon_F$. As a comparison we show the correction to the chemical potential for weak couplings obtained in the Hartree-Fock

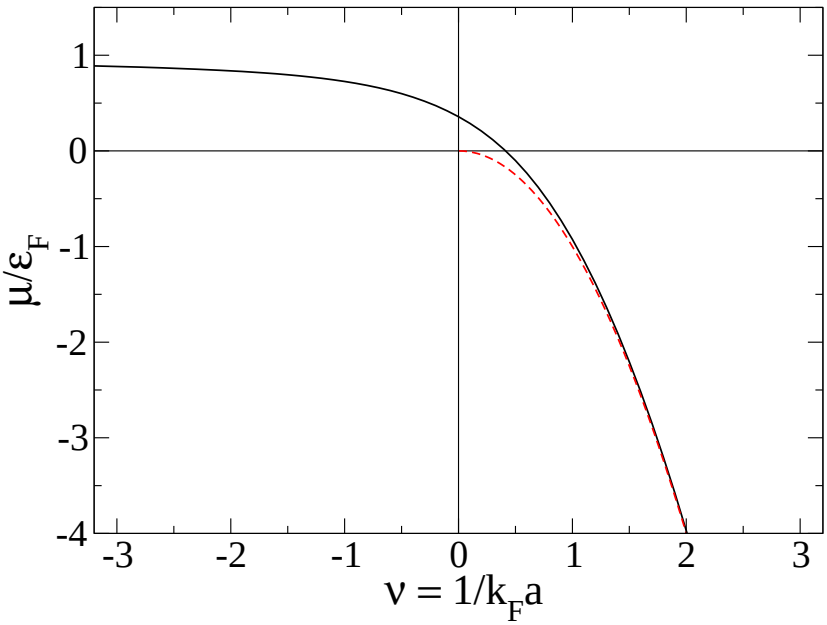

Figure 5.7: Typical behavior of the T = 0 chemical potential. As the pairing strength increases from 0, the chemical potential μ starts to decrease and then becomes negative. The coupling constant at which the chemical potential vanish is where the system changes from fermionic ($\mu > 0$) to bosonic ($\mu < 0$). The region comprised between this value and $\nu \sim -1$ defines the unitary region.

approximation which is given by the formula

$$\frac{\mu}{\varepsilon_F} = 1 + \frac{3}{4\pi} k_F a \tag{5.1}$$

and is represented by the dotted red line. On this side of the crossover there are essentially no bound pairs, the system is a Fermi liquid and only below the critical temperature T_c there will be a few cooper pairs. In Figure 5.7 the chemical potential μ is compared, on the Bose side, with the binding energy (red-dashed line). In the strong coupling limit $1/k_F a \gg 1$ the fermions are bound together into dimers and we expect $\mu \to -\varepsilon_b/2 = -\varepsilon_F \nu^2$. The full line approaches the red-dashed line from above for $\nu \to \infty$, hence the difference $\mu + \varepsilon_b/2$ is positive and represent an energy due to the repulsive interaction of the pairs. Clearly for coupling strengths $\nu \gg 1$ the absolute value of the chemical potential μ is much greater than the Fermi energy $\mu \ll -\varepsilon_F$. This means that the dimers need more than a Fermi energy ε_F to break into two free fermions and so the quantum fluctuation are too weak to break up the pairs. We can then conclude that, if the system is at a temperature which is smaller than the dissociation temperature $k_B T^* \sim \varepsilon_b$, the fermions are bound into pairs and the system behaves like a Bose gas.

The value of the dimensionless coupling constant where the chemical potential μ vanishes can be

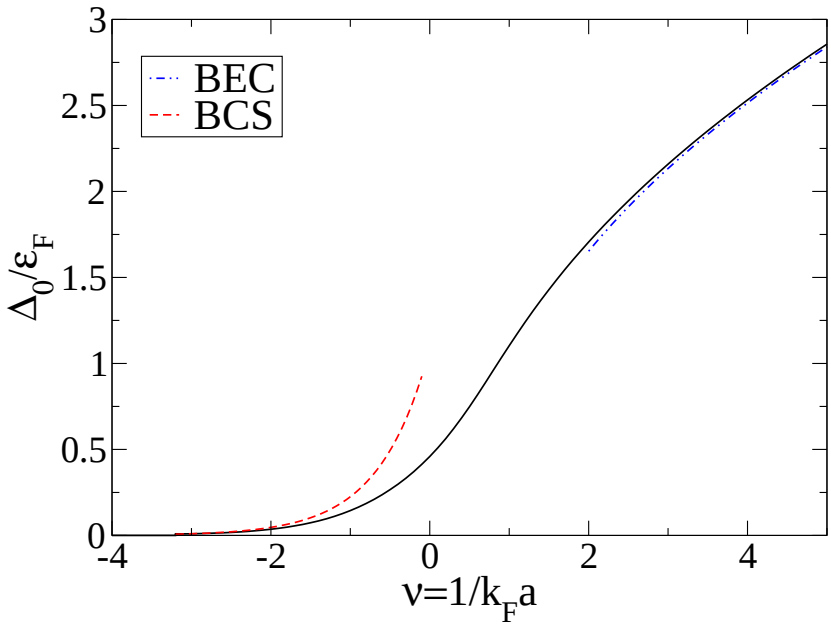

Figure 5.8: Order parameter at zero temperature as a function of the dimensionless coupling constant (solid black line). The numerical result are compared with the BCS result $\Delta^{(BCS)}(T = 0)/\varepsilon_F = 8/e^2 \exp(-\pi/2k_F|a|)$ (red dashed line) in the weak coupling limit and with the square root behaviour $\Delta(T = 0) = \varepsilon_F \sqrt{16/3\pi k_F|a|}[1 - 1/2^{1/2}(8/3\pi k_F a)^{3/2}]$ (blue dash-dotted line) in the strong coupling limit.

viewed as a crossing point. For positive values of μ the system has a remnant Fermi surface, and we say that it is "fermionic". For negative μ, the Fermi surface is gone and the material is "bosonic". In our calculation this crossing point occurs at the value $\nu \approx 0.41$.

The order parameter of the super-fluid transition at zero temperature is shown in Figures 5.8. Its behaviour in the two limits, is clearly visible in the plot where our numerical result is compared with the limits for $\nu \gg 1$ and $\nu \ll -1$. The black solid line represent the gap as a function of the dimensionless coupling constant at zero temperature. The curve is compared for $\nu \lesssim -1$ with the BCS-result (red dashed line)

$$\Delta^{(BCS)}(T = 0) = \frac{8\varepsilon_F}{e^2} \exp(-\pi/2k_F|a|),$$

which has already been derived in section 3.3. In the strong coupling region the gap is related to the boson order parameter Ψ_B via (3.50). For zero temperature the order parameter for the bosonic system can be explicitly calculated [17]

$$|\Psi_B|^2 = \frac{n_F}{2} \cdot \left\{ 1 - \sqrt{\frac{1}{2}} \cdot \left[\frac{8}{3\pi} k_F a \right]^{3/2} \right\}. \tag{5.2}$$

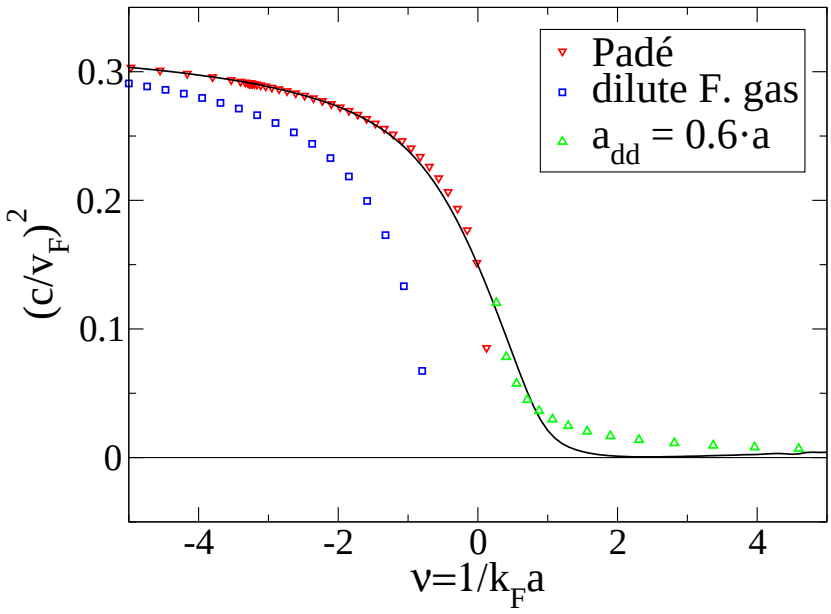

Figure 5.9: Isothermal sound speed $mc^2 = \partial p/\partial n$ as a function of $\nu = 1/k_F a$ for $T = 0$. The different curves are explained in the main text.

Combining the two results (3.50) and (5.2) we obtain for the order parameter in the strong coupling regime $\nu \gg 1$ the approximation

$$\Delta(T=0) = \varepsilon_F \sqrt{16/3\pi k_F|a| \cdot \left(1 - \sqrt{\frac{1}{2}} \cdot \left(\frac{8}{3\pi} k_F a\right)^{3/2}\right)}. \tag{5.3}$$

The asymptotic behaviour defined by (5.3) is is represented in Figure 5.8 by the blue dot-dashed line.

Another interesting quantity, which can be derived starting from our numerical results is the sound speed. At low temperatures the entropy has to vanish, in accordance with the third law of thermodynamics. The way it does, is in fact universal along the full BCS-BEC crossover. Indeed, at low temperatures, the two-component Fermi gas is in a super-fluid state, independent of the strength of the attractive interaction. On quite general grounds therefore, the low lying excitations above the ground state are sound modes of the Bogoliubov-Anderson type, which are the Goldstone modes of the broken gauge symmetry in a neutral super-fluid. These sound modes give rise to an entropy

$$S(T) = V \frac{2\pi^2}{45} k_B \left(\frac{k_B T}{\hbar c}\right)^3 + \dots \tag{5.4}$$

which vanishes like T^3 for arbitrary coupling strength. The constant c in (5.4) is the sound speed which is constant at low temperatures and may be determined from the pressure via the relation $mc^2 = \partial p/\partial n$.

We can thus obtain the curve of the sound velocity over the whole crossover by deriving the numerical data of the calculated pressure. Figure 5.9 displays $(c/v_F)^2$ at $T = 0$ as a function of coupling strength in units of the the Fermi velocity v_F. The dilute interacting Fermi gas limit $(c/v_F)^2 = (1 + 2/(\pi\nu))/3$ and the BEC limit $(c/v_F)^2 = k_F a_{dd}/(6\pi)$ for $a_{dd} = 0.62a$ are represented by the blue squares and the green triangles respectively. The red triangles are obtained by extending the expression of the ground state energy of a dilute weakly interacting Fermi gas [69, 70] with the help of a Padé approximation to the strong coupling regime [71, 72]

$$\frac{E}{\varepsilon_F N} \simeq \frac{3}{5} + \frac{\frac{2}{3\pi}k_F a}{1 - \frac{6}{35\pi}(11 - 2\ln 2)k_F a} \tag{5.5}$$

and the thermodynamic identity

$$c^2 = \frac{1}{m}\frac{\partial}{\partial n}\left(n^2 \frac{\partial E/N}{\partial n}\right) . \tag{5.6}$$

The agreement of our numerical result with the Padé approximation on the negative side of the crossover up to the point where the dimensionless coupling constant becomes zero is surprisingly good. However in the regime defined by $\nu \gtrsim 1$ our result underestimate the pressure and consequently the sound speed which is derived from it.

5.3 Unitary limit

A nontrivial point of the phase diagram is where the scattering length becomes infinite, or equivalently when the parameter which tunes the strength of the interaction, the dimensionless coupling constant $\nu = 1/k_F a$, vanishes. This point is essentially where the Feshbach resonance lies, here the full many-body problem is characterized by a single energy scale given by the Fermi energy ε_F. A consequence of this feature is that the free energy per particle in units of the Fermi energy ε_F, and thus all the thermodynamic quantities, is an universal function of the ratio $\theta = k_B T/\varepsilon_F$ [73].

The study the physics near a Feshbach resonance is a very interesting problem because, from a theoretical point of view the many body problem at unitarity is still not completely understood. On the other hand the big effort that in the last few years many groups put in studying the problem gives us the possibility to compare our results with a few experimental and numerical data obtained independently.

On the theoretical side, fixed node Green's function Monte Carlo calculations provide for an homogeneous system at zero temperature reliable results for the gap parameter [74] [75], the equation of state [76], the momentum distribution, condensate fraction and pair size [77] of the ground state for arbitrary values of the dimensionless coupling strength. Numerical calculations of the negative Hubbard model provide the critical temperature the energy and the chemical potential at unitarity. Further, field-theoretic results at finite temperature have been recently obtained by Nishida [87, 88, 89] and Nikolić and Sachdev [90].

As we already mentioned, within the zero range pseudo-potential formulation of the crossover, at

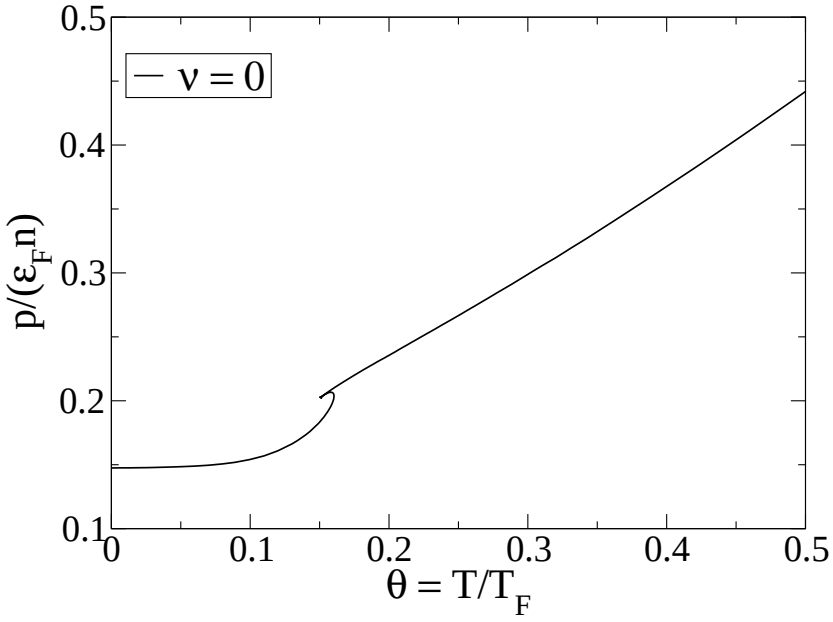

Figure 5.10: Pressure at unitarity as a function of the dimensionless temperature $\theta = T/T_F$ calculated using (4.40) and (4.51).

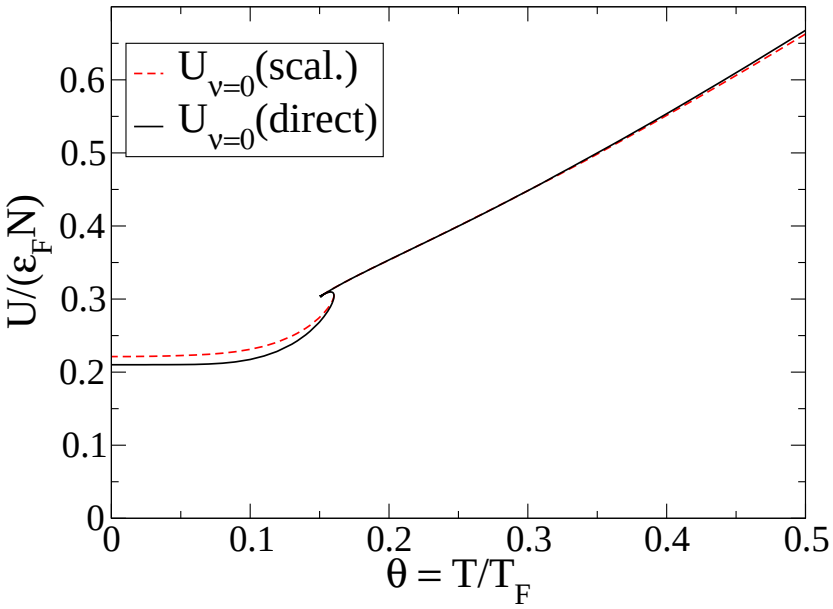

Figure 5.11: Energy at unitarity as a function of the dimensionless temperature $\theta = T/T_F$ calculated using (4.41) and (4.53).The red dashed curve is obtained from the calculated pressure using the scaling formula $U = \frac{3}{2}pV$ valid at unitarity.

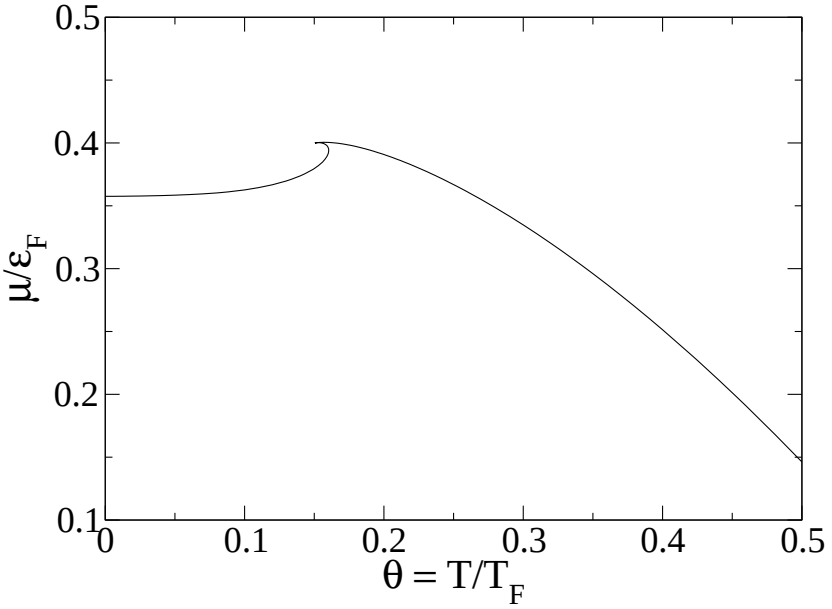

Figure 5.12: Chemical potential at unitarity as a function of the dimensionless temperature $\theta = T/T_F$.

the point $\nu = 1/k_F a = 0$ the only relevant length scale is the Fermi wave length set by the density and the energy scale is determined by the Fermi energy ε_F. All the thermodynamic functions acquire thus a self-similar form [73]

$$F(T, V, N) = f(\theta) N \varepsilon_F. \tag{5.7}$$

In this section we report a series of plots which depict the behaviour of some thermodynamic quantities at the unitary point as a function of the dimensionless temperature $\theta = T/T_F$. Figure 5.10 shows the pressure obtained from the calculated values for the grand-thermodynamic potential by using the formulas (4.40) and (4.51) and the relation $p = -\Omega/V$. In Figure 5.11 is depicted the temperature dependence of the internal energy calculated in two different ways. The solid black line is the numerical result obtained from the formulas (4.41) and (4.53). As comparison in the same Figure we show (red dashed line) the result obtained from the calculated pressure by using the scaling relation $U = 3/2pV$ valid at the unitary point. Above T_c the scaling is fulfilled perfectly, however below T_c we note a violation of the scaling law which is a consequence of the fact that we forced the Thouless criterion for $T < T_c$.

The chemical potential at unitarity as a function of the dimensionless temperature is depicted in Figure 5.12. Below the critical temperature T_c the chemical potential $\mu(T/T_F)$ is an increasing function, this behaviour can be understood from the fact that the thermodynamic at low temperature is determined by the Bogoliubov-Anderson modes. In fact at a given volume and for all the values of the coupling constant $\nu = 1/k_F a$ the chemical potential can be related to the entropy and via the Maxwell

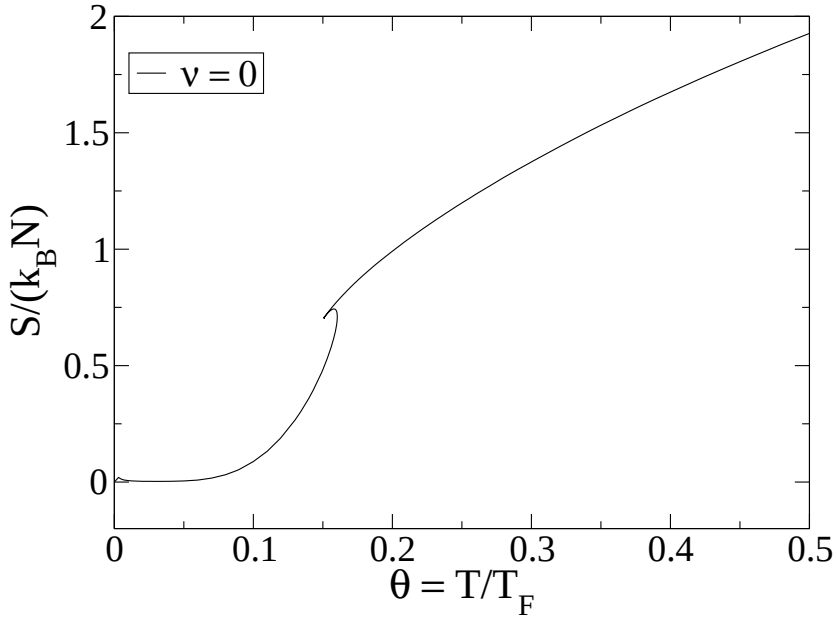

Figure 5.13: Entropy at unitarity as a function of the dimensionless temperature $\theta = T/T_F$ calculated using (4.43) and (4.54).

relation

$$\left.\frac{\partial\mu}{\partial T}\right|_{N,V} = -\left.\frac{\partial S}{\partial N}\right|_{T,V}. \tag{5.8}$$

In this way we can connect the temperature dependence of the chemical potential to the density dependence of the entropy. According to (5.4), the entropy approaches zero with the power law $\sim T^3$ thus the relation (5.8) shows that at low temperatures the chemical potential exhibits a T^4 dependence with a pre-factor determined by

$$\frac{\partial\mu}{\partial T} = \frac{3S}{2Vmc_s^2}\frac{\partial^2 p}{\partial n^2} > 0\,. \tag{5.9}$$

Obviously, this argument is not confined to the unitarity point, showing that the chemical potential at low T has a behaviour $\mu(T) = \mu(0) + O(T^4)$ for arbitrary coupling strengths along the BCS-BEC crossover. For completeness we plot again the curve of the entropy at unitarity as a function of the temperature which was discussed in section 5.1.

5.4 Comparison with theoretical and experimental results

The data at zero temperature, together with the thermodynamic potentials and their values at the unitary limit furnish information which allows us to compare our theory with recent experimental data, field theoretic results and numerical results provided by Monte Carlo simulations. A well documented

Table 5.1: Recent experimental results for β compared with calculated values.

		β
Experimental results	Bartenstein *et al.* [41]	$-0.68^{+0.13}_{-0.10}$
	Bourdel (2004) *et al.* [44]	−0.64(15)
	Duke (2005) [78]	−0.49(4)
	Partridge *et al.* [79]	−0.54(5)
Calculated values	Astrakharchik *et al.* [76]	−0.58(1)
	Carlson *et al.* [74, 75]	−0.56(1)
	Hu/Liu/Drummond [80]	−0.599
	Perali *et al.* [81]	−0.545
	Padé approximation [71, 72]	−0.67
	present work	−0.64

quantity which determines the density profile of dilute fermions in a trap at unitarity and T = 0 is the so called β parameter defined via

$$\mu(T = 0) = \varepsilon_F(1 + \beta) \, . \tag{5.10}$$

Very recently several experimental groups [41, 44, 78, 79] managed to measure this quantity in trapped fermionic gases. All the experimental results for the $\beta-$parameter are relatively close to each other and compatible within the error bars. That being so, its numerical estimation assumes a big relevance. Our value of $\beta \sim -0.640$ is very close to $\beta = -0.67$ obtained via simply Padé approximating the weak coupling result for the ground state energy [71, 72] and the experimental results of Bartenstein *et al.* [41] $\beta = -0.68^{+0.13}_{-0.10}$ and Bourdel *et al.* [44] $\beta = -0.64 \pm 15$ but smaller than the results obtained at Duke [78], at Rice [79] (see Table 5.1) and recent QMC results [74, 75, 76] (see Table 5.3). Currently experimental uncertainties however preclude a detailed comparison with theoretical results. A promising route in the direction of thermometry for trapped gases is provided via the reversible adiabatic (isentropic) sweeps [41, 82] from the BEC limit. In Fig. 5.14 we depict the resulting changes in temperature when moving across the unitarity limit for the homogeneous case. For the trapped case this cooling mechanism was first advocated by Carr *et al.* [83] and recently quantitatively refined by Hu *et al.* [84].

Finally, to facilitate quantitative comparison with various Quantum Monte Carlo and field-theoretic results, we have collected available data from the literature. In Table 5.1 we collect data at the critical temperature T_c taken from Burovski *et al.* [85] and Bulgac *et al.* [86]. Field-theoretic results have been obtained very recently by Nishida [87, 88, 89] and by Nikolić and Sachdev [90]. Apart from the value for T_c which is explicitly quoted in the paper by Bulgac (with errors) we have estimated the remaining quantities from their presented results and utilized the scaling relation $U = 3/2pV$ valid at unitarity to fill in the missing data below. The $T = 0$ results are fixed node QM results by Astrakharchik *et al.* [76] and Carlson *et al.* [74, 75].

Our results are in excellent agreement with those of Burovski *et al.* except for the value of the

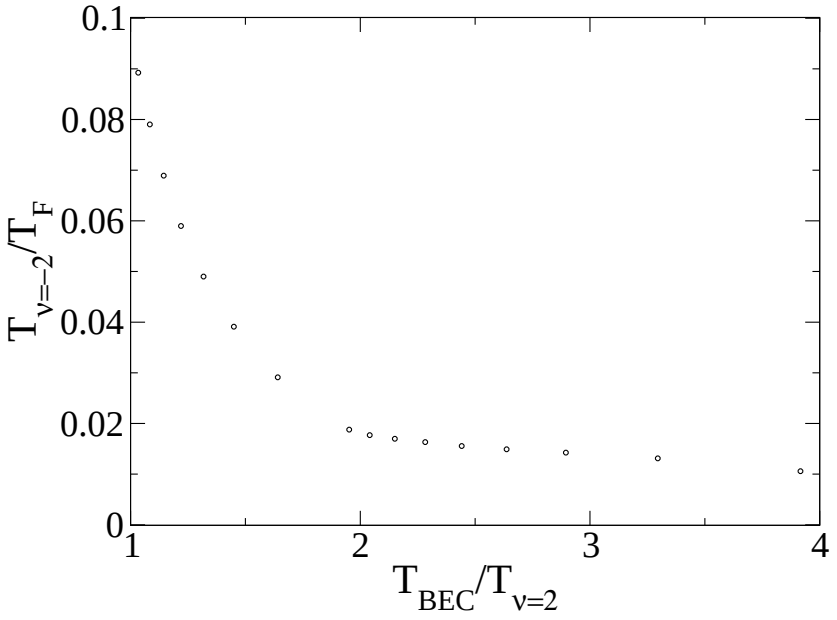

Figure 5.14: Temperature reduction on performing an isentropic sweep across $v = 0$ from $v = 2$ to $v = -2$.

Table 5.2: Comparison with diagrammatic determinant Monte Carlo (Burovski *et al.* [85]), quantum Monte Carlo (Bulgac *et al.* [86]), $\varepsilon = 4 - d$ expansion (Nishida and Son [87, 88, 89]), Borel-Padé approximation connecting an expansion in $\varepsilon = 4 - d$ and one in $\varepsilon = d - 2$ [87]) and a $1/N$ expansion (Nikolić and Sachdev)[90] at $T = T_c$.

	T_c/ε_F	μ/ε_F	$U/N\varepsilon_F$	$P/n\varepsilon_F$	S/N
Bulgac	0.23(2)	0.45	0.41	0.27	0.99
Burovski	0.152(7)	0.493(14)	0.31(1)	0.207(7)	–
Nikolić ($N = 1$)	0.136	0.585	0.164	0.109	
Nishida ($\varepsilon = 1$)	0.249	0.18	0.212	0.135	0.698
Borel-Padé	0.183	0.294	0.270	0.172	0.642
present work	0.160	0.394	0.304	0.204	0.71

Table 5.3: Comparison with fixed node Green's function Monte Carlo (Astrakharchik *et al.* [76] and Carlson *et al.* [74, 75]) at $T = 0$.

	μ/ε_F	$U/N\varepsilon_F$	$P/n\varepsilon_F$	Δ
Astrakharchik	0.41(2)	0.25(1)	0.17(1)	
Carlson	0.43(1)	0.26(1)	0.17(1)	0.54
present work	0.36	0.21	0.15	0.46

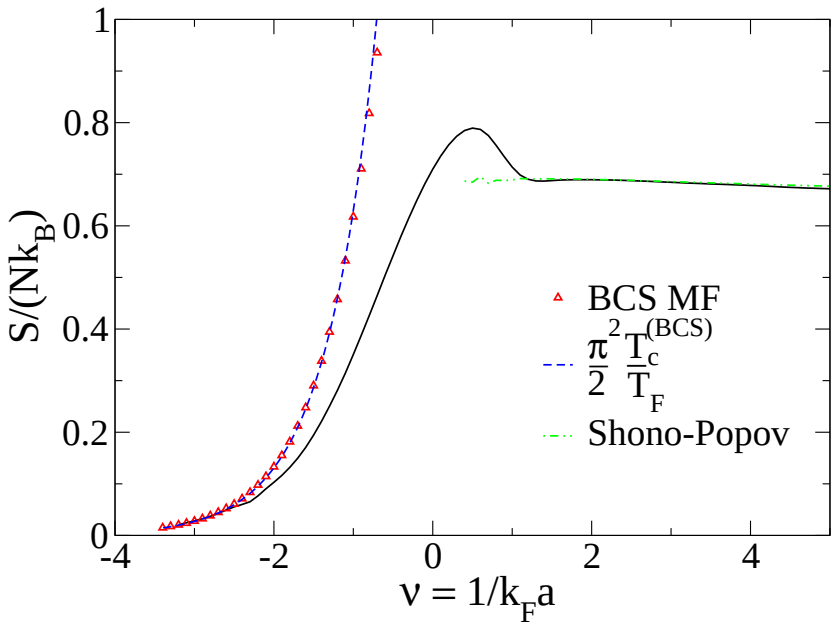

Figure 5.15: Entropy at T_c as a function of $\nu = 1/k_F a$. Numerical result (solid black) line obtained with (4.43) and (4.46) compared with the limiting results: the BCS mean-field result (red triangles) from (4.43) and (blue dashed) from (5.11) and the Shohno-Popov result (green dotted-dashed line) from (5.13) and (5.14).

dimensionless chemical potential μ/ε_F and that of the entropy per particle at T_c. Now Burovski *et al.* have obtained their values for the pressure $p/n\varepsilon_F$ and the entropy S/Nk_B indirectly from the internal energy and the chemical potential by using $3pV = 2U$ right at unitarity and the Gibbs-Duhem relation. The different results for the chemical potential then entail the considerable discrepancy in the value of S/Nk_B at T_c. For the entropy they obtain the value 0.2 ± 0.2 [91] which is meaningless due to the too large error bar. Within our numerical scheme, the chemical potential is the most directly - via (4.14) - obtainable quantity among the thermodynamic data.

In figure 5.15 is depicted the evolution of the of the entropy per particle $S(T_c)/Nk_B$ right at the critical temperature as a function of the dimensionless coupling $\nu = 1/k_F a$. In the BCS limit, the entropy associated with single particle excitations can be calculated from the exactly soluble reduced BCS-Hamiltonian and gives [57]

$$S(T_c)/Nk_B = (\pi^2/2)(T_c/T_F)\,. \tag{5.11}$$

Since the ratio T_c/T_F is exponentially small in the weak coupling limit, the entropy (5.11) associated with fermionic excitations is dominant compared to the contribution arising from the collective Bogoliubov-Anderson mode. Indeed, extrapolating the corresponding low temperature entropy (5.4)

associated with collective excitations up to the critical temperature gives rise to a contribution of order $(T_c/T_F)^3$, which is negligible compared to (5.11). At very large coupling strengths, where the strongly bound fermion pairs assumes the behaviour of Bose gas, for the entropy at right at the transition temperature we obtain the universal number

$$S(T_c)/Nk_B = \frac{5\zeta(5/2)}{4\zeta(3/2)} = 0.6417\ldots . \tag{5.12}$$

where we have to note that the number of bosons $N_B = N/2$ in this limit is just half the number of fermions.

As can be clearly seen from Figure 5.15, the limiting value of the ideal Bose gas (5.12) is in good agreement with the entropy of a noninteracting gas of bosonic quasi-particles which is obtained from the Shohno-Popov theory of noninteracting bosonic quasi-particles in the range $v > 1$, according to the formula

$$S/Nk_B = L^d \int \frac{d^dK}{(2\pi)^d}\{(1+n^B_{\mathbf{K}})\ln(1+n^B_{\mathbf{K}}) - n^B_{\mathbf{K}}\ln n^B_{\mathbf{K}}\} \tag{5.13}$$

with the standard distribution function

$$n^B_{\mathbf{K}} = 1/[\exp(\beta E^B_{\mathbf{K}}) - 1]\,. \tag{5.14}$$

The corresponding spectrum of excitation energies

$$E^B_{\mathbf{K}} = [(\hbar^2\mathbf{K}^2/2m_B)^2 + (\hbar^2\mathbf{K}^2/2m_B)\,2g_B|\Psi_B|^2]^{1/2} \tag{5.15}$$

has the well known form of a Bogoliubov spectrum with a temperature dependent condensate density $n_{B,0} = |\Psi_B|^2$ and a positive Bose-Bose scattering amplitude g_B.

It is interesting to note, that the entropy per particle right at T_c exhibits a maximum as a function of the coupling constant of order $S(T_c)/Nk_B \approx 0.78$ around the same coupling, where the critical temperature exhibits a maximum.

Noting that the evolution of the entropy at the critical temperature $S(T_c)/Nk_B$ over the whole crossover is smooth, we can argue that the value for the entropy obtained by Burovski *et. al* at unitarity would be too small. On the other hand the result obtained by Bulgac *et al.* seems to be too high.

5.5 Conclusions

In the next Chapter we will give an exhaustive explanation of the numerical procedure used in this work. Anyway, before entering into the numerical details, it is worth to summarize the main aspects of the theoretical background of the present thesis and the results which have been achieved. Furthermore, we would like to mention the shortcomings of the present approach, highlight new interesting problems and indicate possible future extension.

In this work we have studied the behaviour of a homogeneous attractive Fermi system in which the strength of the interatomic potential can be varied to explore the whole regime from extremely weak coupling to strong couplings. The problem has an experimental motivation. In fact, in the last decade, a high number of very successful and interesting experiments has been carried out in the field of cold atoms. The progress done in cooling techniques and in the laser trapping of atoms together with the increasing ability of controlling atomic Feshbach resonances, made possible to realize systems in which the interaction between the atoms can be tuned in a very precise way. By ramping across the Feshbach resonance, one can continuously transform a fermionic atomic gas to a bosonic molecular gas, both above and below the superfluid transition temperature thus making possible to observe the formation of condensed pairs [37, 38, 39].

The results presented in this work are based on a self-consistent, $\Phi-$derivable, conserving theory, whose formal basis has been first posed by Luttinger and Ward and De Dominicis and Martin. According to the approach of these autors, the exact one- or two-particle Green's functions serve as an infinite set of variational parameters. Further, by means of the one- and two-particle Green's functions, it is possible to derive functionals which are related with the thermodynamic functionals of the system.

In order to obtain consistent thermodynamic results within our approach, it is essential that the Green's functions satisfy self-consistency conditions which reflect the stationarity of the appropriate thermodynamic potentials. Formulations in which the free Green's function is replaced by a full one according to a choice of G_0G_0, GG_0, GG at will, would, in general, not be enough to obey conservation laws and thermodynamic identities which are granted to be obeyed in Φ-derivable formulations like the one presented here. Self-consistency is a necessary issue of the formalism. Indeed, within the formulation of Luttinger and Ward or De Dominicis and Martin, an appropriate functional for the grand thermodynamic potential or for the entropy is made stationary by determing the space and time dependent Green's functions from the stationarity conditions. A very important issue of the present formalism is the fact that self-consistency is only assured at the stationarity point of these functionals. Indeed, only at this point it is possible to get functionals which can be associated to thermodynamic quantities.

The stationarity conditions of the thermodynamic potentials have also been used to prove the thermodynamic equivalence of the Luttinger and Ward and the De Dominicis and Martin formalisms on the level of our approximate for the grand thermodynamic potential or the entropy.

The knowledge of the Green's function and the vertex function allows us to provide quantitative

results for the thermodynamic properties of the system over a range of temperatures which covers the relevant regime of the degenerate gas and for values of the coupling constant over the whole crossover from BCS super-fluidity to Bose-Einstein condensation.

The numerical calculations provide results for a number of universal ratios characterizing the unitary Fermi gas both at zero temperature and at the critical temperature which agree remarkably well with the results of most of the recent numerical and field-theoretic calculations at the unitarity point.

A shortcoming of the present approach is clearly visible from the three-dimensional figures which depict thermodynamic quantities such as the pressure and the entropy and the order parameter of the super-fluid transition. According to the numerical data, our super-fluid phase transition appears to be first order instead of being continuous. Moreover, in the region of strong coupling, where the physics is dominated by bosonic degrees of freedom, the calculation provides which seem to be less accurate than the ones provided for the weakly interacting regime. An evidence of this loss in the accuracy can be seen in the figure depicting the sound speed at zero temperature.

A possible extension of the theory could be focused on the calculation of the fermionic spectral functions $A(\mathbf{k}, \varepsilon)$ which are related to the fermion Green's function. The position and the shape of peaks in the spectral function would give an indication of the nature of the quasi-particles of the system at different values of the coupling constant. In particular, it could be possible to estimate the lifetime of the fermionic quasi-particles in the three different regime of weak, intermediate and strong coupling and get information on the formation of dimers.

Another extension is suggested by new experiment carried out recently by a few experimental group which have focused their work on fermionic super-fluidity in strongly interacting atomic gases with controlled population imbalance in two spin components. These experimental studies open up new intriguing problems. In particular, an increase in the imbalance leads to the disappearance of super-fluidity. Further, phase separation of a unitary gas in a trap has been observed. This significant experimental development could motivate future work aimed to the definition of a phase diagram in the entire BCS-BEC crossover also in the case of a fermionic gas with an imbalanced population in the spin component.

Chapter 6

Numerical calculations

The most challenging part of this work is the numerical calculation of the thermodynamic potentials. The present chapter is written with the purpose to point out the relevant informations which, from our point of view, are necessary to handle the problem in a satisfactory way. The central point of the numerics is to solve the self consistent equations for the Green's function and the vertex function. Once these functions are calculated, it is in principle possible to compute the thermodynamic potentials expressed by the formulas derived Chapter 4.

The functions that appears in the self-consistent equations are related to each other by a Fourier transformation thus the numerics is essentially based on a high precision Fourier transformation which allows us to transform the Green's function together with the self-energy and the vertex function several times back and forth from the momentum space to the real space and from the Matsubara frequencies to the imaginary time until the convergence is reached. Furthermore, we need to integrate the functionals defining the thermodynamic potentials. These functional have a singular behaviour that needs to be regularized.

In the first section of this Chapter we will give an overview of the method we used to compute the Green's functions and the vertex function.

In the second part we describe how we regularized the functions involved in the self-consistent equation and in the last section we will describe the numerical Fourier transformation which has been used for the calculations.

6.1 Solution of the self-consistent equations

In chapter 2 a two sets of self-consistent equations have been derived which give an analytical expression for the matrix Green's function $G(\mathbf{k}, \omega_n)$ and for the vertex function $\Gamma(\mathbf{K}, \Omega_n)$.

The Dyson equation (3.11) together with the self-energy (3.23) form the set of equation through which the matrix Green's function can be calculated. The second set of equation, which accounts for the renormalized vertex function, is given by the Bethe-Salpeter equation (3.18) and the renormalized

pair propagator (3.20). The Dyson equation and and the Bethe-Salpeter equation contain the three parameters that describe the state of the system. The temperature T, hidden in the bosonic and fermionic Matsubara frequencies Ω_n and ω_n through $\beta = 1/k_B T$, the chemical potential μ which appears in the Dyson equation (3.11) and the inverse s-wave scattering length contained in the renormalized interaction $g = m/(4\pi\hbar^2 a_F)$ that appears in the renormalized Bethe-Salpeter equation (3.18). The system can be equivalently described by the three parameters T, a_F^{-1} and n_F if the parameter μ is replaced by the fermionic density $n_F = k_F^3/3\pi^2$.

Because of the local nature of the interaction the self-consistent equations are scaling invariant. The scaling invariance can be exploited to study the system at a constant fermion density $n_F = -2 \cdot \mathcal{G}(\mathbf{r} = 0, \tau = -0)$, where all the quantities are rescaled by n_F. The lengths will be then rescaled by the Fermi wave number k_F and the energies by the Fermi energy $\varepsilon_F = \hbar^2 k_F^2/2m$. The Green function, the vertex function, the self-energy and the renormalized pair propagator, can be thus rewritten in terms of scaling functions depending on dimensionless variables

$$G_{\alpha\alpha'}(\mathbf{k}, \omega_n) = \varepsilon_F^{-1} \cdot \tilde{G}_{\alpha\alpha'}(\mathbf{k}/k_F, \hbar\omega_n/\varepsilon_F), \tag{6.1}$$

$$\Sigma_{\alpha\alpha'}(\mathbf{r}, \tau) = k_F^3 \varepsilon_F^2 \cdot \tilde{\Sigma}_{\alpha\alpha'}(k_F\mathbf{r}, \varepsilon_F\tau/\hbar), \tag{6.2}$$

$$\Gamma_{\alpha\alpha'}(\mathbf{K}, \Omega_n) = k_F^{-3} \varepsilon_F \cdot \tilde{\Gamma}_{\alpha\alpha'}(\mathbf{K}/k_F, \hbar\Omega_n/\varepsilon_F), \tag{6.3}$$

$$M_{\alpha\alpha'}(\mathbf{r}, \tau) = k_F^6 \cdot \tilde{M}_{\alpha\alpha'}(k_F\mathbf{r}, \varepsilon_F\tau/\hbar). \tag{6.4}$$

We can now replace the functions in the equations (3.18), (3.11), (3.23) and (3.20) with (6.1)-(6.4) to obtain a dimensionless set of self-consistent equations for the scaling functions :

$$\tilde{G}^{-1}_{\alpha\alpha'}(\mathbf{k}/k_F, \hbar\omega_n/\varepsilon_F) = \tilde{G}^{-1}_{0,\alpha\alpha'}(\mathbf{k}/k_F, \hbar\omega_n/\varepsilon_F) - \tilde{\Sigma}_{\alpha\alpha'}(\mathbf{k}/k_F, \hbar\omega_n/\varepsilon_F), \tag{6.5}$$

$$\tilde{\Sigma}_{\alpha\alpha'}(k_F\mathbf{r}, \varepsilon_F\tau/\hbar) = \tilde{\Sigma}_{1,\alpha\alpha'}\delta(k_F\mathbf{r})\,\delta_F(\varepsilon_F\tau/\hbar) + \tilde{G}_{\alpha\alpha'}(-k_F\mathbf{r}, -\varepsilon_F\tau/\hbar)\,\tilde{\Gamma}_{\alpha\alpha'}(k_F\mathbf{r}, \varepsilon_F\tau/\hbar), \tag{6.6}$$

$$\tilde{\Gamma}^{-1}_{\alpha\alpha'}(\mathbf{K}/k_F, \hbar\Omega_n/\varepsilon_F) = \frac{1}{8\pi}\frac{1}{k_F a_F}\delta_{\alpha\alpha'} + \tilde{M}_{\alpha\alpha'}(\mathbf{K}/k_F, \hbar\Omega_n/\varepsilon_F), \tag{6.7}$$

$$\tilde{M}_{\alpha\alpha'}(k_F\mathbf{r}, \varepsilon_F\tau/\hbar) = \left[\tilde{G}_{\alpha\alpha'}(k_F\mathbf{r}, \varepsilon_F\tau/\hbar)\right]^2 - \tilde{C}\,\delta_{\alpha\alpha'}\delta(k_F\mathbf{r})\delta_B(\varepsilon_F\tau/\hbar). \tag{6.8}$$

The pre-factor $\tilde{C}$ of the delta functions that appear in equation (6.4) is a dimensionless infinite constant defined by $\tilde{C} = \varepsilon_F^{-1} k_F^2 C$, where C is given by the integral (3.17).

At a fixed fermion density n_F, the state of the system over the whole crossover from BCS superconductivity to Bose-Einstein condensation can be described as a function of the dimensionless interaction strength $\nu = 1/k_F a_F$. The only two relevant parameters are in this case the dimensionless temperature $\theta = k_B T/\varepsilon_F$ and the dimensionless interaction strength, which varies from $-\infty$ in the BCS limit to ∞ in the BEC limit.

The dimensionless Green's function $\tilde{G}_{\alpha\alpha'}(\mathbf{k}/k_F, \hbar\omega_n/\varepsilon_F)$ and vertex function $\tilde{\Gamma}_{\alpha\alpha'}(\mathbf{K}/k_F, \hbar\Omega_n/\varepsilon_F)$ can be numerically evaluated solving iteratively the equations (6.5)-(6.8). We start from the free Green's function $\tilde{G}_{0,\alpha\alpha'}(\mathbf{k}/k_F, \hbar\omega_n/\varepsilon_F)$, using equation (6.8) we can get $\tilde{M}_{\alpha\alpha'}(\mathbf{K}/k_F, \hbar\Omega_n/\varepsilon_F)$ and

through the (6.7) the dimensionless vertex function $\tilde{\Gamma}_{\alpha\alpha'}(\mathbf{K}/k_F, \hbar\Omega_n/\varepsilon_F)$. Once we have the vertex function we can calculate the self-energy $\tilde{\Sigma}_{\alpha\alpha'}(k_F\mathbf{r}, \varepsilon_F\tau/\hbar)$ and use it to obtain the dressed Green's function and the vertex function to the first order. The process has to be iterated until convergence is achieved to get higher order approximations for $\tilde{G}$ and $\tilde{\Gamma}$.

In the whole process the functions defined by the equation (6.5)-(6.8), which have a nontrivial behaviour over several decades on a logarithmic scale, must be repeatedly Fourier transformed from the normal space variable $\mathbf{r}$ to the momenta $\mathbf{k}$ and $\mathbf{K}$, and from the Matsubara frequencies Ω_n and ω_n to the imaginary time τ and vice-versa. The numerical computation has to be done in such a way that the precision of the Fourier integrals is preserved in the all iteration process. To achieve the degree of accuracy needed, a rather sophisticated procedure [63] had to be developed which will be discussed in detail in section 6.3.

Furthermore we must note that the functions $\tilde{G}$ and $\tilde{\Gamma}$ are slowly decreasing function for large values of the variables $(\mathbf{k}/k_F, \hbar\omega_n/\varepsilon_F)$ and $(\mathbf{K}/k_F, \hbar\Omega_n/\varepsilon_F)$ respectively. This kind of behaviour of the functions for large momenta and large Matsubara frequencies implies a singular behaviour for small values of the variables $(k_F\mathbf{r}, \varepsilon_F\tau/\hbar)$ of the function in real space. Because of their singular behaviour, the functions $\tilde{G}(k_F\mathbf{r}, \varepsilon_F\tau/\hbar)$ and $\tilde{\Gamma}(k_F\mathbf{r}, \varepsilon_F\tau/\hbar)$ can not be integrated numerically for $(k_F\mathbf{r}, \varepsilon_F\tau/\hbar) \to (\mathbf{0}, 0)$. To make the calculation possible we must first eliminate the singular behaviour of the function. We perform this numerical "regularization" subtracting suitable *gauge*-functions from $\tilde{G}$, $\tilde{\Gamma}$, $\tilde{M}$ and $\tilde{\Sigma}$. Once the singular behaviour has been weakened we can proceed with the numerical integration of the differences $\Delta\tilde{G}$, $\Delta\tilde{\Gamma}$, $\Delta\tilde{M}$ and $\Delta\tilde{\Sigma}$.

An rather delicate issue of the whole process is the choice of the *gauge*-functions that need to be subtracted from the original functions: we need to find functions which can be computed analytically and that resemble the behaviour of the original function for small values of their arguments. Once we have such functions, we can subtract them to the functions we need to calculate and only then we can proceed with the numerical integration. The difference functions which have to be transformed by the numerical procedure must be smooth enough and they must decay at least like $\Delta G, \Delta\Gamma \sim 1/k^2$ for large values of the integrating variable.

The details of the process will be given in section 6.2 where the *gauge*-functions and their Fourier Transformation will be explicitly derived. To make the notation lighter, in the discussion that follows we will refer to the *gauge*-functions by using letters without *tilde*. For the same reason we will also refer to the dimensionless variables with the shorter symbols $(\mathbf{r}, \tau)$, $(\mathbf{k}, \omega_n)$ and $(\mathbf{K}, \Omega_n)$.

6.2 Derivation of the gauge-functions

If we study the system for temperatures $T > T_c$, the calculations simplify considerably. In fact, above the critical temperature T_c the anomalous Green's function defined by (3.4) vanishes and we have to deal only with functions instead of matrices. We start discussing this particular case because all the relevant issue already appear at this level and the results obtained can be extended to the case $T < T_c$.

$$\begin{array}{ccccc} G^{(0)}(\mathbf{k},\omega_n) & \xrightarrow{-} & \Delta G(\mathbf{k},\omega_n) = G - G^{(0)} & & \\ \Big\downarrow FT & & \Big\downarrow NFT & \longrightarrow & G(\mathbf{r},\tau) \\ G^{(0)}(\mathbf{r},\tau) & \xrightarrow{+} & \Delta G(\mathbf{r},\tau) & & \end{array}$$

Figure 6.1: Schematic diagram for the numeric evaluation of the Fourier integral for the Green's function

In this case the singular behaviour of the Green's function is given by the free fermion Green's function

$$G_0(\mathbf{k},\omega_n) = \frac{1}{-i\omega_n + (\varepsilon_k - \mu)^2} \tag{6.9}$$

which, in real space and imaginary time variables can be written as:

$$G^{(0)}(\mathbf{r},\tau) = \sum_{n=0}^{\infty}(-1)^n \frac{e^{\mu(\tau+n\beta)}}{[4\pi(\tau+n\beta)]^{\frac{3}{2}}} e^{-\frac{r^2}{4(\tau+n\beta)}} , \tag{6.10}$$

where the series is obtained using the Matsubara frequency sum (C.1) given in appendix C. Clearly the $n = 0$ term of the series is divergent, in fact the limit $\tau \to 0^+$ is a delta function:

$$e^{\mu\tau}\frac{e^{-\frac{r^2}{4\tau}}}{(4\pi\tau)^{\frac{3}{2}}} \xrightarrow{\tau\to 0^+} \delta(\mathbf{r}) .$$

To be able to perform the Fourier integral numerically, we need to regularize the Green's function $G(\mathbf{k},\omega_n)$ by subtracting the free fermion Green's function. The Green's function in the Fourier space can then be obtained by adding to the function $\Delta G(\mathbf{r},\tau)$ the following function:

$$G^{(0)}(\mathbf{r},\tau) = \begin{cases} \sum_{n=0}^{\infty}(-1)^n \frac{e^{\mu(\tau+n\beta)}}{[4\pi(\tau+n\beta)]^{\frac{3}{2}}} e^{-\frac{r^2}{4(\tau+n\beta)}} & \text{for } \tau \neq 0 \\ \\ \sum_{n=1}^{\infty}(-1)^n \frac{e^{\mu(n\beta)}}{[4\pi(n\beta)]^{\frac{3}{2}}} e^{-\frac{r^2}{4n\beta}} + \delta(\mathbf{r}) & \text{for } \tau = 0. \end{cases} \tag{6.11}$$

A schematic view of the numerical evaluation of the Green's function defined by the equations (6.5)-(6.6) is given by the diagram depicted in figure 6.1. Furthermore, since we are above the transition temperature, we removed the Nambu indices $\alpha\alpha'$, this won't cause any misunderstanding because the only functions that have to be "regularized" are the diagonal elements of the matrices defined in section 3.1. The *gauge*-functions are denoted in the diagrams by the superscript (0) and this notation will be used also in the next sections.

The zeroth order pair propagator in $(\mathbf{K}, \Omega_n)$ space defined by the product of two Green's functions

$$\chi_0(\mathbf{k}; \mathbf{K}, \Omega_n) = \frac{1}{\beta} \sum_{\omega_n} \mathcal{G}_0\left(\frac{1}{2}\mathbf{K} + \mathbf{k}, \Omega_n - \omega_n\right) \mathcal{G}_0\left(\frac{1}{2}\mathbf{K} - \mathbf{k}, \omega_n\right) \tag{6.12}$$

which is explicitly given by the sum

$$\chi_0(\mathbf{k}; \mathbf{K}, \Omega_n) = \frac{1}{\beta} \sum_{\omega_n} \frac{1}{-i(\Omega_n - \omega_n) + \frac{1}{2}\left(\frac{1}{2}\mathbf{K} + \mathbf{k}\right)^2 - \mu} \cdot \frac{1}{-i\omega_n + \frac{1}{2}\left(\frac{1}{2}\mathbf{K} - \mathbf{k}\right)^2 - \mu}. \tag{6.13}$$

The series (6.13) can be summed by using contour integration (see Appendix C). As a result we obtain

$$\chi_0(\mathbf{k}; \mathbf{K}, \Omega_n) = \frac{1}{-i\Omega_n + \frac{1}{2}\left(\frac{K^2}{2} + 2k^2 - 2\mu\right)} \cdot \left(1 - \frac{1}{e^{\frac{1}{2}(\frac{1}{2}\mathbf{K}+\mathbf{k})^2 - \mu} + 1} - \frac{1}{e^{\frac{1}{2}(\frac{1}{2}\mathbf{K}-\mathbf{k})^2 - \mu} + 1}\right). \tag{6.14}$$

The renormalized pair propagator is defined in the zero order as follows

$$M_0(\mathbf{K}, \Omega_n) = 4\pi \int \frac{d^3k}{(2\pi)^3} \left[\frac{1}{\beta} \sum_{\omega_n} \mathcal{G}_0\left(\frac{1}{2}\mathbf{K} + \mathbf{k}, \Omega_n - \omega_n\right) \mathcal{G}_0\left(\frac{1}{2}\mathbf{K} - \mathbf{k}, \omega_n\right) - \frac{1}{k^2}\right]. \tag{6.15}$$

In equation (6.15), the sum over the fermionic Matsubara frequencies defines the pair propagator $\chi_0(\mathbf{k}; \mathbf{K}, \Omega_n)$ explicitly written in (6.14). In order to regularize $M(\mathbf{r}, \tau)$ in the vicinity of the origin we need to know explicitly the behaviour of the pair propagator for large wave vectors and then subtract its Fourier transform from $M(\mathbf{r}, \tau)$. It is clear from equations (6.15) and (6.14) that the asymptotic behaviour of the regularized pair propagator for $|k| \to \infty$ is given by the expression

$$M_0(\mathbf{K}, \Omega_n) \approx \frac{1}{-i\Omega_n + \frac{1}{2}\left(\frac{K^2}{2} + 2k^2 - 2\mu\right)}. \tag{6.16}$$

Integrating this contribution over the fermionic wave vector we obtain the function needed for the regularization

$$\begin{aligned} M^{(0)}(\mathbf{K}, \Omega_n) &= -4\pi \int \frac{d^3k}{(2\pi)^3} \left(\frac{1}{i\Omega_n + \frac{1}{2}\left(-\frac{K^2}{2} - 2k^2 + 2\mu\right)} + \frac{1}{k^2}\right) \\ &= -\left[\left(-i\Omega_n + \frac{K^2}{4} - 2\mu\right)\right]^{\frac{1}{2}}. \end{aligned} \tag{6.17}$$

The formula (6.15) tells us the asymptotic behaviour of the pair propagator. This expression contains the most singular divergence in the limit $(\mathbf{r}, \tau) \to 0$. In practice, we found that, in order to obtain stable numerical results it was necessary to perform further subtractions. In particular for the renormalized pair propagator $M(\mathbf{K}, \Omega_n)$ we find that, for the procedure to work properly, the following gauge function has to be subtracted.

$$
\begin{array}{ccc}
M^{(0)}(\mathbf{r},\tau) & \xrightarrow{\ -\ } & \Delta M(\mathbf{r},\tau) = M - M^{(0)} \\
{\scriptstyle FT}\downarrow & & \downarrow{\scriptstyle NFT+FT} \\
M^{(0)}(\mathbf{k},\tau) & & \left[G^2 - M^{(0)}\right](\mathbf{k},\tau) - C\delta(\tau) \\
{\scriptstyle FT}\downarrow & & \downarrow{\scriptstyle NFT} \\
M^{(0)}(\mathbf{k},\Omega_n) & \xrightarrow{\ +\ } & \left[G^2 - M^{(0)}\right](\mathbf{k},\Omega_n) \longrightarrow M(\mathbf{k},\Omega_n)
\end{array}
$$

Figure 6.2: Schematic diagram for the numeric evaluation of the Fourier integral for the renormalized pair-function. The function M is obtained from the Green's function calculated as described in Figure 6.1 by using equation (6.8)

$$
\begin{aligned}
M^{(0)}(\mathbf{K},\Omega_n) \approx & -\frac{1}{8\pi}\sqrt{-i\Omega_n + \frac{K^2}{4} - 2\mu_0} \\
& + \frac{1}{16\pi}\frac{1}{\sqrt{-i\Omega_n + \frac{K^2}{4} - 2\mu_0}}(\mu - \mu_0) \\
& + \frac{1}{64\pi}\frac{1}{\left(-i\Omega_n + \frac{K^2}{4} - 2\mu_0\right)^{\frac{3}{2}}}(\mu - \mu_0)^2 \ .
\end{aligned}
\tag{6.18}
$$

Using the results (C.3) (C.4) and (C.5) we can calculate the contribution of $M^{(0)}(\mathbf{K},\Omega_n)$ to the renormalized pair propagator in real space and imaginary time:

$$
M^{(0)}(\mathbf{r},\tau) = \begin{cases} \frac{1}{8\pi^3}\sum_{n=0}^{\infty} e^{2\mu_0(\tau+n\beta)} e^{-\frac{x^2}{2(\tau+n\beta)}}\left[\frac{1}{[2(\tau+n\beta)]^3} + \frac{\mu-\mu_0}{[2(\tau+n\beta)]^2} + \frac{(\mu-\mu_0)^2}{2}[2(\tau+n\beta)]\right] & \text{for } \tau \neq 0 \\ \\ \frac{1}{8\pi^3}\sum_{n=1}^{\infty} e^{2\mu_0 n\beta} e^{-\frac{x^2}{2n\beta}}\left[\frac{1}{(2n\beta)^3} + \frac{\mu-\mu_0}{(2n\beta)^2} + \frac{(\mu-\mu_0)^2}{2}\cdot 2n\beta\right] & \text{for } \tau = 0\ . \end{cases}
\tag{6.19}
$$

Once we have found an analytical expression for the function $M^{(0)}(\mathbf{r},\tau)$ we can proceed following the diagram depicted in figure 6.2 to get the renormalized pair propagator $M(\mathbf{K},\Omega_n)$. As we have already done for the pair propagator, to regularize the vertex function we need to know its asymptotic behaviour for large K. From the definition (6.7) we can deduce that the vertex function has the same asymptotic form as the pair propagator. Thus the zeroth order vertex function is dominated for large wave vectors by the term

$$
\Gamma_0(\mathbf{K},\Omega_n) = 8\pi\frac{1}{\frac{1}{k_F a} - \sqrt{-i\frac{\Omega_n}{2} + \frac{K^2}{4} - \mu}}\ .
\tag{6.20}
$$

$$\begin{array}{ccc} \Delta\Gamma(\mathbf{K},\Omega_n) & \xrightarrow{NFT} & \Delta\Gamma(\mathbf{r},\tau) \\ + & \xrightarrow{\Sigma(\mathbf{r},\tau)=G(-\mathbf{r},-\tau)\Gamma(\mathbf{r},\tau)} & + \\ \Gamma^{(0)}(\mathbf{K},\Omega_n) & \xrightarrow{FT} & \Gamma^{(0)}(\mathbf{r},\tau) \end{array} \qquad \begin{array}{ccc} \Delta\Sigma(\mathbf{k},\tau) & \xrightarrow{NFT} & \Delta\Sigma(\mathbf{k},\omega_n) \\ + & & + \\ \Sigma^{(0)}(\mathbf{k},\tau) & \xrightarrow{FT} & \Sigma^{(0)}(\mathbf{k},\omega_n) \end{array} \rightarrow \Sigma(\mathbf{k},\omega_n)$$

Figure 6.3: Schematic diagrams of the Fourier integration process for the vertex function and for the self-energy defined by the equations (6.7) and (6.6).

To obtain higher order terms we expand in $\mu-\mu_0$ and ν to get

$$\begin{aligned} \frac{1}{8\pi}\Gamma_0(\mathbf{K},\Omega_n) \approx & -\frac{1}{\sqrt{-i\frac{\Omega_n}{2}+\frac{K^2}{4}-\mu}} - \frac{\mu-\mu_0}{2\left(-i\frac{\Omega_n}{2}+\frac{K^2}{4}-\mu\right)^{\frac{3}{2}}} - \frac{3}{8}\frac{(\mu-\mu_0)^2}{\left(-i\frac{\Omega_n}{2}+\frac{K^2}{4}-\mu\right)^{\frac{5}{2}}} \\ & + \left(-\frac{1}{-i\frac{\Omega_n}{2}+\frac{K^2}{4}-\mu} - \frac{\mu-\mu_0}{\left(-i\frac{\Omega_n}{2}+\frac{K^2}{4}-\mu\right)^2} - \frac{(\mu-\mu_0)^2}{\left(-i\frac{\Omega_n}{2}+\frac{K^2}{4}-\mu\right)^3}\right)\nu \\ & + \left(-\frac{1}{\left(-i\frac{\Omega_n}{2}+\frac{K^2}{4}-\mu\right)^{\frac{3}{2}}} - \frac{3}{2}\frac{\mu-\mu_0}{\left(-i\frac{\Omega_n}{2}+\frac{K^2}{4}-\mu\right)^{\frac{5}{2}}} - \frac{15}{8}\frac{(\mu-\mu_0)^2}{\left(-i\frac{\Omega_n}{2}+\frac{K^2}{4}-\mu\right)^{\frac{7}{2}}}\right)\nu^2 . \end{aligned} \tag{6.21}$$

In practice it turns out that some of the terms in (6.21) are redundant and don't affect the precision of the numerical Fourier transformation procedure. For the regularization purpose it is then enough to build the *gauge*-function for Γ by retaining the following terms of the expansion (6.21)

$$\begin{aligned} \Gamma^{(0)}(\mathbf{K},\Omega_n) \approx & -\frac{8\pi}{\sqrt{-i\frac{\Omega_n}{2}+\frac{K^2}{4}-\mu}} - 8\pi\frac{\mu-\mu_0}{2\left(-i\frac{\Omega_n}{2}+\frac{K^2}{4}-\mu\right)^{\frac{3}{2}}} \\ & - \frac{8\pi}{-i\frac{\Omega_n}{2}+\frac{K^2}{4}-\mu}\nu - \frac{8\pi}{\left(-i\frac{\Omega_n}{2}+\frac{K^2}{4}-\mu\right)^{\frac{3}{2}}}\nu^2 . \end{aligned} \tag{6.22}$$

The (6.22) can be now used to construct the function $\Delta\Gamma(\mathbf{K},\Omega_n)$, which will be transformed numerically. Once the vertex function is known, it is straightforward to get the self-energy via equation (6.6). Schematically we can proceed as described by the diagram depicted in figure 6.3. The Fourier transformation of the function defined by (6.22) can be explicitly done by following the calculation reported in Appendix C. The series over the bosonic Matsubara frequencies Ω_n can be determined using the results (C.2), (C.4) and (C.5). A further integration over the wave vector $\mathbf{K}$ produces

$$\Gamma^{(0)}(\mathbf{r},\tau) = \begin{cases} -\sum_{n=0}^{\infty} e^{2\mu_0(\tau+n\beta)} e^{-\frac{x^2}{2(\tau+n\beta)}}\left[\frac{16\pi}{[2\pi(\tau+n\beta)]^2} + \frac{16[(\mu-\mu_0)+2\nu]}{2\pi(\tau+n\beta)} + \frac{16\pi\nu}{[2\pi(\tau+n\beta)]^{\frac{3}{2}}}\right], & \text{for } \tau \neq 0 \\ -\sum_{n=1}^{\infty} e^{2\mu_0 n\beta} e^{-\frac{x^2}{2n\beta}}\left[\frac{16\pi}{[2\pi n\beta]^2} + \frac{16[(\mu-\mu_0)+2\nu]}{2\pi n\beta} + \frac{16\pi\nu}{[2\pi n\beta]^{\frac{3}{2}}} + 16\pi\nu\delta(\mathbf{r})\right], & \text{for } \tau = 0 . \end{cases} \tag{6.23}$$

Following the same reasoning done for $G^{(0)}$, $M^{(0)}$ and $\Gamma^{(0)}$ we can get the *gauge*-function $\Sigma^{(0)}$ for the self-energy that appears in the diagram in figure 6.3. For the self-energy we need to distinguish three cases. In fact, the definition $\Sigma(\mathbf{r},\tau) = \mathcal{G}(-\mathbf{r},-\tau)\Gamma(\mathbf{r},\tau)$ implies that the self-energy assumes a singular behaviour for both $\tau = 0$ and $\tau = \beta$. The singularity in $\tau = 0$ is produced by the vertex function while the Green's function $\mathcal{G}(-\mathbf{r},\tau = 0)$ is finite[1]. On the other hand, in the case $\tau = \beta$, the Green's function $\mathcal{G}(-\mathbf{r},-\beta)$ assumes a singular behaviour, while the vertex function is regular.

$$\Sigma(\mathbf{r},\tau) = \begin{cases} -\mathcal{G}(\mathbf{r},\beta-\tau)\Gamma(\mathbf{r},\tau) & \forall\mathbf{r},\ \tau \neq 0,\beta \\ -\mathcal{G}(\mathbf{r},\beta)\Gamma(\mathbf{r},0) + 16\pi\nu\mathcal{G}(\mathbf{r},\beta)\delta(\mathbf{r}) & \forall\mathbf{r},\ \tau = 0 \\ -\mathcal{G}(\mathbf{r},0)\Gamma(\mathbf{r},\tau) - \Gamma(\mathbf{r},\beta)\delta(\mathbf{r}) & \forall\mathbf{r},\ \tau = \beta. \end{cases} \tag{6.24}$$

The integration over the space variable $\mathbf{r}$ doesn't give any problems and can be integrated numerically without much effort. However the Fourier integral over the imaginary time τ needs to be regularized. We define the function $\Sigma^{(0)}(\mathbf{k},\tau)$

$$\Sigma^{(0)}(\mathbf{k},\tau) = \begin{cases} 16\sqrt{\pi}\mathcal{G}(\mathbf{0},\beta)\sum_{n=0}^{\infty}(-1)^n e^{-(\frac{k^2}{2}-2\mu_0)(\tau n\beta)}\left[\frac{1}{\sqrt{2(\tau+n\beta)}} + \left(\mu-\mu_0+2\nu^2\right)\sqrt{2(\tau+n\beta)}\right] & \\ \qquad +16\pi\nu\mathcal{G}(\mathbf{0},\beta)\frac{e^{-(\frac{k^2}{2}-2\mu_0)\tau}}{1+e^{-(\frac{k^2}{2}-2\mu_0)\beta}} - \Gamma(\mathbf{0},\beta)\frac{e^{-(\frac{k^2}{2}-2\mu_0)(\beta-\tau)}}{1+e^{-(\frac{k^2}{2}-2\mu_0)\beta}} & \tau \neq 0 \\ 16\sqrt{\pi}\mathcal{G}(\mathbf{0},\beta)\sum_{n=1}^{\infty}(-1)^n e^{-(\frac{k^2}{2}-2\mu_0)n\beta}\left[\frac{1}{\sqrt{2n\beta}} + \left(\mu-\mu_0+2\nu^2\right)\sqrt{2n\beta}\right] & \\ \qquad +16\pi\nu\frac{\mathcal{G}(\mathbf{0},\beta)}{1+e^{-(\frac{k^2}{2}-2\mu_0)\beta}} - \Gamma(\mathbf{0},\beta)\frac{e^{-(\frac{k^2}{2}-2\mu_0)\beta}}{1+e^{-(\frac{k^2}{2}-2\mu_0)\beta}} + 16\pi\nu\mathcal{G}(\mathbf{0},\beta) & \tau = 0 \\ 16\sqrt{\pi} - \mathcal{G}(\mathbf{0},\beta)\sum_{n=1}^{\infty}(-1)^n e^{-(\frac{k^2}{2}-2\mu_0)n\beta}\left[\frac{1}{\sqrt{2n\beta}} + \left(\mu-\mu_0+2\nu^2\right)\sqrt{2n\beta}\right] & \\ \qquad +16\pi\nu\frac{\mathcal{G}(\mathbf{0},\beta)}{1+e^{-(\frac{k^2}{2}-2\mu_0)\beta}} - \frac{\Gamma(\mathbf{0},\beta)}{1+e^{-(\frac{k^2}{2}-2\mu_0)\beta}} - \Gamma(\mathbf{0},\beta) & \tau = \beta\,. \end{cases} \tag{6.25}$$

Subtracting the *gauge*-function $\Sigma^{(0)}(\mathbf{k},\tau)$ to the product $\mathcal{G}(-\mathbf{r},-\tau)\Gamma(\mathbf{r},\tau)$ reduces the discontinuities at $\tau = 0$ and $\tau = \beta$ considerably. This allows us to successfully find the spline coefficient needed to build the cubic interpolation which will be used for the numerical integration of the Fourier integral (see section 6.3). Of course the function $\Sigma^{(0)}(\mathbf{k},\tau)$ contains terms that are necessary to get the correct asymptotic behaviour in the variables $(\mathbf{k},\omega_n)$. Thus once we have performed the numerical integration we need to add the contribution $\Sigma^{(0)}(\mathbf{k},\omega_n)$ generated by the *gauge*-function, to recover the Fourier

[1]The Green's function is antiperiodic in the variable τ: $\mathcal{G}(\mathbf{r},\tau) = -\mathcal{G}(\mathbf{r},\beta-\tau)$

transformation of the "full" self-energy.

$$\begin{aligned}\Sigma^{(0)}(\mathbf{k},\omega_n) =& \mathcal{G}(\mathbf{0},\beta)\frac{8\pi}{\sqrt{-i\frac{\omega_n}{2}+\frac{k^2}{4}-\mu_0}} + \mathcal{G}(\mathbf{0},\beta)\frac{8\pi\nu}{-i\frac{\omega_n}{2}+\frac{k^2}{4}-\mu_0} \\ &+ \mathcal{G}(\mathbf{0},\beta)\frac{4\pi(\mu-\mu_0+2\nu^2)}{\left(-i\frac{\omega_n}{2}+\frac{k^2}{4}-\mu_0\right)^{\frac{3}{2}}} + \Gamma(\mathbf{0},\beta)\frac{1}{-i\omega_n+k-\mu_0}.\end{aligned} \tag{6.26}$$

Once the Green's function and the vertex function are computed, we can use them to obtain the thermodynamic potentials given by the formulas (4.40)- (4.43) and (4.51)- (4.54).

6.2.1 Extension to the superfluid regime

If we want to solve the self-consistent equations for the superfluid system $T < T_c$ the numerical calculation gets slightly more complicated. However the complications are only due to the fact that below the transition temperature T_c the order parameter is finite and the Green's and the vertex functions are not diagonal anymore and the procedure becomes a bit heavier and time consuming. The off-diagonal terms in the matrices G and Γ does not need to be regularized and can be directly integrated by the numerical procedure.

The anomalous Green's function given by the formula (3.27) is regularized by the term $\Delta/2\mathbf{k}^2$. The vertex function in the superfluid regime is given by the matrix

$$\Gamma^{-1}(\mathbf{K},\Omega_n) = \begin{pmatrix} \frac{\nu}{8\pi} + M_{11}(\mathbf{K},\Omega_n) & M_{12}(\mathbf{K},\Omega_n) \\ M_{12}(\mathbf{K},\Omega_n) & \frac{\nu}{8\pi} + M_{11}^*(\mathbf{K},\Omega_n) \end{pmatrix} \tag{6.27}$$

where the off-diagonal terms $M_{12}(\mathbf{K},\Omega_n)$ are obtained as a product of two anomalous Green's functions and is thus finite, on the other hand the diagonal terms need to be regularized. If we invert the matrix we find that Γ_{11} reads

$$\Gamma_{11}(\mathbf{K},\Omega_n) = \frac{\nu/8\pi + M_{11}^*(\mathbf{K},\Omega_n)}{|\nu/8\pi + M_{11}(\mathbf{K},\Omega_n)|^2 - M_{12}^2}. \tag{6.28}$$

The irregular behaviour in the limit $|k| \to \infty$ is given by the contribution

$$\begin{aligned}\Gamma_{0,11}(\mathbf{K},\Omega_n) &\approx \frac{\nu/8\pi + M_{11}^*(\mathbf{K},\Omega_n)}{|\nu/8\pi + M_{11}(\mathbf{K},\Omega_n)|^2} \\ &= 8\pi\frac{1}{\frac{1}{k_F a} - M_{11}(\mathbf{K},\Omega_n)} = 8\pi\frac{1}{\frac{1}{k_F a} - \sqrt{-i\frac{\Omega_n}{2}+\frac{K^2}{4}-\mu}}.\end{aligned} \tag{6.29}$$

This expression is exactly (6.20), hence the matrix vertex function can be easily regularized by using the results obtained in section 6.2. Once we know how to regularize $\Gamma(\mathbf{K},\Omega_n)$ we can proceed with the regularization of the self-energy as we did for the case $T > T_c$.

6.3 Fourier transformation procedure

In the theory occur two kind of functions. First there are fermionic functions like the matrix green function $G(\mathbf{r},\tau)$ and the self energy $\Sigma(\mathbf{r},\tau)$. Secondly there are bosonic functions like the vertex function $\Gamma(\mathbf{r},\tau)$ and the pair propagator $\chi(\mathbf{r},\tau)$ and the renormalized pair propagator $M(\mathbf{r},\tau)$. The Fourier transformation of these functions for arbitrary dimension are defined by

$$G(\mathbf{r},\tau) = \int \frac{d^d k}{(2\pi)^d} \frac{1}{\beta} \sum_{\omega_n} e^{i(\mathbf{k}\cdot\mathbf{r}-\omega_n\tau)}\, G(\mathbf{k},\omega_n)\,, \tag{6.30}$$

$$\Gamma(\mathbf{r},\tau) = \int \frac{d^d K}{(2\pi)^d} \frac{1}{\beta} \sum_{\Omega_n} e^{i(\mathbf{K}\cdot\mathbf{r}-\Omega_n\tau)}\, \Gamma(\mathbf{K},\Omega_n)\,. \tag{6.31}$$

The two integrals differs only in the Matsubara frequencies. The fermionic function are transformed with respect to the frequencies $\omega_n = (2n+1)\pi/\beta$, which are odds, while the bosonic functions are transformed with respect to the even frequencies $\Omega_n = 2n\pi/\beta$. In the three-dimensional case we can simplify the integral by exploiting the spherical symmetry of the system. If we do that the functions in the integrals (6.30) and (6.31) only depend on the absolute value of the variables $\mathbf{k}$, $\mathbf{K}$, $\mathbf{r}$ and the Fourier transformation becomes two dimensional. For the Green's function we have

$$G(r,\tau) = \frac{1}{\beta(2\pi)^2} \sum_{\omega_n} e^{-i\omega_n\tau} \int_0^\infty dk\, \frac{2k\sin(kx)}{x}\, G(k,\omega_n). \tag{6.32}$$

We then only need to develop a continuous Fourier transform procedure that transforms the variable $k \leftrightarrow r$, $K \leftrightarrow r$, $\tau \to \omega_n$ and $\tau \to \Omega_n$ respectively. Furthermore we need to transform the Matsubara frequencies ω_n and Ω_n into the imaginary times τ via a Fourier series. The integral over k in equation (6.32) can be rewritten as follows:

$$\begin{aligned}
\frac{1}{2\pi^2 x}\int_0^\infty dk\, k\sin(kx)G(k,\omega_n) &= \frac{1}{2\pi^2 x}\int_0^\infty dk\ \sin(kx) f_{\omega_n}(k) \\
&= \frac{1}{4\pi^2 x}\int_{-\infty}^\infty dk\ \sin(kx) f_{\omega_n}(k) \\
&= \frac{1}{4\pi^2 x}\Im m\left[\int_{-\infty}^\infty dk\, e^{ikx} f_{\omega_n}(k)\right],
\end{aligned} \tag{6.33}$$

since we are interested in the continuous Fourier transformation we will omit in the following discussion the dependence on the Matsubara frequency ω_n. The second equality in (6.33) is justified by the fact that the function we are dealing with are even function in the variable k and x, hence the integrand $k\sin(kx)G(k,\omega_n) = \sin(kx) f_{\omega_n}(k)$ is also an even function and the integral can be extended to the whole real axis. The problem is thus reduced to the evaluation of integrals of the type:

$$f(x) = \int_{-\infty}^\infty dk\, e^{ikx} f(k) \tag{6.34}$$

As has been already pointed out in section 6.1, the functions that need to be transformed numerically have a nontrivial singular behaviour for values of the variable close to the origin, furthermore the physical properties of the fermionic system are included in the functions G and Γ at intermediate values of their variables. On the other hand it is important to get the correct behaviour of the function for large values of their variables to get the right behaviour of the same function for small values of the variables in the Fourier space. Therefore we need to develop a Fourier transformation procedure which has a good resolution at small, intermediate and large values of the variables. We will sample the functions at the following points:

$$k_m = (\gamma)^{-1} \sinh(\gamma\, \Delta k\, m) \qquad m = 0, \pm 1, \pm 2, \cdots, \pm N. \tag{6.35}$$

This choice of the sampling points automatically gives a good resolution on a logarithmic scale.

In order to perform the Fourier transformation we need to evaluate the sum

$$\mathrm{FT}_{\Delta k}\left[f(k)\right](x) = \sum_{k_{min}}^{k_{max}} \Delta k\, e^{ikx} f(k), \tag{6.36}$$

where k is a discrete variable and the integration step Δk is constant. The sum (6.36) defines the trapezoid sum of the integral

$$\int_{k_{min}}^{k_{max}} dk\, e^{ikx} f(k).$$

If the value of the function is known at the points $k_m,\ m = 0, \pm 1, \pm 2, \cdots, \pm N$ covering the whole interval $[x_{\min}, x_{\max}]$, the sum (6.36) can be divided into a sum of N trapezoid sums

$$\begin{aligned} \mathrm{FT}_{\Delta k}\left[f(k)\right](x) &= \sum_{k_{min}}^{k_{max}} \Delta k\, e^{ikx} f(k) = \sum_{m=0}^{N} \left\{ \sum_{k_m}^{k_{m+1}} \Delta k\, e^{ikx} f(k) \right\} \\ &= \sum_{m=0}^{N} e^{ik_m x} \left\{ \sum_{0}^{l_m} \Delta k\, e^{ixh_m} f(k_m + h_m) \right\} = \sum_{m=0}^{N} e^{ik_m x} I_m \ . \end{aligned} \tag{6.37}$$

where $k_0 = k_{min}$, $k_{N+1} = k_{max}$, $l_m = k_{m+1} - k_m$ and $h_m = k - k_m$. Since the formula (6.37) defines the trapez sum of an integral, at the boundaries k_{min} and k_{max} the summand contributes only $\frac{1}{2}$ to the total sum. The quantities $k_{max} - k_{min}$ and $l_m = k_{m+1} - k_m$ must be integer multiples of Δk.

The choice (6.35) for the sampling interval doesn't allow us to use a standard procedure like a *Fast Fourier transform* routine. Therefore a special procedure to calculate the Fourier integrals is needed. The idea is to interpolate the sampled function $f(k)$ for continuous values of k in the interval between two sampling points with a cubic spline

$$f(k_m + h_m) = a_m + b_m h_m + c_m h_m^2 + d_m h_m^3 \ . \tag{6.38}$$

The spline polynomial and its first two derivative are continuous at k_m and k_{m+1}, thus

$$\begin{cases} a_m + b_m h_m + c_m h_m^2 + d_m h_m^3 = a_{m+1} \\ b_m + 2c_m h_m + 3d_m h_m^2 = b_{m+1} \\ 2c_m + 6d_m h_m = 2c_{m+1} \ . \end{cases} \tag{6.39}$$

Furthermore, in the case of a natural spline the coefficient c_0 and c_{N+1} vanish. Once the spline coefficient have been calculated we can then easily evaluate the integral of the cubic polynomial over the interval $[k_m, k_{m+1}]$. At this stage, the only thing that is left to do is to sum up the single contribution to get the value of the whole integral. We now need to calculate explicitly the sums in the last equality of equation (6.37) where we substitute the function $f(k_m + h_m)$ with its cubic interpolation (6.38). The sum I_m that appears in the equality (6.37) reads:

$$I_m = a_m S_0(l_m) + b_m S_1(l_m) + c_m S_2(l_m) + d_m S_3(l_m) \tag{6.40}$$

where

$$S_j(l_m) = \sum_0^{l_m} \Delta k \, h_m^j e^{ixh_m}. \tag{6.41}$$

The sums $S_j(l_m)$ can be easily evaluated. Defining $l_m = \Delta k \, n$ and $h_m = \Delta k \, s$ we get for the sum $S_0(l_m)$:

$$\begin{aligned} S_0(l_m) = \sum_{s=0}^{n} \Delta k \, e^{ix\Delta k \, s} &= \Delta k \left[\frac{1}{2} + \sum_{s=1}^{n-1} e^{ix\Delta k \, s} + \frac{1}{2} e^{ix\Delta k \, n} \right] \\ &= \frac{\Delta k}{2} \left[\sum_{s=0}^{n-1} \left(e^{ix\Delta k} \right)^s + \sum_{s=1}^{n} \left(e^{ix\Delta k} \right)^s \right] \\ &= \frac{\Delta k}{2} \left[\frac{e^{ix\Delta k \, n} - 1}{e^{ix\Delta k} - 1} + \frac{e^{ix\Delta k \, n+1} - e^{ix\Delta k}}{e^{ix\Delta k} - 1} \right] \\ &= \frac{\Delta k}{2i} \cot\left(\frac{x\Delta k}{2} \right) \cdot \left(e^{ix\Delta k \, n} - 1 \right) \\ &= -i g_0 \, (x, \Delta k) \cdot \left(e^{ixl_m} - 1 \right), \end{aligned} \tag{6.42}$$

once $S_0(l_m)$ is computed, the remaining sums can be derived by noting that

$$S_j(l_m) = \left(-i \frac{\partial}{\partial x} \right)^j \sum_0^{l_m} \Delta k e^{ixh_m} \ . \tag{6.43}$$

From equation (6.43) follows:

$$S_1(l_m) = -g_1(x, \Delta k) \cdot \left(e^{ixl_m} - 1 \right) - i g_0(x, l_m) \cdot l_m e^{ixl_m}, \tag{6.44}$$

$$S_2(l_m) = i g_2(x, \Delta k) \cdot \left(e^{ixl_m} - 1 \right) - 2 g_1(x, l_m) l_m e^{ixl_m} - i l_m^2 g_0(x, l_m) e^{ixl_m}, \tag{6.45}$$

and

$$S_3(l_m) = g_3(x,\Delta k)\cdot\left(e^{ixl_m}-1\right) + 3il_m g_2(x,l_m)e^{ixl_m} - 3l_m^2 g_1(x,l_m)e^{ixl_m} - il_m^3 g_0(x,l_m)e^{ixl_m}. \tag{6.46}$$

where the functions $g_j(x,\Delta k)$ are defined in the following way:

$$g_j(x,\Delta k) = \left(\frac{\partial}{\partial x}\right)^j \frac{\Delta k}{2}\cot\left(\frac{x\Delta k}{2}\right). \tag{6.47}$$

Exploiting the results obtained for the $S_j(l_m)$ and the property (6.39) of the spline polynomial, it is now possible to evaluate the sum I_m:

$$\begin{aligned} I_m = &- ig_0(x,\Delta k)\left(a_{m+1}e^{ixl_m} - a_m\right) - g_1(x,\Delta k)\left(b_{m+1}e^{ixl_m} - b_m\right) \\ &+ ig_2(x,\Delta k)\left(c_{m+1}e^{ixl_m} - c_m\right) + g_3(x,\Delta k)\left(e^{ixl_m}-1\right)\ . \end{aligned} \tag{6.48}$$

Multiplying I_m with e^{ixk_m} and sum the terms over the whole range we finally obtain a discretized expression for the Fourier integral (6.34):

$$\begin{aligned} \mathrm{FT}_{\Delta k}\left[f(k)\right](x) = &- ig_0(x,\Delta k)\sum_{m=0}^{N}\left[a_{m+1}e^{ixl_{m+1}} - a_m e^{ixl_m}\right] \\ &- g_1(x,\Delta k)\sum_{m=0}^{N}\left[b_{m+1}e^{ixl_{m+1}} - b_m e^{ixl_m}\right] \\ &+ ig_2(x,\Delta k)\sum_{m=0}^{N}\left[c_{m+1}e^{ixl_{m+1}} - c_m e^{ixl_m}\right] \\ &+ g_3(x,\Delta k)\sum_{m=0}^{N}\left[e^{ixl_{m+1}} - e^{ixl_m}\right]d_m\ , \end{aligned} \tag{6.49}$$

all terms in the first three sums cancel except the end terms hence, using a natural spline for the calculation, the final form of the discretized Fourier integral reads:

$$\begin{aligned} \mathrm{FT}_{\Delta k}\left[f(k)\right](x) = &- ig_0(x,\Delta k)\left[a_{N+1}e^{ixl_{N+1}} - a_0 e^{ixl_0}\right] \\ &- g_1(x,\Delta k)\left[b_{N+1}e^{ixl_{N+1}} - b_0 e^{ixl_0}\right] \\ &+ g_3(x,\Delta k)\sum_{m=0}^{N}\left[e^{ixl_{m+1}} - e^{ixl_m}\right]d_m\ . \end{aligned} \tag{6.50}$$

If we take the limit $\Delta k \to 0$ in the functions $g_j(x, \Delta k)$ that appear in the formula (6.50), we get

$$\begin{cases} g_0(x,\Delta k) \xrightarrow{\Delta k\to 0} \dfrac{1}{x} \\ g_1(x,\Delta k) \xrightarrow{\Delta k\to 0} -\dfrac{1}{x^2} \\ g_2(x,\Delta k) \xrightarrow{\Delta k\to 0} \dfrac{2}{x^3} \\ g_3(x,\Delta k) \xrightarrow{\Delta k\to 0} -\dfrac{6}{x^4} \end{cases},$$

substituting the limit $g_j(x, 0)$ in the the discrete sums (6.42), (6.44), (6.45), and (6.46) we exactly recover the continuous Fourier integral. An important point still needs to be stressed, in fact the Fourier integral of a cubic polynomial produces terms of the order x^{-4}, x^{-3}, x^{-2} and x^{-1} thus, while for big values of x the procedure described above works fine without much effort, it breaks down in the limit $x \to 0$. This limit need a more careful approach, the discrete Fourier sum for $x = 0$ is given by:

$$\mathrm{FT}_{\Delta k}\left[f(k)\right](x=0) = \sum_{k_{min}}^{k_{max}} \Delta k\, f(k) = \sum_{m=0}^{N} \left\{ \sum_{k_m}^{k_{m+1}} \Delta k\, f(k) \right\} = \sum_{m=0}^{N} I_m\,, \tag{6.51}$$

where I_m is defined by (6.40) and the sums $S_j(l_m)$ by:

$$S_j^{(x=0)}(l_m) = \sum_{0}^{l_m} \Delta k\, (h_m)^j. \tag{6.52}$$

The $S_j^{(x=0)}(l_m)$ can be evaluated directly following the same calculation done for the general case:

$$S_0^{(x=0)}(l_m) = l_m, \tag{6.53}$$

$$S_1^{(x=0)}(l_m) = \frac{1}{2} l_m^2, \tag{6.54}$$

$$S_2^{(x=0)}(l_m) = \frac{1}{3} l_m^3 \cdot \left(1 + \frac{\Delta k^2}{2 l_m^2}\right), \tag{6.55}$$

$$S_3^{(x=0)}(l_m) = \frac{1}{4} l_m^4 \cdot \left(1 + \frac{\Delta k^2}{2 l_m^2}\right). \tag{6.56}$$

Summing up all the term and considering that we are using a natural spline interpolation, the $x \to 0$ limit of the discretized Fourier integral can be written in the form:

$$\begin{aligned} \mathrm{FT}_{\Delta k}\left[f(k)\right](x=0) = &\left[a_{N+1}k_{N+1} - a_0 k_0\right] - \frac{1}{2}\left[b_{N+1}k_{N+1}^2 - b_0 k_0^2\right] \\ &- \frac{1}{4}\sum_{m=0}^{N} d_m \left\{ \left(k_{m+1}^4 - k_m^4\right) + \Delta k^2 \left(k_{m+1}^2 - k_m^2\right) \right\}. \end{aligned} \tag{6.57}$$

The formulas (6.50) and (6.57) provide an expression that allows us to evaluate numerically Fourier integrals of the type (6.33) either in the limit $k_m x > 1$ and $k_m x \to 0$.

The results obtained above can be used, with some little modifications, to perform the Fourier transformation from the discrete Matsubara frequencies to the imaginary time. The sums that we need to evaluate are of the type:

$$f(\tau) = \frac{1}{\beta} \sum_{\nu_n} e^{-i\nu_n \tau} f(\nu_n) = \frac{1}{2\pi} \sum_{\nu_n} 2\nu_0 e^{-i\nu_n \tau} f(\nu_n) \tag{6.58}$$

where ν_n can be even or odd integer multiple of $\nu_0 = \pi/\beta$ and the function $f(\tau)$ is defined on the interval $0 \leq \tau \leq \beta$. In this case we have to consider only those values $f_m = \nu_n^{(m)}$ corresponding to the Matsubara frequencies $\nu_n^{(m)}$ that lie closer to the sampling points x_m given by the formula (6.35). The procedure to evaluate the Matsubara sums follows what has already been done in the case of the Fourier integral but in order to use the formulas (6.50) and (6.57) it is necessary to identify $\Delta k = 2\nu_0$, $k_m = (2n_m + 1)\nu_0$ in case we need to transform a fermionic function and $k_m = 2n_m\nu_0$ in case the Fourier sum involves bosonic Matsubara frequencies.

Appendix A

Comparison between the Luttinger and Ward and De Dominicis and Martin functional at stationarity

The statement that, at stationarity, the functionals obtained in the Luttinger and Ward formalism coincides with the ones obtained within the theory of De Dominicis and Marin can be directly verified by calculating the functional with the values of the Green's function and the vertex function obtained by the stationarity condition (2.42). We start with the functional

$$\begin{aligned}\Omega[G,\Gamma] = &-2\,L^d \int \frac{d^dk}{(2\pi)^d}\,(\varepsilon_{\mathbf{k}}-\mu)\,\mathcal{G}(\mathbf{k},\tau=-0) \;+\; L^d\,g_0|\mathcal{F}(\mathbf{0},0)|^2 \\ &- L^d \int \frac{d^dk}{(2\pi)^d}\,\frac{1}{\beta}\sum_{\omega_n}\mathrm{Tr}\{-\ln[G(\mathbf{k},\omega_n)] + [-i\hbar\omega_n G(\mathbf{k},\omega_n)-1]\} \\ &+ \frac{1}{2}\,L^d \int \frac{d^dK}{(2\pi)^d}\,\frac{1}{\beta}\sum_{\Omega_n}\mathrm{Tr}\{g_0\,[\chi(\mathbf{K},\Omega_n) - \chi(\mathbf{K},\Omega_n)\,\Gamma(\mathbf{K},\Omega_n)\,\chi(\mathbf{K},\Omega_n)] \\ &\qquad\qquad - \chi(\mathbf{K},\Omega_n)\,\Gamma(\mathbf{K},\Omega_n) - \ln[1-\chi(\mathbf{K},\Omega_n)\,\Gamma(\mathbf{K},\Omega_n)]\},\end{aligned} \tag{A.1}$$

First we rewrite the frist term of the functional by means of the identity (4.19):

$$2L^d \int \frac{d^dk}{(2\pi)^d}\frac{1}{\beta}\sum_{\omega_n}(\varepsilon_k-\mu)\mathcal{G}(\mathbf{k},\omega_n) = L^d \int \frac{d^dk}{(2\pi)^d}\frac{1}{\beta}\sum_{\omega_n}\mathrm{Tr}\left\{\left(G_0^{-1}(\mathbf{k},\omega_n)+i\hbar\omega_n\right)G(\mathbf{k},\omega_n)\right\}, \tag{A.2}$$

It is now possible to simplify the functional (A.1) by combining the two intergals over the fermionic variables together

$$-L^d \int \frac{d^dk}{(2\pi)^d}\,\frac{1}{\beta}\sum_{\omega_n}\mathrm{Tr}\{-\ln[G(\mathbf{k},\omega_n)] + [G_0(\mathbf{k},\omega_n)^{-1}G(\mathbf{k},\omega_n)-1]\}, \tag{A.3}$$

Finally we consider the last integral in (A.1), we group together the first thre argument of the trace to obtain

$$\begin{aligned} &g_0\chi(\mathbf{K},\Omega_n) - g_0\chi(\mathbf{K},\Omega_n)\,\Gamma(\mathbf{K},\Omega_n)\,\chi(\mathbf{K},\Omega_n) - \chi(\mathbf{K},\Omega_n)\,\Gamma(\mathbf{K},\Omega_n) \\ &= \chi(\mathbf{K},\Omega_n)\,[g_0 - g_0\Gamma(\mathbf{K},\Omega_n)\,\chi(\mathbf{K},\Omega_n) - \Gamma(\mathbf{K},\Omega_n)] \end{aligned}$$

if the vertex function fulfill the stationarity condition $\delta_\Gamma\Omega[G,\Gamma] = 0$, the quantity in the square brackets vanishes, thus we are left with the logarithm only, which, using the Bethe-Salpeter equation, can be rewritten in the following way:

$$-\ln[1 - \chi(\mathbf{K},\Omega_n)\Gamma(\mathbf{K},\Omega_n)] = \ln[g_0\Gamma^{-1}(\mathbf{K},\Omega_n)]. \tag{A.4}$$

With this furter simplification the functional (A.1) reads:

$$\begin{aligned} \Omega[G,\Gamma] = &- L^d \int \frac{d^dk}{(2\pi)^d}\,\frac{1}{\beta}\sum_{\omega_n} \mathrm{Tr}\{-\ln[G(\mathbf{k},\omega_n)] + [G_0(\mathbf{k},\omega_n)^{-1}G(\mathbf{k},\omega_n) - 1]\} \\ &+ L^d\, g_0|\mathcal{F}(\mathbf{0},0)|^2 \;+\; \frac{1}{2}\,L^d \int \frac{d^dK}{(2\pi)^d}\,\frac{1}{\beta}\sum_{\Omega_n} \mathrm{Tr}\{\ln[g_0\,\Gamma^{-1}(\mathbf{K},\Omega_n)]\}. \end{aligned} \tag{A.5}$$

The Luttinger and Ward grand-potential derived in section 4.1 reads

$$\begin{aligned} \Omega[G] = &-L^d \int \frac{d^dk}{(2\pi)^d}\,\frac{1}{\beta}\sum_{\omega_n} \mathrm{Tr}\{-\ln[G(\mathbf{k},\omega_n)] + [G_0(\mathbf{k},\omega_n)^{-1}G(\mathbf{k},\omega_n) - 1]\} \\ &+ L^d\, g_0|\mathcal{F}(\mathbf{0},0)|^2 \;+\; \frac{1}{2}\,L^d \int \frac{d^dK}{(2\pi)^d}\,\frac{1}{\beta}\sum_{\Omega_n} \mathrm{Tr}\{\ln[1 + g_0\,\chi(\mathbf{K},\Omega_n)]\}. \end{aligned} \tag{A.6}$$

The integral over the bosonic variables in the functional (A.6) can be rewritten in the same form as in (A.5) using again the Bethe-Salpeter equation. Hence the Luttinger and Ward theory can be recovered from the functional obtained within the formalism of De Dominicis and Martin if the stationarity condition are fulfilled.

Appendix B

Calculation of the pair propagator

In Chapter 6 we use the explicit expression of the pair propagator $\chi_0(\mathbf{K}, \Omega_n)$ to define the asymptotic behaviour of the vetex function in the limit $|k| \to \infty$. In the following we report the detailed calculation to get from the definition of the pair propagator (6.13) to the final results (6.14) and (6.16). We need to sum the series

$$\chi(\mathbf{k}; \mathbf{K}, \Omega_n) = \frac{1}{\beta} \sum_{\omega_n} \frac{1}{-i\left(\Omega_n - \omega_n\right) + \xi_1} \cdot \frac{1}{-i\omega_n + \xi_2} \tag{B.1}$$

where

$$\xi_1 = \frac{1}{2}\left(\frac{\mathbf{K}}{2} + \mathbf{k}\right)^2 - \mu, \tag{B.2}$$

$$\xi_2 = \frac{1}{2}\left(\frac{\mathbf{K}}{2} - \mathbf{k}\right)^2 - \mu. \tag{B.3}$$

The sum (B.1) is the result of the contour integral

$$I = \int_{C_R} \frac{dz}{2\pi i} \frac{1}{z - i\Omega_n + \xi_1} \cdot \frac{1}{-z + \xi_2} \cdot \frac{1}{e^{\beta z} + 1} \tag{B.4}$$

the contour C_R being plotted in Figure B.1. A solution for the integral (B.4) is given by the sum over the residues that lie into the the circle C_R. The function $n_F(z) = 1/e^{\beta z} + 1$ has an infinite number of poles on the imaginary axis at the values $z = i\omega_n$, and its residues assume the value $-1/\beta$. The two fraction in the integral have a pole for $z = i\Omega_n + \xi_1$ and $z = \xi_2$ respectively. The integral I is hence given by the following sum

$$\begin{aligned} I =& \frac{1}{\beta} \sum_{\omega_n} \frac{1}{-i\left(\Omega_n - \omega_n\right) + \xi_1} \cdot \frac{1}{-i\omega_n + \xi_2} \\ &+ \frac{1}{-i\Omega_n + \xi_1 + \xi_2} \cdot \left(\frac{1}{e^{-\xi_1\beta} + 1} - \frac{1}{e^{-\xi_2\beta} + 1}\right). \end{aligned} \tag{B.5}$$

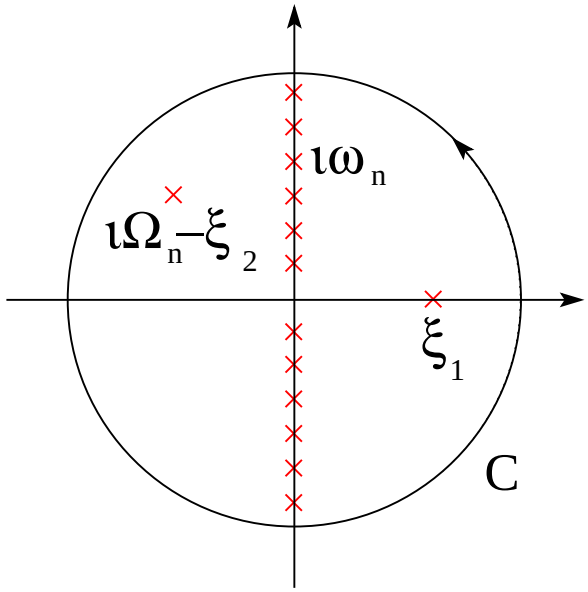

Figure B.1: Contour for evaluation of frequency sum (B.1)

The first sum correspond to the definition (B.1) of the pair propagator, the sum $\xi_1 + \xi_2$ in the denominator of the fraction in front of the second term can be rewritten by using the definitions (B.2) and (B.3). If we now let the radius of the contour C_R go to infinity, according to the Jordan's lemma, the contour integral (B.4) vanishes thus and we get the equality

$$\begin{aligned}\frac{1}{\beta}\sum_{\omega_n}\frac{1}{-i\left(\Omega_n-\omega_n\right)+\frac{1}{2}\left(\frac{1}{2}\mathbf{K}+\mathbf{k}\right)^2-\mu}\cdot\frac{1}{-i\omega_n+\frac{1}{2}\left(\frac{1}{2}\mathbf{K}-\mathbf{k}\right)^2-\mu}=\\ \frac{1}{-i\Omega_n+\frac{1}{2}\left(\frac{K^2}{2}+2k^2-2\mu\right)}\cdot\left(1-\frac{1}{e^{\frac{1}{2}(\frac{1}{2}\mathbf{K}+\mathbf{k})^2-\mu}+1}-\frac{1}{e^{\frac{1}{2}(\frac{1}{2}\mathbf{K}-\mathbf{k})^2-\mu}+1}\right)\end{aligned} \tag{B.6}$$

which is exactly the result (6.14). We are now intrested in the behaviour at large wave vectors of the pair propagator, it is easy to see that in tat limit the leading contribution is given by the first term of (B.6). This is exactly the term we have to integrate over the fermionic wave vectors to get the result (6.17).

The asympotic behaviour of the renormalized pair propagator is given by the integral

$$M^{(0)}(\mathbf{K},\Omega_n)=-4\pi\int\frac{d^3k}{(2\pi)^3}\left(\frac{1}{i\Omega_n+\frac{1}{2}\left(-\frac{K^2}{2}-2k^2\right)+2\mu}+\frac{1}{k^2}\right). \tag{B.7}$$

Exploiting the spherical symmetry of the problem we can reduce the integral (B.7) to a one-dimentional integral. By integrating out the angles we are left with the integral over the module of the wave vector

k, which, with the change of variable $y = k/[i\Omega_n + -\frac{K^2}{4} + 2\mu]$ becomes:

$$\begin{aligned} M^{(0)}(\mathbf{K}, \Omega_n) &= -\frac{2}{\pi} \int_0^\infty dk \left(\frac{1}{i\Omega_n + -\frac{K^2}{4} - k^2 + 2\mu} + \frac{1}{k^2} \right) \\ &= \sqrt{i\Omega_n + -\frac{K^2}{4} + 2\mu} \int_0^\infty dy \frac{1}{1-y^2} \\ &= -\frac{2}{\pi} \cdot \frac{i\pi}{2} \sqrt{i\Omega_n - \frac{K^2}{4} + 2\mu} = \sqrt{-i\Omega_n + \frac{K^2}{4} - 2\mu}. \end{aligned}$$

Appendix C

Sum over Matsubara frequencies

To calculate the Fourier transformation for of *gauge*-functions defined in Chapter 6, we need to perform a few sums over bosonic and fermionic Matsubara frequencies.

$$\frac{1}{\beta}\sum_{\omega_n} e^{-i\omega_n\tau}\frac{1}{-i\omega_n+\xi} = \frac{e^{-\xi\tau}}{1+e^{-\beta\xi}} \tag{C.1}$$

where $\omega_n = (2n+1)\pi/\beta$ are fermionic Matsubara frequencies.

$$\frac{1}{\beta}\sum_{\Omega_n} e^{-i\Omega_n\tau}\frac{1}{-\frac{i\Omega_n}{2}+\xi} = \frac{2e^{-2\xi\tau}}{1-e^{-2\beta\xi}} \tag{C.2}$$

$\Omega_n = 2n\pi/\beta$ on the left hand side of (C.2) and in the rest of the discussion are bosonic Matsubara frequencies. The evaluation of (C.1) and (C.2) is straightforward and we will skip the details.

$$\frac{1}{\beta}\sum_{\Omega_n} e^{-i\Omega_n\tau}\sqrt{-i\frac{\Omega_n}{2}+\xi} = \frac{1}{\sqrt{\pi}}\sum_{m=0}^{\infty}\frac{e^{-2\xi(\tau+m\beta)}}{\left[2\left(\tau+m\beta\right)\right]^{3/2}}. \tag{C.3}$$

The most direct approach for evaluating (C.3) is to perform a contour integration on a meromorphic function with poles at the even integers. In figure C.1 is depicted the contour for the evaluation of the sum (C.3), on this contour the integral

$$\oint \frac{dz}{2\pi i}\cdot e^{-z\tau}\sqrt{-\frac{z}{2}+\xi}\frac{e^{\beta z}}{e^{\beta z}-1}$$

exactly reproduces the sum on the left hand side of (C.3), in fact the integrand has an infinite sequence of singles poles at $z = i\Omega_n$ with residue

$$\frac{1}{\beta}e^{-i\Omega_n\tau}\sqrt{-\frac{i\Omega_n}{2}+\xi}.$$

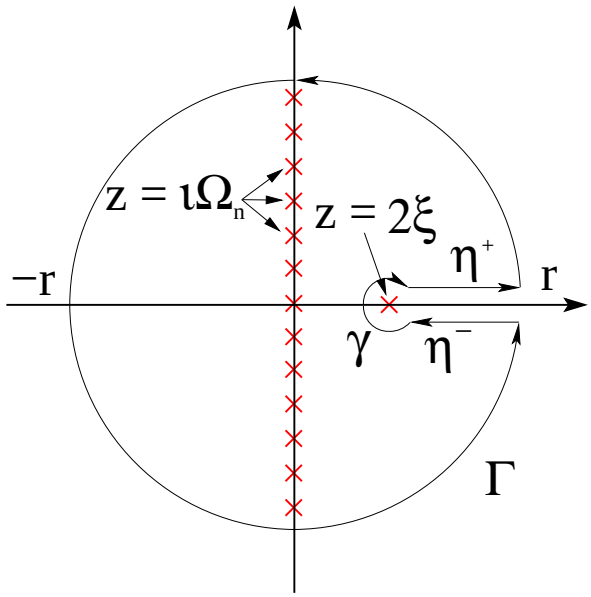

Figure C.1: Contour for evaluation of frequency sum (C.3), (C.4) and (C.5)

If $r \to \infty$ Jordan's lemma shows that the contribution of Γ vanish and the only non vanishing terms, in the limit $\gamma \to 0$, are given by the integrals:

$$i\int_{2\xi}^{\infty}\frac{dx}{2\pi i}e^{-\tau x}\sqrt{\frac{x}{2}-\xi}\cdot\frac{e^{\beta x}}{e^{\beta x}-1}+i\int_{\infty}^{2\xi}\frac{dx}{2\pi i}e^{-\tau x}\sqrt{\frac{x}{2}-\xi}\cdot\frac{e^{\beta x}}{e^{\beta x}-1}.$$

The two contributions can be added together to give:

$$\frac{2}{\pi}\int_0^{\infty}dy\,\sqrt{y}\frac{e^{-2\tau(y+\xi)}}{1-e^{2\beta(y+\xi)}}=\frac{2}{\pi}\int_0^{\infty}dy\,\sqrt{y}\sum_{m=0}^{\infty}e^{-2\beta m(y+\xi)}e^{-2\tau(y+\xi)}=\frac{1}{\sqrt{\pi}}\sum_{m=0}^{\infty}\frac{e^{-2\xi(\tau+m\beta)}}{\left[2\left(\tau+m\beta\right)\right]^{3/2}}.$$

In the same way we can evaluate the sum:

$$\frac{1}{\beta}\sum_{\Omega_n}e^{-i\Omega_n\tau}\frac{1}{\sqrt{-\frac{i\Omega_n}{2}+\xi}}=\frac{2}{\sqrt{\pi}}\sum_{m=0}^{\infty}\frac{e^{-2\xi(\tau+m\beta)}}{\sqrt{2\left(\tau+m/\theta\right)}}. \tag{C.4}$$

The proof of the next result is more tricky. We need to calculate

$$\frac{1}{\beta}\sum_{\Omega_n}\frac{e^{-i\Omega_n\tau}}{\left(-\frac{i\Omega_n}{2}+\xi\right)^{3/2}}.$$

Again we can reproduce the sum using a contour integral

$$\oint \frac{dz}{2\pi i} \frac{e^{-z\tau}}{\left(-\frac{z}{2}+\xi\right)^{3/2}} \frac{e^{\beta z}}{e^{\beta z}-1}$$

the integration contour being the same as in Figure C.1. When $r \to \infty$ Jordan's lemma tells us that the contribution of the arch Γ to the integral vanishes and we are left with the integrals over γ, η^+ and η^-. The contribution of the arch γ, in the limit $\gamma \to 0$, is

$$I_\gamma \approx \frac{4}{\pi}\frac{1}{\sqrt{\varepsilon}} \frac{e^{-2\xi\tau}}{1-e^{-2\beta\xi}} = \frac{4}{\pi}\frac{1}{\sqrt{\varepsilon}} \sum_{m=0}^{\infty} e^{-2(\tau-m\beta)\xi},$$

where $\varepsilon \to 0$ is the radius of the small arch γ. Letting $r \to \infty$ the last two integrals become

$$I_{\eta^-} + I_{\eta^+} = -\frac{1}{\pi}\int_{2\xi+\varepsilon}^{\infty} dx \frac{e^{-x\tau}}{\left(\frac{x}{2}+\xi\right)^{3/2}} \frac{e^{\beta x}}{e^{\beta x}-1}.$$

We can rewrite the last fraction on the right hand side of the previous equation as a geometric series and then make a change of variables to obtain

$$I_{\eta^-} + I_{\eta^+} = -\frac{2}{\pi}\sum_{m=0}^{\infty}\left[e^{-2\xi(\tau+m\beta)}\int_{\varepsilon}^{\infty} du \frac{e^{-2u(\tau+m\beta)}}{u^{3/2}}\right].$$

The integral in the square brackets can be evaluated in terms of the error function [1] as follows

$$\int_{\varepsilon}^{\infty} du \frac{e^{-2u(\tau+m\beta)}}{u^{3/2}} = \frac{2e^{-2\varepsilon(\tau+m\beta)}}{\sqrt{\varepsilon}} - 2\sqrt{2\pi(\tau+m\beta)}\cdot\left(1-\frac{2}{\pi}\sqrt{2\varepsilon(\tau+m\beta)}\right).$$

With the last result we get, in the limit $\varepsilon \to 0$:

$$I_{\eta^-} + I_{\eta^+} = -\frac{4}{\pi}\frac{1}{\sqrt{\varepsilon}}\sum_{m=0}^{\infty} e^{-2\xi(\tau+m\beta)} + \frac{4}{\sqrt{\pi}}\sum_{m=0}^{\infty}\sqrt{2\left(\tau+m\beta\right)}\cdot e^{-2\xi(\tau+m\beta)}$$

and finally, putting together the contributions I_γ, I_{η^-} and I_{η^+}, we can write the sum as:

$$\frac{1}{\beta}\sum_{\Omega_n} e^{-i\Omega_n\tau}\frac{1}{\left(-\frac{i\Omega_n}{2}+\xi\right)^{3/2}} = \frac{4}{\sqrt{\pi}}\sum_{m=0}^{\infty}\sqrt{2\left(\tau+m\beta\right)}\cdot e^{-2\xi(\tau+m\beta)}. \tag{C.5}$$

[1] To evaluate the integral we used the results

$$\int_{\varepsilon}^{\infty} dx \frac{e^{-\alpha x}}{x^{3/2}} = \frac{2e^{-\alpha\varepsilon}}{\sqrt{\varepsilon}} - 2\sqrt{\pi\alpha}\left(1-Erf\left(\sqrt{\alpha\varepsilon}\right)\right), \quad Erf\left(\sqrt{\alpha\varepsilon}\right) \approx \frac{2}{\sqrt{\pi}}\left[(\alpha\varepsilon)^{1/2} - \frac{(\alpha\varepsilon)^{3/2}}{3}\right]$$

and considered the first order only.

Bibliography

[1] S. N. Bose, Z. Phys **26**, 178 (1924).

[2] A. Einstein, Sitz. Ber. Preussischen Akad. Wiss. Phys. Math. Kl. **261**, 3 (1924).

[3] M. H. Anderson *et al.*, Science **269**, 198 (1995).

[4] C. C. Bradley, C. A. Sackett, J. J. Tollett, and R. G. Hulet, Phys. Rev. Lett. **75**, 1687 (1995).

[5] K. B. Davis *et al.*, Phys. Rev. Lett. **75**, 3969 (1995).

[6] C. J. Pethick and H. Smith, *Bose-Einstein Condensation in Dilute Gases* (Cambridge University, Cambridge, England, 2002).

[7] L. P. Pitaevskii and S. Stringari, *Bose-Einstein Condensation* (Oxford University, Oxford, UK, 2003).

[8] F. Dalfovo, S. Giorgini, L. P. Pitaevskii, and S. Stringari, Rev. Mod. Phys. **71**, 463 (1999).

[9] A. J. Leggett, Rev. Mod. Phys. **73**, 307 (2001).

[10] L. N. Cooper, Phys. Rev. **104**, 1189 (1956).

[11] J. Bardeen, L. N. Cooper, and J. R. Schrieffer, Phys. Rev. **108**, 1175 (1957).

[12] D. M. Eagles, Phys. Rev. **186**, 456 (1969).

[13] A. J. Leggett, J. Phys. C (Paris) **41**, 7 (1980).

[14] P. Nozières and S. Schmitt-Rink, J. Low. Temp. Phys **59**, 195 (1985).

[15] M. Drechsler and W. Zwerger, Ann. Phys. **1**, 15 (1992).

[16] S. Stintzing and W. Zwerger, Phys. Rev. B **56**, 9004 (1997).

[17] R. Haussmann, Z. Phys. B **91**, 291 (1993).

[18] R. Haussmann, *Self-consistent quantum-field theory and bosonization for strongly correlated electron systems* (Springer, Berlin, 1999).

[19] B. DeMarco and D. S. Jin, Science **285**, 1703 (1999).

[20] F. Schreck *et al.*, Phys. Rev. Lett. **87**, 080403 (2001).

[21] A. G. Truscott, K. E. Strecker, W. I. McAlexander, and G. B. P. R. G. Huletdagger, Science **291**, 2570 (2001).

[22] S. R. Granade, M. E. Gehm, K. M. O'Hara, and J. E. Thomas, Phys. Rev. Lett. **88**, 120405 (2002).

[23] Z. Hadzibabic *et al.*, Phys. Rev. Lett. **88**, 160401 (2002).

[24] G. Roati, F. Riboli, G. Modugno, and M. Inguscio, Phys. Rev. Lett. **89**, 150403 (2002).

[25] S. Inouye *et al.*, Nature **392**, 151 (1998).

[26] P. Courteille *et al.*, Phys. Rev. Lett. **81**, 69 (1998).

[27] J. L. Roberts *et al.*, Phys. Rev. Lett. **81**, 5109 (1998).

[28] V. Vuletić, A. J. Kerman, C. Chin, and S. Chu, Phys. Rev. Lett. **82**, 1406 (1999).

[29] T. Loftus *et al.*, Phys. Rev. Lett. **88**, 173201 (2002).

[30] K. Dieckmann *et al.*, Phys. Rev. Lett. **89**, 203201 (2002).

[31] T. Bourdel *et al.*, Phys. Rev. Lett. **91**, 020402 (2003).

[32] S. Jochim *et al.*, Phys. Rev. Lett. **89**, 273202 (2002).

[33] J. Cubizolles *et al.*, Phys. Rev. Lett. **91**, 240401 (2003).

[34] S. Jochim *et al.*, Phys. Rev. Lett. **91**, 240402 (2003).

[35] K. E. Strecker, G. B. Partridge, and R. G. Hulet, Phys. Rev. Lett. **91**, 080406 (2003).

[36] K. Xu *et al.*, Phys. Rev. Lett. **91**, 210402 (2003).

[37] M. Greiner, C. A. Regal, and D. S. Jin, Nature **426**, 537 (2003).

[38] M. W. Zwierlein *et al.*, Phys. Rev. Lett. **91**, 250401 (2003).

[39] S. Jochim *et al.*, Science **302**, 2101 (2003).

[40] C. A. Regal, M. Greiner, and D. S. Jin, Physical Review Letters **92**, 040403 (2004).

[41] M. Bartenstein *et al.*, Physical Review Letters **92**, 120401 (2004).

[42] M. W. Zwierlein *et al.*, Physical Review Letters **92**, 120403 (2004).

[43] J. Kinast *et al.*, Physical Review Letters **92**, 150402 (2004).

[44] T. Bourdel *et al.*, Physical Review Letters **93**, 050401 (2004).

[45] J. M. Luttinger and J. C. Ward, Phys. Rev. B **118**, 1417 (1960).

[46] W. E. Parry, in *The Many-Body Problem*, edited by B. Bleaney and D. H. Wilkinson (Oxford University Press, London, 1973).

[47] C. D. Dominicis and P. Martin, J. Math. Phys. **5**, 14 and 31 (1964).

[48] G. Baym and L. Kadanoff, Phys. Rev. **124**, 287 (1961).

[49] G. Baym, Phys. Rev. **127**, 1391 (1962).

[50] J. M. Luttinger, Phys. Rev. **119**, 1153 (1960).

[51] D. J. Amit, *Field Theory, the Renormalization Group, and Critical Phenomena* (McGraw-Hill, New York, 1978).

[52] D. J. Thouless, Ann. Phys. (N.Y.) **10**, 553 (1960).

[53] Y. Nambu, Phys. Rev **117**, 648 (1960).

[54] G. C. Strinati and P. Pieri, Europhys. Lett. **71**, 359 (2005).

[55] P. C. Hohenberg and P. C. Martin, Ann. Phys. **34**, 291 (1965).

[56] L. P. Gorkov and T. K. Melik-Barkhudarov, Sov. Phys. JETP **13**, 1018 (1961).

[57] A. L. Fetter and J. D. Walecka, *Quantum Many-Particle System* (Mc Graw-Hill, New York, 1971).

[58] D. S. Petrov, C. Salomon, and G. V. Shlyapnikov, Physical Review Letters **93**, 090404 (2004).

[59] G. Baym *et al.*, Phys. Rev. Lett. **83**, 1703 (1999).

[60] G. Baym *et al.*, Eur. Phys. J. B **24**, 107 (2001).

[61] G. Baym, J.-P. Blaizot, and J. Zinn-Justin, Europhys. Lett. **49**, 150 (2000).

[62] M. Randeria, in *Bose-Einstein Condensation*, edited by D. W. S. A. Griffin and S. Stringari (Cambridge University Press, NY, 1995), p. 355.

[63] R. Haussmann, Phys. Rev. B **49**, 12975 (1994).

[64] C. A. R. Sá de Melo, M. Randeria, and J. R. Engelbrecht, Phys. Rev. Lett. **71**, 3202 (1993).

[65] P. Arnold and G. Moore, Phys. Rev. Lett. **87**, 120401 (2001).

[66] P. Arnold and G. D. Moore, Phys. Rev. E **64**, 066113 (2001).

[67] V. A. Kashurnikov, N. V. Prokof'ev, and B. V. Svistunov, Phys. Rev. Lett. **87**, 120402 (2001).

[68] G. Ortiz and J. Dukelsky, Physical Review A **72**, 043611 (2005).

[69] W. Lenz, Z. Phys. **56**, 778 (1929).

[70] K. Huang and C. Yang, Phys. Rev. **105**, 767 (1957).

[71] J. G. A. Baker, Phys. Rev. C **60**, 054311 (1999).

[72] H. Heiselberg, Phys. Rev. A **63**, 043606 (2001).

[73] T.-L. Ho, Physical Review Letters **92**, 090402 (2004).

[74] J. Carlson, S.-Y. Chang, V. R. Pandharipande, and K. E. Schmidt, Physical Review Letters **91**, 050401 (2003).

[75] S. Y. Chang, V. R. Pandharipande, J. Carlson, and K. E. Schmidt, Physical Review A (Atomic, Molecular, and Optical Physics) **70**, 043602 (2004).

[76] G. E. Astrakharchik *et al.*, Physical Review Letters **93**, 200404 (2004).

[77] G. E. Astrakharchik, J. Boronat, J. Casulleras, and S. Giorgini, Physical Review Letters **95**, 230405 (2005).

[78] J. Kinast *et al.*, Science **307**, 1296 (2005).

[79] G. B. Partridge *et al.*, Science **311**, 503 (2006).

[80] H. Hu, X. J. Liu, and P. D. Drummond, Europhys. Lett **74**, 574 (2006).

[81] A. Perali, P. Pieri, and G. C. Strinati, Physical Review Letters **93**, 100404 (2004).

[82] C. Chin *et al.*, Science **305**, 1128 (2004).

[83] L. D. Carr, G. V. Shlyapnikov, and Y. Castin, Physical Review Letters **92**, 150404 (2004).

[84] H. Hu, X.-J. Liu, and P. D. Drummond, Physical Review A (Atomic, Molecular, and Optical Physics) **73**, 023617 (2006).

[85] E. Burovski, N. Prokof'ev, B. Svistunov, and M. Troyer, Physical Review Letters **96**, 160402 (2006).

[86] A. Bulgac, J. E. Drut, and P. Magierski, Physical Review Letters **96**, 090404 (2006).

[87] Y. Nishida and D. T. Son, cond-mat/0607835 (2006).

[88] Y. Nishida and D. T. Son, Physical Review Letters **97**, 050403 (2006).

[89] Y. Nishida, cond-mat/0608321 (2006).

[90] P. Nikolic and S. Sachdev, cond-mat/0609106 (2006).

[91] E. Burovski, N. Prokof'ev, B. Svistunov, and M. Troyer, Physical Review Letters **97**, 239902 (2006).

Acknowledgements

First I would like to thank Prof. Zwerger for giving me the opportunity to study this interesting and actual problem, for being patient and always helpful. I also want to thank him for having given me the chance to meet and work with many young physicist in Munich at the Ludwig Maximilians Universität first and at the Technische Universität during the last year, and in Innsbruck at the Leopold-Franzens Universität.

I would like to thank the people I worked with at the LMU. Patrick Werner, who helped me a lot at the beginning of my staying in Munich, Richard Neher and Dr. Sigmund Stintzing.

Next I wish to thank the group that Prof. Zwerger had in Innsbruck, Dr. Jean-Noël Fuchs and Dr. Walter Rantner to whom go special thanks. He was always ready to talk about the complicated physics underlying the problem we worked on and he was always very acute in finding solution to the technical problems connected with the numerics. Another thank goes to Rudolf Hausmann for his helpful suggestion about the numerics. For the wonderful time I spent in Innsbruck I also want to tank Alessio Recati, Janos Ashbot, Uwe Dorner, Andrea Micheli and Ignacio Wilson-Rae and Claudia Peça, which I had the pleasure to meet again in Munich during the last months of my Ph. D..

Finally, I wish to thank Dong Chen, Martin Oberkofler, Matthias Punk, Stefan Wellenzohn, Cyril Belardinelli, Daniela Neufang and all the members of the department of theoretical physics for the nice working atmosphere.

A special thank goes also to Ester, my friends and my family which sustained and pushed me during the last four years.